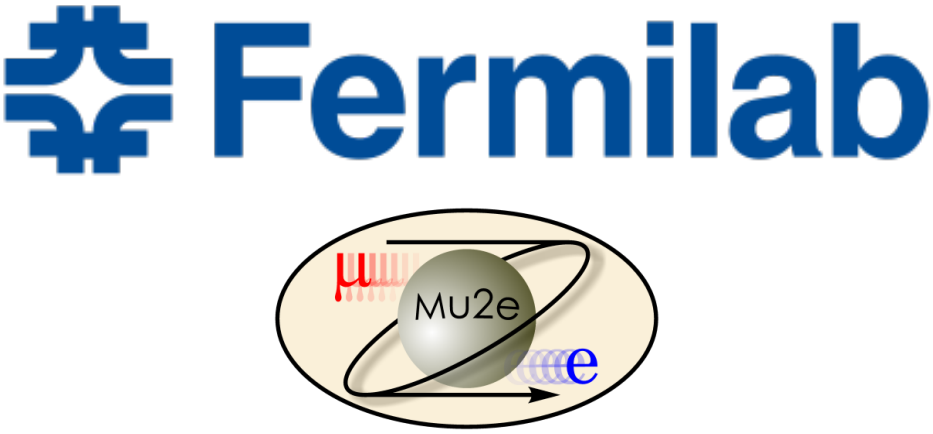

Verification of the Mu2e Proton Beam Dump Heat Removal System

Supervisor:
Kavin Ammigan
ammikav@fnal.gov

Intern:
Davide Venturini
dave.venturini@gmail.com

Co-supervisor:
Zunping Liu
zunping@fnal.gov

The following report is the result of the Italian Summer Internship Program at FNAL (Batavia, Jul-Sept 2024)

Abstract

Davide Venturini

Università di Pisa, Scuola Superiore Sant'Anna
dave.venturini@gmail.com

The purpose of this report is the verification of the working and accident conditions of the Mu2e Proton Beam Dump Heat Removal System. Energy from the Mu2e proton beam is deposited inside of the Proton Beam Dump, which has to be cooled by its Heat Removal System. Many simulations are carried out to check if the temperature of the concrete stays below 95 °C for material properties reasons and the results are analyzed. The report discusses in detail the meshing and the boundary conditions of both the solid and the fluid components of the ANSYS coupled simulations. Sensitivity analysis on the air volumetric flow are carried out and results are compared with the previously available calculations to determine the applicability of the numbers found.

The final results suggest that the heat transfer coefficients are bigger than the ones calculated previously. The previous calculations are thus very cautelative and it is possible to lower the air volumetric flow without problems. It has to be said that, of all the simulations carried out, the most reliable one is that with a volumetric airflow of 165 CFM. In fact, simulations with a bigger volumetric airflow do not exactly satisfy the global energy conservation equation, a necessary condition to evaluate if the result is realistic. To achieve more accurate results with higher volumetric airflows or in different conditions, it is seen that it is necessary to increase the coupling iterations and the Fluent iterations.

Contents

Introduction

1.1 Purpose of the Mu2e experiment

Mu2e (or Muon-to-Electron Conversion Experiment) is a particle physics experiment carried out at Fermilab, US. The goal of the experiment is to lower the upper known boundary of the probability of flavor violating decay of muon into electron and gamma.[1] The theoretical probability of this event is estimated by the Standard Model in being 1 in 10^{54} events and Mu2e will be able to detect if this is true for a maximum of 10^{17} muon decays. Detecting signals over the background could be a strong clue of physics beyond the Standard Model while not detecting any signal would put a strong constraint in the development of beyond the Standard Model theories.[2]

Figure 1.1: Mu2e decay[3]

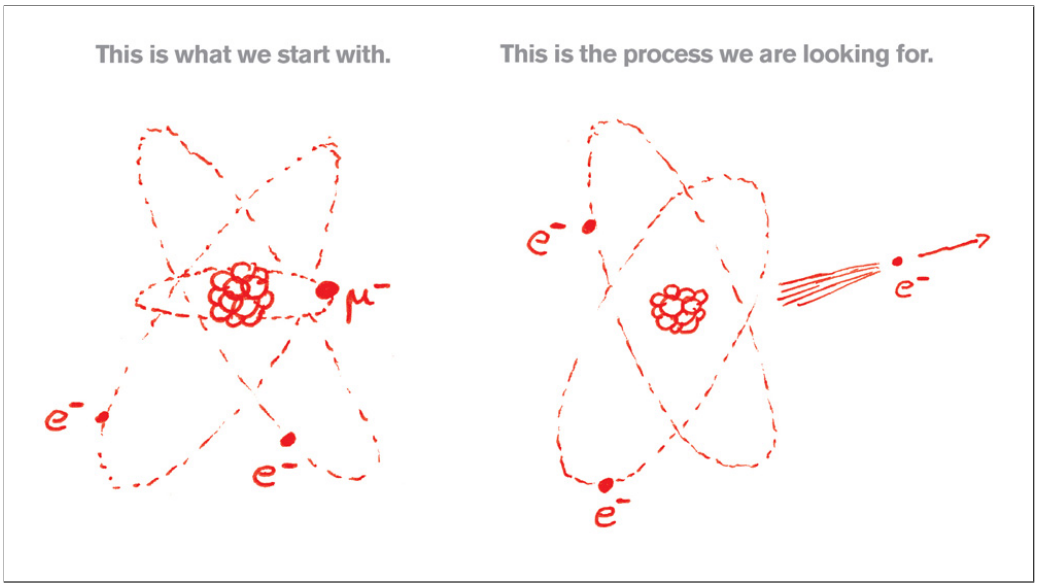

1.2 Carrying out the Mu2e experiment

Everything starts with a proton beam with a power of 8 kW. This beam collides with a tungsten target and generates pions that fastly decay in muons. These muons are carried by an S-shaped solenoid structure towards a 0.2 mm thick aluminum target in which different types of decays can happen. Detectors are able to say if the neutrinoless muon-to-electron conversion happens or not by measuring the energy of the generated electron.

[1] https://en.wikipedia.org/wiki/Mu2e
[2] https://mu2ewiki.fnal.gov/wiki/PhysicsIntro
[3] https://mu2e.fnal.gov/graphics.shtml

Figure 1.2: Mu2e assembly[4]

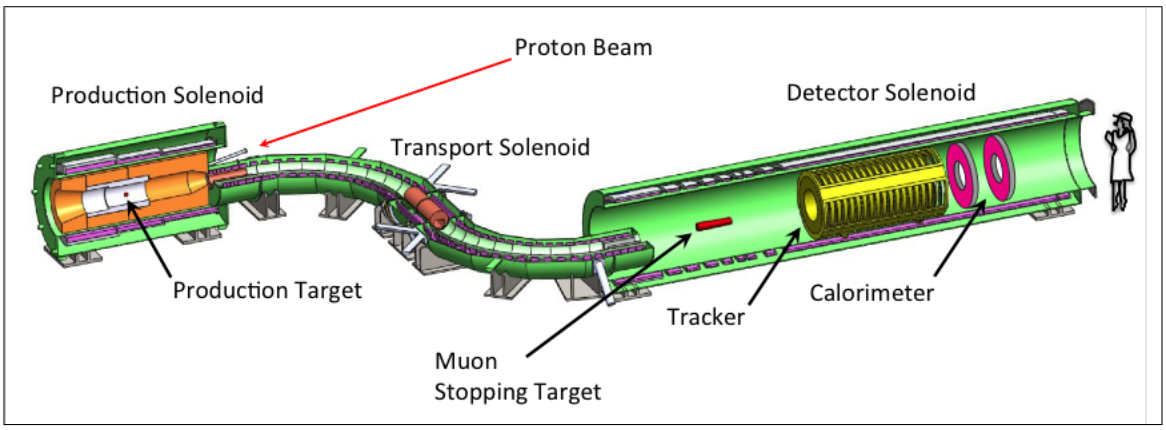

1.3 Proton Beam Dump

The Proton Beam Dump is made of seven steel plates surrounded by a steel baffle and kept in position by two concrete blocks. On the upper part of the assembly there are some plates and supports for the Extinction Monitor pipe. Normally, not all the proton beam energy is delivered inside of the tungsten target due to scattering and particle deviations. Moreover, there is the possibility that the proton beam is not centered on the target and in the worst case it could totally miss the target. So there is the need for an absorbing structure that has the purpose to stop both the partial energy of the beam in ordinary conditions and the almost total energy of the beam in accident conditions. The Proton Beam Dump is the assembly that has this purpose.

Figure 1.3: Proton Beam Dump

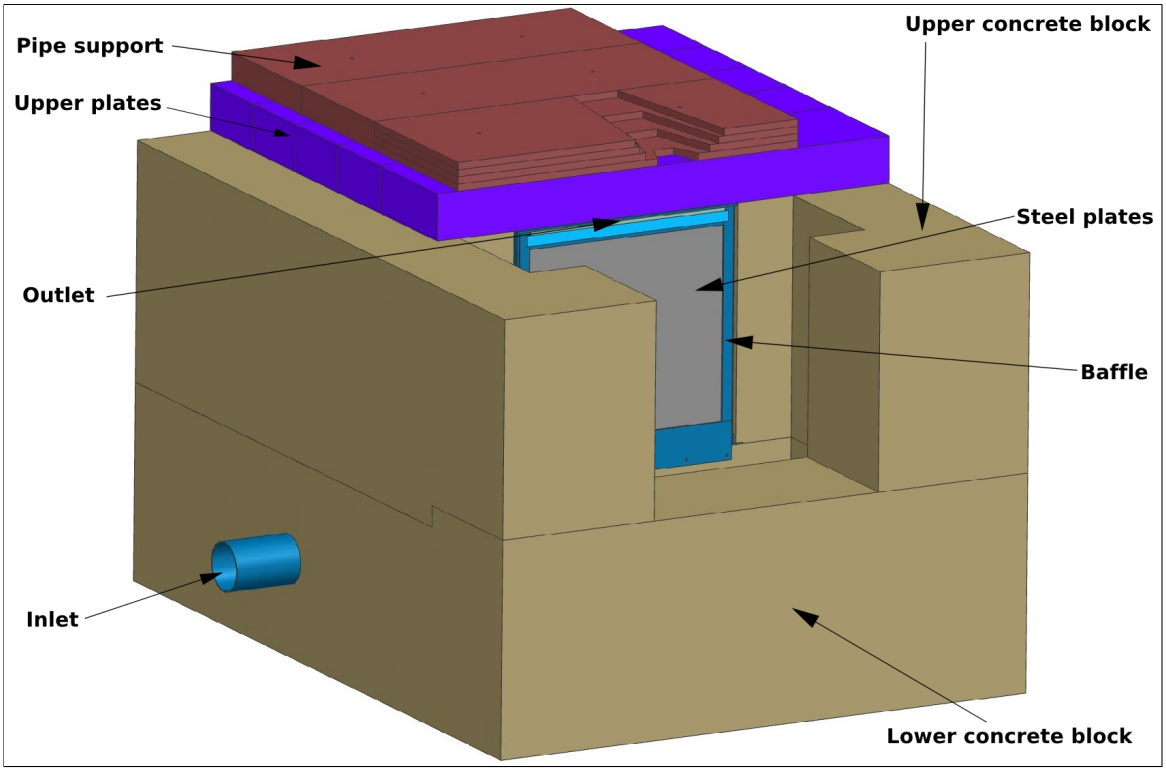

[4]https://mu2ewiki.fnal.gov/wiki/File:FullDetector.png

1.4 Heat Removal System

The Heat Removal System consists of a building supply duct positioned inside the lower concrete block. The duct is connected to a crossover line that is connected to the supply header. The header drives the air into six individual feed pipes that have two outlets each. The air coming from the pipes flows inside the horizontal gap under the core. Then, the airflow path is vertical around the steel plates and converges towards the upper horizontal gap. Then, it flows out to the upper outlet that is positioned in the front of the assembly.

The energy deposited inside of the steel plates and the concrete blocks due to the proton beam makes the temperature of the system go up. This is not a big problem for steel: it is estimated that the increase of temperature for the steel without any Heat Removal System is well below any problematic threshold. But this is not the case for concrete: to avoid any degradation, it is required that its temperature should stay below 95 °C.

Figure 1.4: Heat Removal System

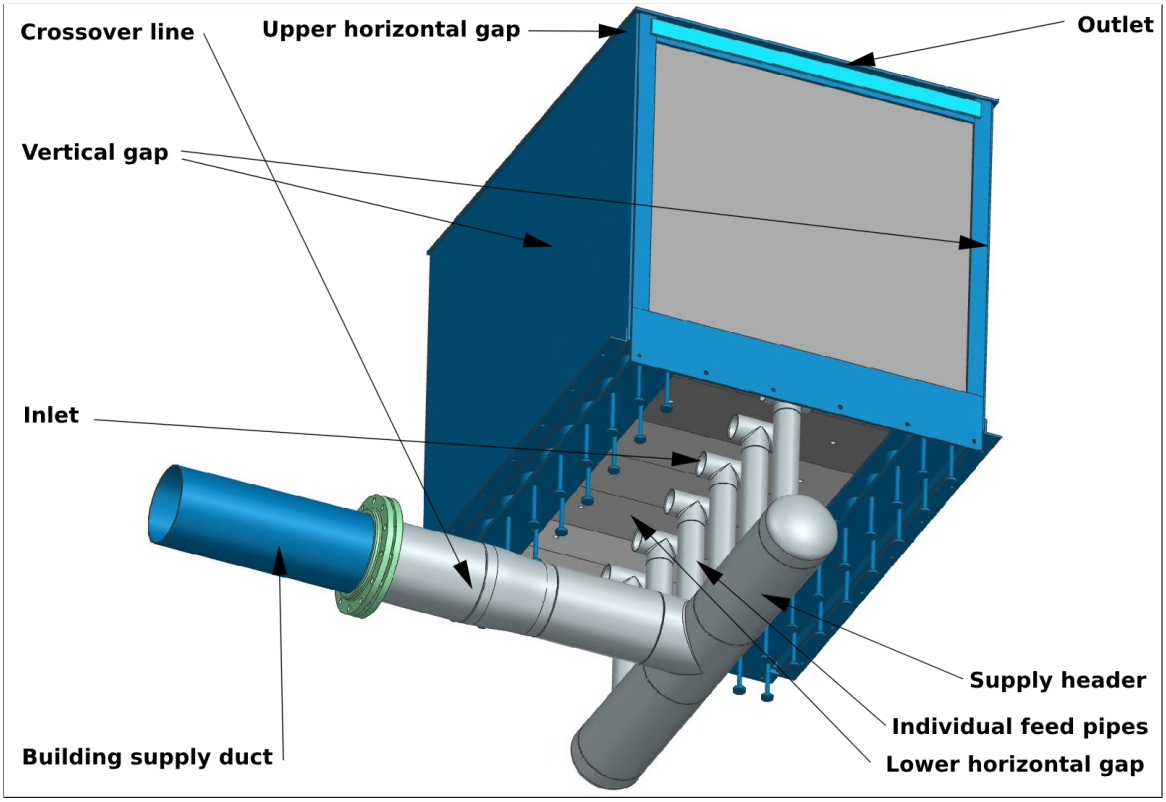

Previous work

Given the design of the Heat Removal System, there is the need to estimate the increase of temperature of the steel walls and the concrete blocks to understand if the concrete temperature is kept below the given constraint of 95 °C. Previously, the main calculations were carried out using an Excel file, an ANSYS thermal simulation and an ANSYS Fluent simulation. Data as the Heat Transfer Coefficients were transferred manually from the Excel file to the ANSYS Thermal simulations. The geometries were available and developed using NX CAD software and are those shown in the previous chapter.

2.1 Excel calculations file

The Excel file calculations divide the airflow path in eight regions: building supply duct, crossover line from building air duct to supply header, supply header, individual feed pipe, horizontal gap under the core, vertical gap between core and wall, horizontal gap on top of the core (lateral flow), horizontal gap on top of the core (longitudinal flow). For each region, the main outputs of the file are: bulk heat transfer coefficient, film heat transfer coefficient, surface temperature, bulk temperature pressure drops and fan horsepower needed.

Figure 2.1: Excel file

	A	B	C	D	E	F	G	H	I	J	K
1	READ ME FIRST: (1) Enable iterative calculations under EXCEL Options/Formulas and then reopen the spreadsheet. (2) Sometimes the heat transfer coefficient calculations won't automatically iterate and must be manually repaired by entering a reasonable initial value in the (INPUT) cell and then inserting the formula pointing to the (CHECK INPUT) cell.					CHECK CALCULATIONS FOR FLOW PATH 4: CHECK CALCULATIONS FOR FLOW PATH 4		CHECK CALCULATIONS FOR FLOW PATH 6: CHECK CALCULATIONS FOR FLOW PATH 6	FLOW PATH DIAGRAM and FEA INPUT CALCULATIONS →		
2					Six 4" feed pipes with tee, 14" supply line.						
3											
4	Standard pressure (1 atmosphere)	Pa	101325	101325	101325	101325	101325	101325	101325	101325	
5	Standard temperature (20 C according to EPA)	C	20	20	20	20	20	20	20	20	
6	Standard density	kg/m^3	1.204	1.204	1.204	1.204	1.204	1.204	1.204	1.204	
8	Molecular weight	g/mol	28.965	28.965	28.965	28.965	28.965	28.965	28.965	28.965	
9											
10	**INPUT:**										
11	Air volumetric flow rate to be used in the calculation	cfm	250	← CHANGE AIR FLOW RATE HERE							
12											
13	Flow path number		1	2	3	4	5	6	7-1	7-2	
14			Building supply duct	Crossover line from building air duct to supply header	Supply header	Individual feed pipe	Horizontal gap under the core	Vertical gap between core and wall (half right)	Horizontal gap on top of the core 1 - lateral flow	Horizontal gap on top of the core 2 - longitudinal flow	Total
104	**Film temperature calculations:**										
105											
106	Surface										
107											
108	Surface area	m^2	0.027	2.025	0.876	0.319	0.650	7.100	3.386	6.297	
109	Assumed surface temperature (INPUT)	C	20.000	20.000	20.000	20.000	86.803	128.352	197.475	223.128	Cell number 128
110	Average film temperature	C	20.000	20.000	20.000	20.000	59.658	102.707	181.794	223.128	
111	Air density	kg/m^3	1.1789	1.1789	1.1789	1.1789	1.0384	0.9195	0.7596	0.6964	
112	Air specific heat	J/kg-K	1005.2	1005.2	1005.2	1005.2	1007.3	1011.3	1022.3	1029.6	
113	Air dynamic viscosity	micro-Pa-s	18.084	18.084	18.084	18.084	19.923	21.802	24.990	26.540	
114	Air thermal conductivity	W/(m-K)	0.026	0.026	0.026	0.026	0.028	0.031	0.036	0.039	
115	Air velocity at film temperature	m/s	1.284	1.284	0.642	2.438	0.241	0.736	0.891	2.636	
116	Reynolds number	-	2.87 E+04	2.87 E+04	1.44 E+04	1.61 E+04	1.35 E+03	3.65 E+03	6.48 E+03	6.80 E+03	
117	Prandtl number	-	0.709	0.709	0.709	0.709	0.707	0.705	0.704	0.703	
118	Stanton Number - *Colburn Equation (Re > 6,000 (ga*	-	0.0037	0.0037	0.0043	0.0042	0.0069	0.0056	0.0050	0.0050	
119	Heat transfer coefficient - *Colburn Equation, +/- 30%*	W/(m^2-K)	5.7	5.7	3.3	12.1	1.7	3.9	3.5	9.4	
120											
121	Smooth tube Darcy friction factor	-	0.0239	0.0239	0.0285	0.0276	0.0607	0.0426	0.0356	0.0351	
122	Nusselt Number - *Petukhov Equation, for liquids (10,*	-	65	65	40	43	9	16	23	24	
123	Heat transfer coefficient - *Petukhov Equation, +/- 6%*	W/(m^2-K)	4.9	4.9	3.0	10.9	2.3	4.2	3.5	9.3	
124											
125	Use the smaller heat transfer coefficient	W/(m^2-K)	4.9	4.9	3.0	10.9	1.7	3.9	3.5	9.3	
126											
127	Tsurface - Taverage bulk air	C	0.000	0.000	0.000	0.000	54.290	51.290	31.362	0.000	

2.2 ANSYS Thermal Simulation

The ANSYS Thermal simulation simulates the behaviour of the Proton Beam Dump using as boundary conditions an imposed temperature of 15 °C on the bottom face of the lower concrete

block and the heat transfer coefficients calculated by the Excel file. There are some problems with the simulation:

- It seems that the simulation uses an old and extremely simplified geometry not including the new baffle structure and the plates covering the baffle and details as fins, upper and lower supports that are in contact with the baffle and are responsible of delivering heat due to conduction
- The boundary conditions imposed on the simulations are just the heat transfer coefficients calculated using the Excel file (so with simplified calculations and assuming uniform HTC in every region)
- The number and dimensions of the steel plates is not up-to-date to the latest design (seen in the CAD file)
- It is not clear how the ambient temperatures that are used together with the heat transfer coefficients to impose convection are calculated

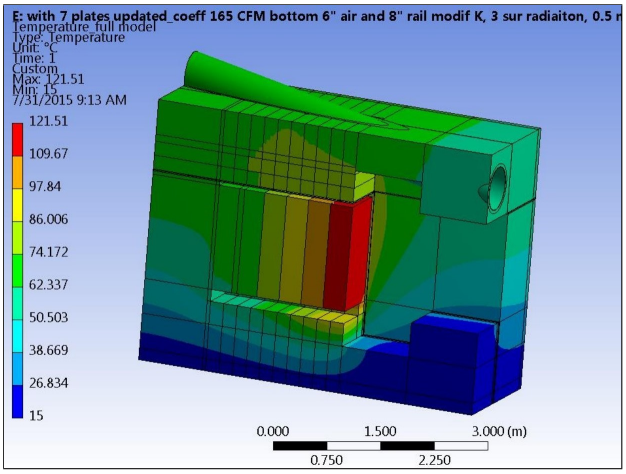

Figure 2.2: Previous thermal simulation with 165 CFM of inlet airflow[1]

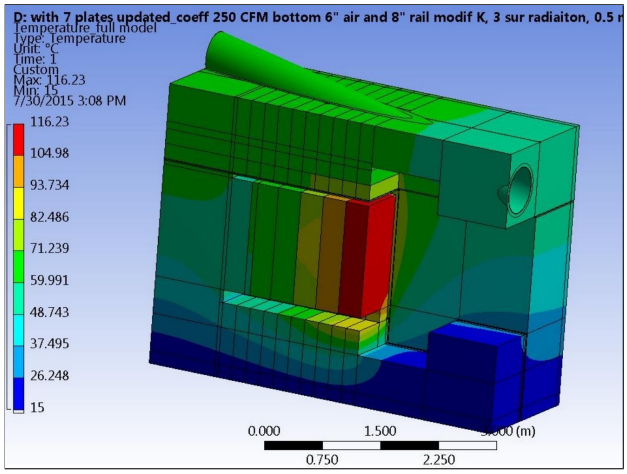

Figure 2.3: Previous thermal simulation with 250 CFM of inlet airflow

2.3 ANSYS Fluent Simulation

A Fluent simulation of the airflow geometry was also available. This simulation did not include any heat exchange.

[1]Pictures taken from Lee, A. and Stefanik A. (2015) Mu2e-doc-5855 Updated Thermal Result for the Proton Absorber

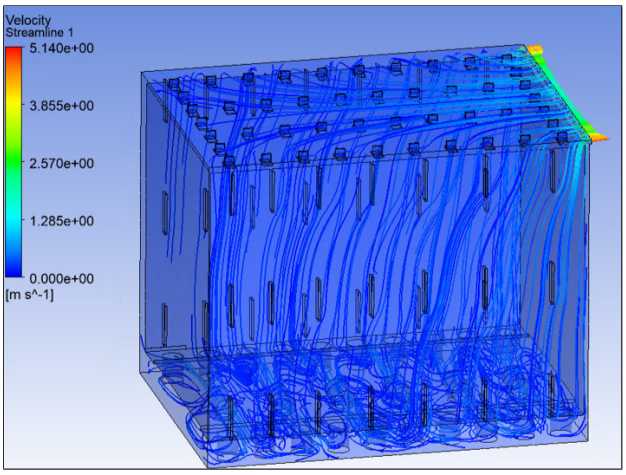

Figure 2.4: Previous Fluent simulation[2]

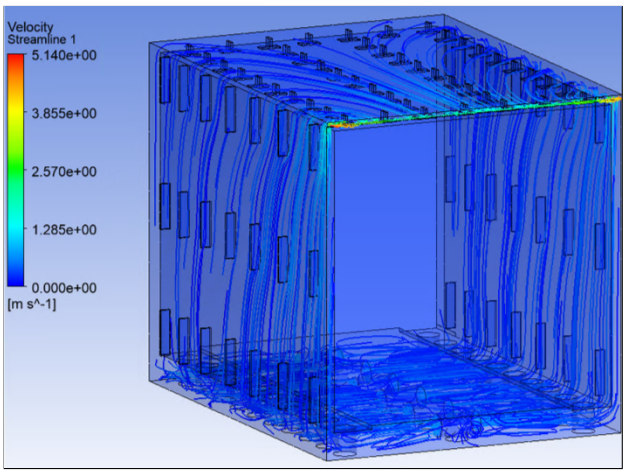

Figure 2.5: Previous Fluent simulation

2.4 Proton Beam Dump CAD geometry file

This is the most complete CAD file of the Proton Beam Dump. For the report, the following actions were taken:

- Simplifying the geometry for the meshing by removing the lower pipe entrance and the internal pipe paths
- Splitting many contact surfaces to assing more accurate boundary and contact conditions between the bodies using the SpaceClaim ANSYS module

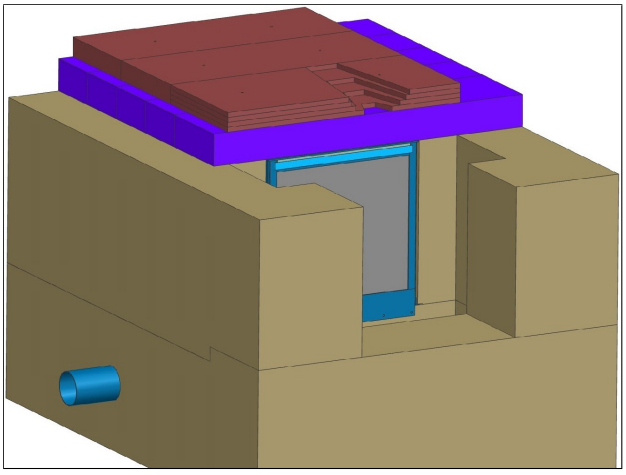

Figure 2.6: Solid CAD

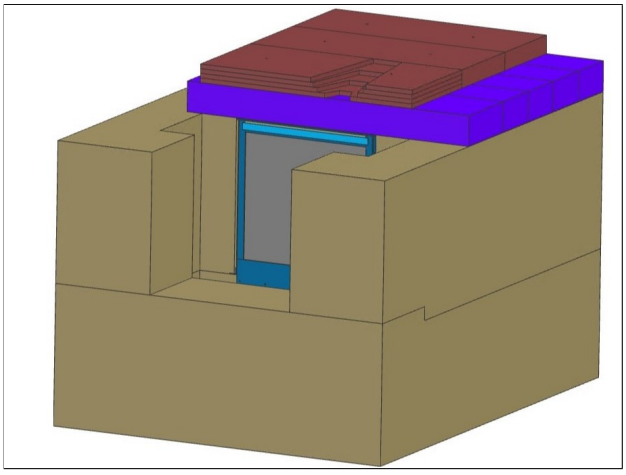

Figure 2.7: Solid CAD

[2]Picture taken from Liu, Z. (2024) Baffle for Mu2e Proton Absorber 5-15-24

2.5 Airflow Path CAD geometry file

This is the same CAD that has been used in the previous ANSYS Fluent simulation. The file describes the air path from the inlet on the bottom of the steel plates up to the outlet on the top of the steel plates. The back and the front of the air volume were removed since from the ANSYS Fluent simulation it was clear that only stagnant air was present. These two surfaces will be substituted with static air boundary conditions.

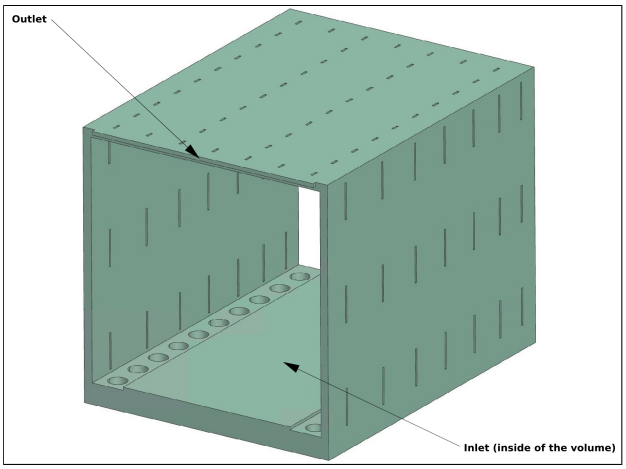

Figure 2.8: Fluid volume with inlet and outlet indicated by the arrows

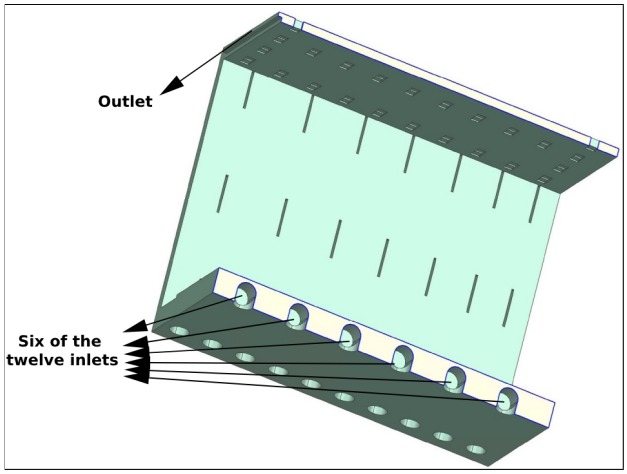

Figure 2.9: Fluid volume section (using a plane of geometric symmetry)

Coupled simulations

From the start, it was clear that to get the most realistic results for the Heat Removal System, a coupled simulation was needed. The already available simulation of the Proton Beam Dump imposing the heat transfer coefficients and the air temperature on the surfaces is computationally fast, but uses some strong simplifications that can be avoided by making the computer simulate also the air component. Note: Fluent alone was not used due to a list of reasons: the focus of the simulations is the solid component, one should have known the energy distribution (e.g. fitting the sources by a gaussian), an UDF should have been defined etc.

3.1 How does a coupled simulation work?

There are two kind of coupled simulations.[1]

3.1.1 One-way coupling

This kind of coupled simulation is useful when we want to simulate accurately only one of the two components and want a low computational time. Data is transferred only from one component to the other and not in the other way. For instance, in a Structural-Fluent simulation, the forces from a fluid that surrounds a body are transferred as pressures on the body's surface but the deformations of the body are not transferred to the fluid. So the solid will be correctly modelled but the fluid not so much (because it is not necessary). Notice the graph below, given for a transient simulation (with more time steps). In the case of a steady-state simulation only one time step is required so the external loop consists only of one transfer from fluid to the solid.

Figure 3.1: One-way coupling graph

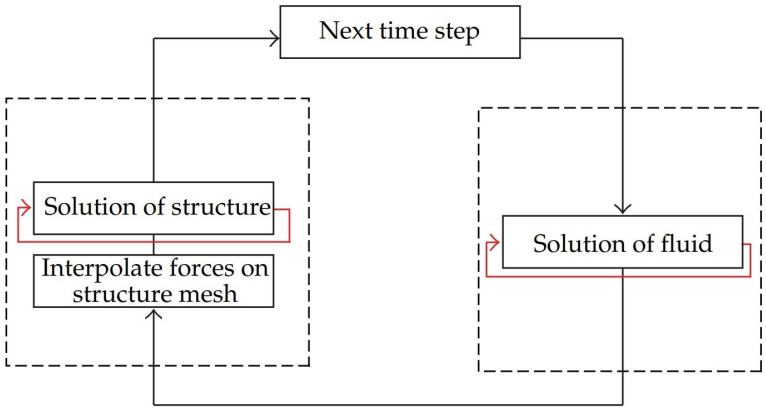

[1]Images and concepts taken from Benra, Friedrich-Karl & Dohmen, Hans & Pei, Ji & Schuster, Sebastian & Wan, Bo. (2011). A Comparison of One-Way and Two-Way Coupling Methods for Numerical Analysis of Fluid-Structure Interactions. Journal of Applied Mathematics. 2011. 10.1155/2011/853560.

3.1.2 Two-way coupling

This kind of coupled simulation is useful when we want to simulate accurately both of the components and are not worried about a higher computational time. Initially one component is solved starting from an initial guess on the coupled physical quantities until the convergence criteria are reached. Then, the calculated coupled physical quantities are transferred at the boundaries. Next, the other component is calculated until the convergence criterion is reached. And the process starts again. The solution is finished when the maximum number of time steps is reached. In the case of a static simulation only one time step is required so the external loop in the graph below consists only of one cycle (but more transfers between solid and fluid are required for convergence, differently from the one-way coupling). For the simulations of this report, a two-way coupling simulation approach is required.

Figure 3.2: Two-way coupling graph

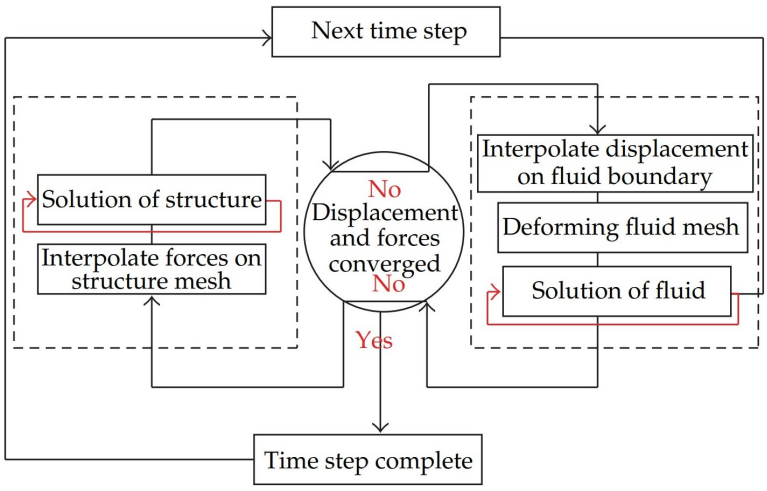

3.2 Software

The software chosen to simulate both the solid and the fluid components is ANSYS. In ANSYS Workbench, some blocks are needed:

- External data for the MARS Heat Generation rate
- Thermal Steady-State for the solid component
- Fluent (with Fluent Meshing) for the airflow. It is important to use Fluent to mesh the air volume, since the Mechanical meshing approach is not correct for fluids.
- System Coupling to set up the data transfer

In this case, it is possible (and computationally convenient) to use a steady-state simulation because the time interval in which the heat deposition occurs is pretty long and so we evaluate only the most conservative case.

Figure 3.3: Workbench blocks

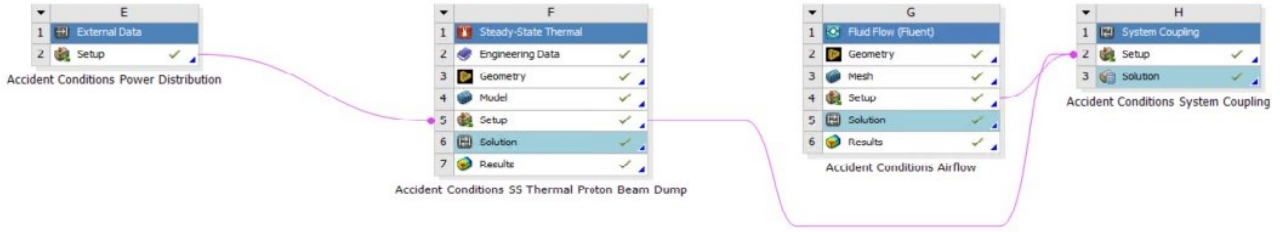

3.3 CAD elaboration

The two separate CADs (the solid one and the fluid one) already available have been merged in one single CAD. Moreover, the fluid CAD was simplified by removing the rear region since from previous simulations it was clear that there the air is pretty much static and no dynamic fluid simulation is required.

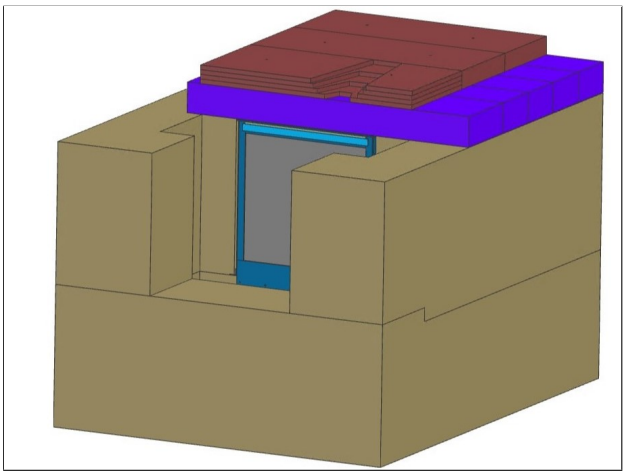

Figure 3.4: Solid CAD

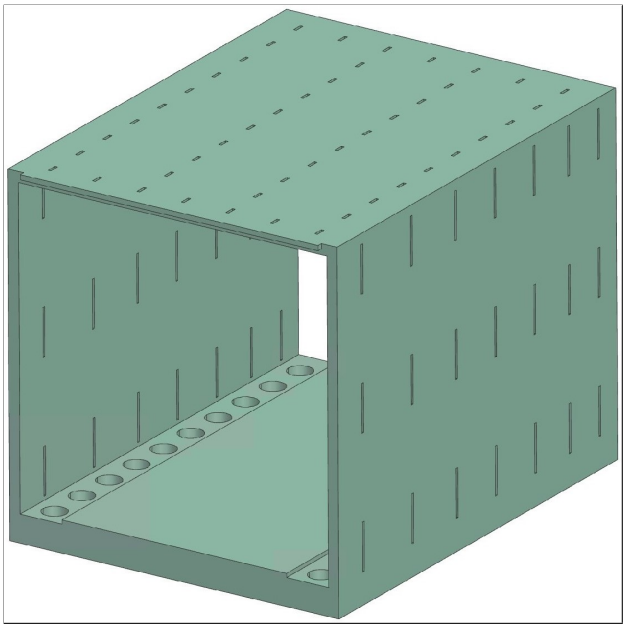

Figure 3.5: Fluid CAD

3.4 Solid Meshing

3.4.1 Process

The meshing has been done using different functions for different regions.

- Concrete blocks: 2 bodies meshed with Cartesian method, element size 0.12 m
- Pipe support: 4 bodies meshed with MultiZone method
- Upper plates: 7 bodies meshed with Cartesian method, element size 0.12 m
- Baffle plates: 3 bodies meshed with Sweep method, sweep element size 0.1 m. Face sizing on the external faces with element size 5e-2 m

- Steel plates: 7 bodies meshed with Sweep method, sweep element size 0.1 m. Face sizing on each one of the frontal faces with element size 7.5e-2 m. These dimensions are important to match the distances of the Heat Generation source nodes in the external distribution to have a one-to-one mapping and preserve the total power generated
- Lateral supports: 42 bodies meshed with MultiZone method.
- Lower supports: 32 bodies meshed with Sweep Axisymmetric method
- Upper supports: 92 bodies meshed with Sweep method
- Cylindrical supports: 20 bodies meshed with Sweep Axisymmetric method
- Cover plates: 16 bodies meshed with Automatic method

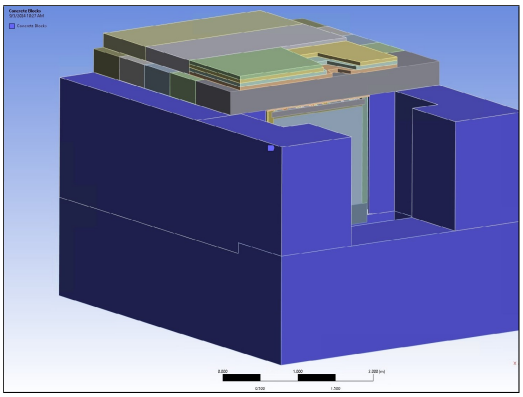

Figure 3.6: Concrete blocks bodies

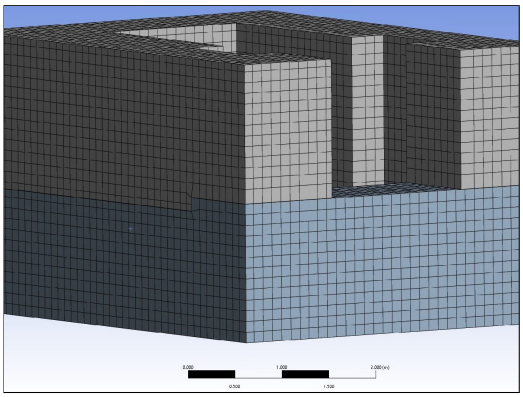

Figure 3.7: Concrete blocks meshing

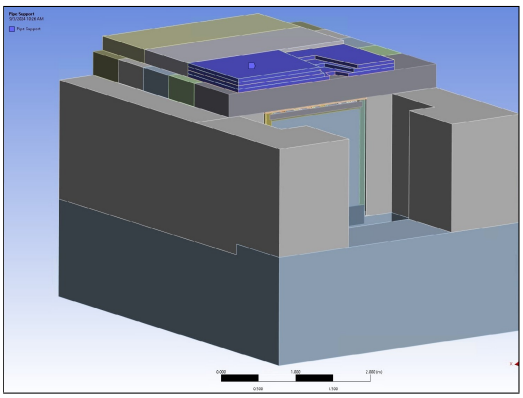

Figure 3.8: Pipe support bodies

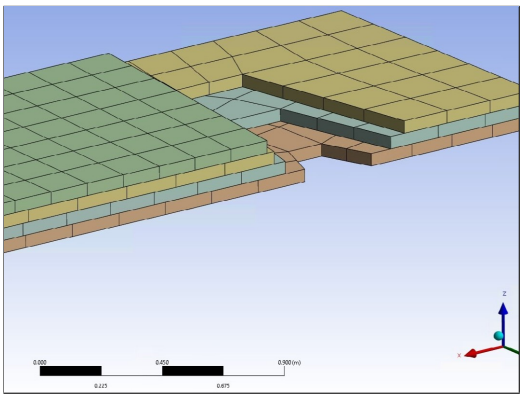

Figure 3.9: Pipe support meshing

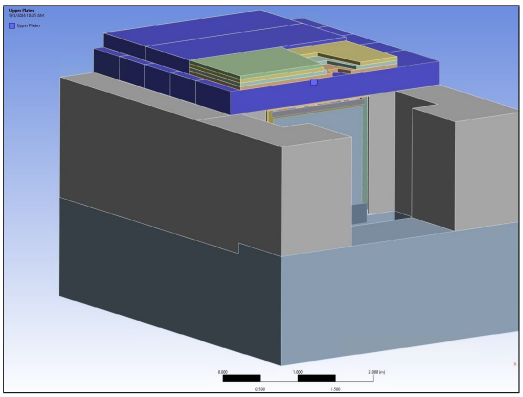

Figure 3.10: Upper plates bodies

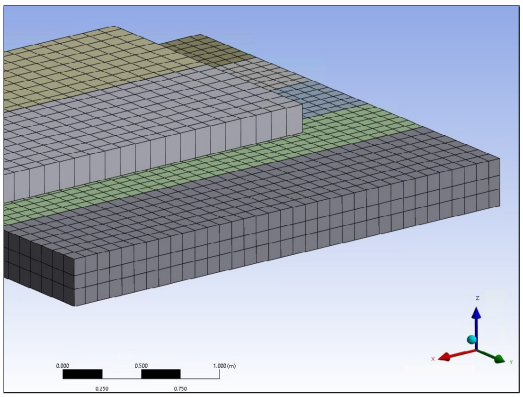

Figure 3.11: Upper plates meshing

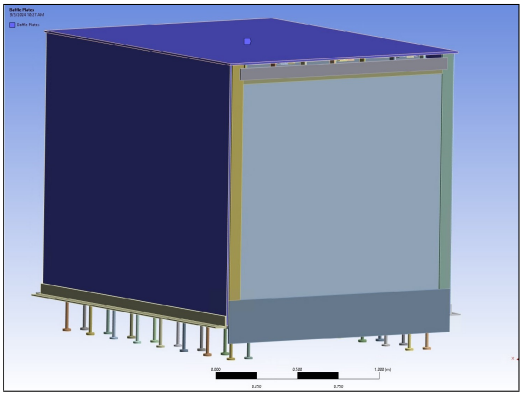

Figure 3.12: Baffle plates bodies

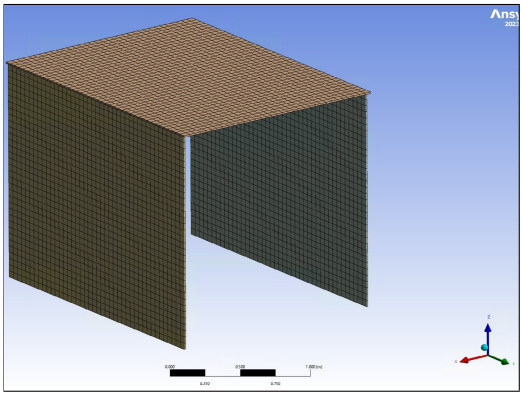

Figure 3.13: Baffle plates meshing

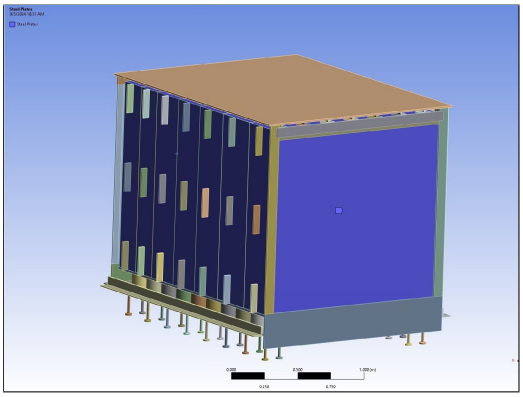

Figure 3.14: Steel plates bodies

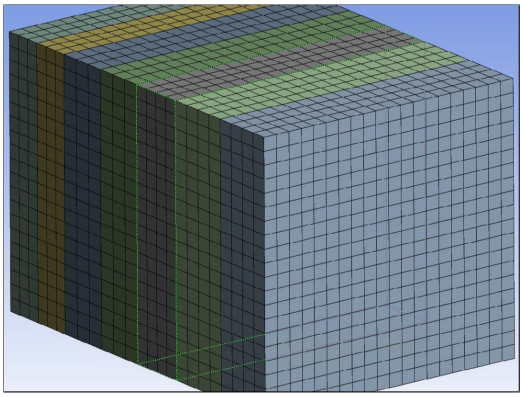

Figure 3.15: Steel plates meshing

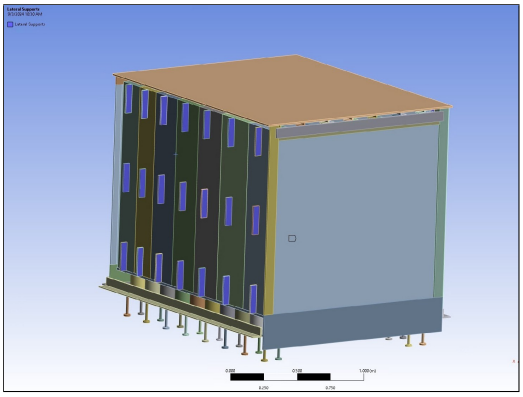

Figure 3.16: Lateral supports bodies

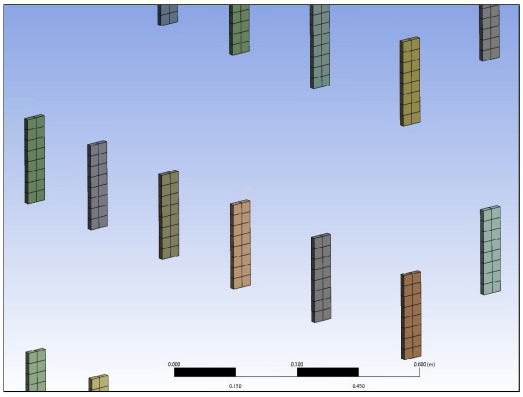

Figure 3.17: Lateral supports meshing

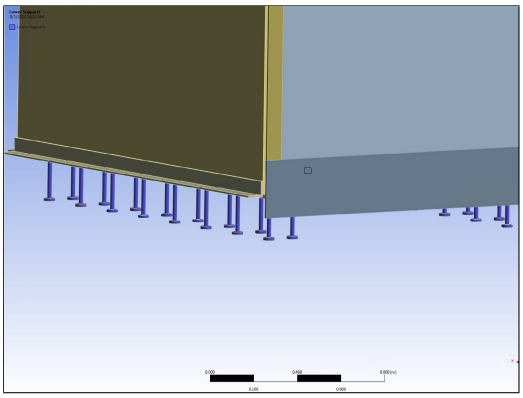

Figure 3.18: Lower supports bodies

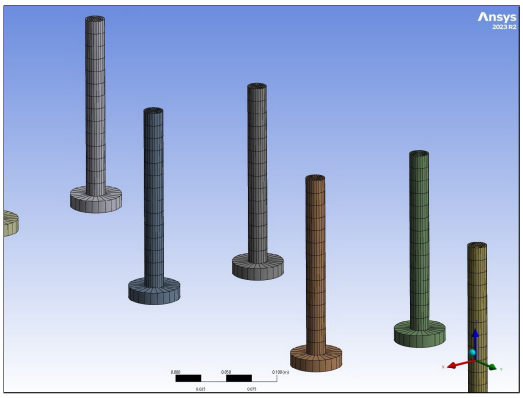

Figure 3.19: Lower supports meshing

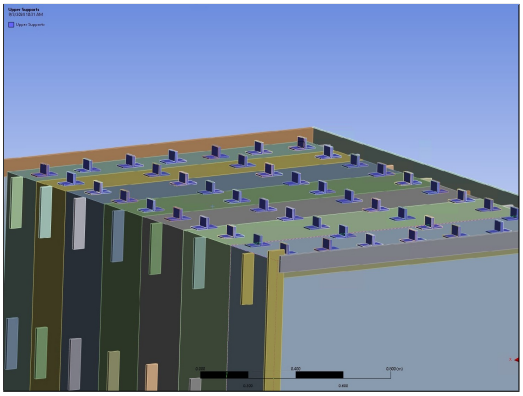

Figure 3.20: Upper supports bodies

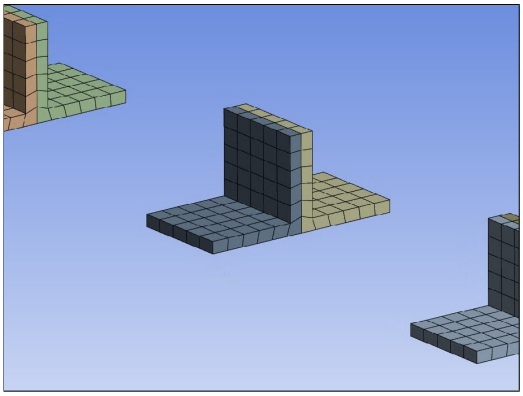

Figure 3.21: Upper supports meshing

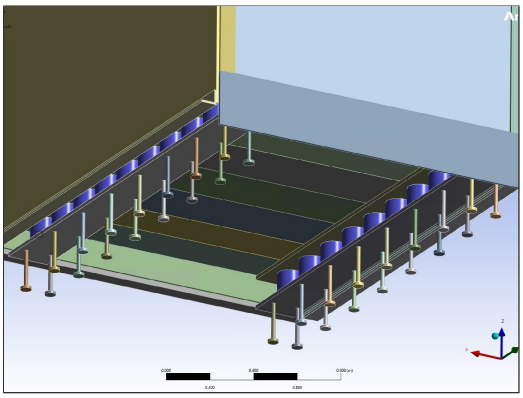

Figure 3.22: Cylinder supports bodies

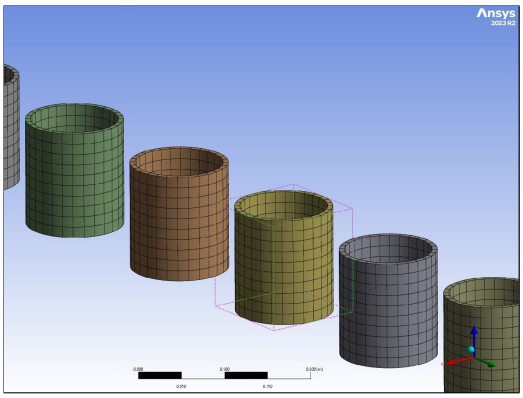

Figure 3.23: Cylinder supports meshing

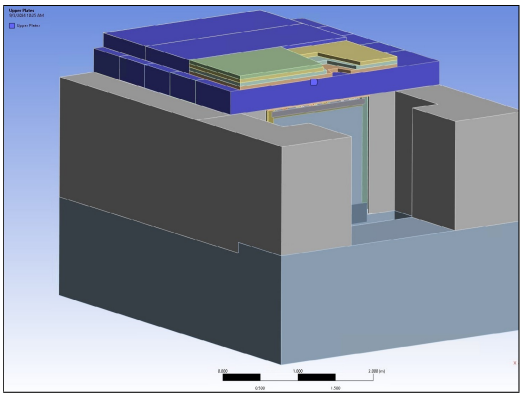

Figure 3.24: Upper plates bodies

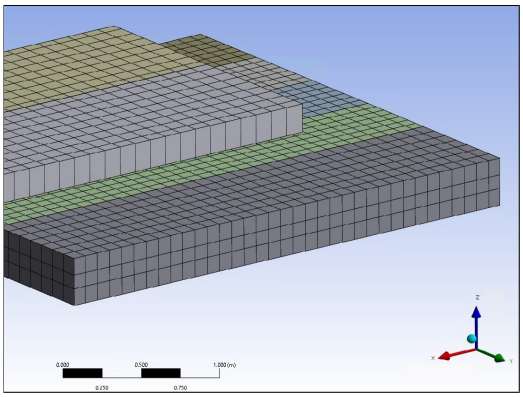

Figure 3.25: Upper bodies meshing

3.4.2 Mesh quality

The quality of the mesh is pretty good on all significant parameters.

Quality Criterion	Warning Limit	Error (Failure) Limit	Worst
Max Aspect Ratio	Default (5)	Default (1000)	28.327
Min Element Quality	Default (0.05)	Default (5e-04)	0.038
Min Jacobian Ratio (Corner Nodes)	Default (0.05)	Default (0.025)	0.123
Min Jacobian Ratio (Gauss Points)	Default (0.05)	Default (0.025)	0.255
Max Element Edge Length	Default (3.716 m)	Default (7.432 m)	0.316 m
Max Corner Angle	Default (150 °)	Default (170 °)	166.64 °
Min Element Edge Length	Default (0.037 m)	Default (3.7e-03 m)	1.1e-03 m
Max Skewness	Default (0.9)	Default (0.999)	0.991
Min Tet Collapse	Default (0.1)	Default (1e-03)	0.146
Max Warping Angle	Default (20 °)	Default (30 °)	NA

Figure 3.26: Mesh quality parameters

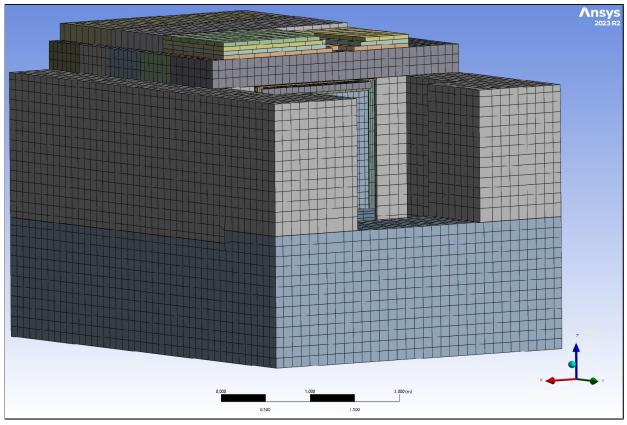

Figure 3.27: Mesh of all bodies

3.5 Fluid Meshing

3.5.1 Process

The fluid meshing is not as easy as that of the solid component. Before doing any simulation, it is difficult to estimate if the flow will be turbulent or laminar. Since a laminar model is not able to simulate a turbulent flow but a laminar flow can be approximated by a turbulent model, to stay safe the decision is to use a turbulent model (more about this in Section 3.8) like the SST k-ω viscous turbulent model. Then, the mesh should be refined on the walls according to the requirements of the SST k-ω model, explained below.

Estimation of the boundary layer thickness

A first guess can be made using the formula[2]:

$$\delta = \frac{0.383}{Re_x^{1/5}} x$$

where x is the coordinate parallel to the flow of air and Re_x is the Reynolds number defined as

$$Re_x = \frac{\rho \cdot u_\infty \cdot x}{\mu}$$

where u_∞ is the free-stream velocity, ρ is the air density, μ is the air dynamic viscosity. The boundary layer thickness depends on the axial coordinate x because its thickness increases when the flow develops. Let's consider the case of the lateral regions of the Heat Removal System. The thickness here is about 5 cm and the lenght of the path (that is the height of the steel plates) is about 1.5 m. One can use the WolframAlpha Boundary Layer tool[3] to see that

[2]Boundary Layer Thickness
[3]Wolphram Alpha Boundary Layer Tool

there is a point in the lateral airflow path where the boundary layers on the inner and outer surfaces merge.

Figure 3.28: Boundary layer along the airflow path[4]

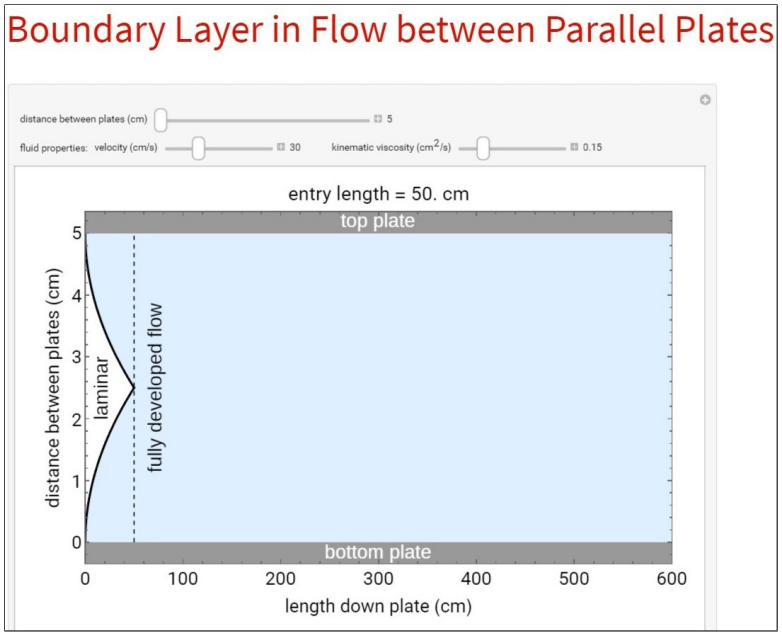

So the value for the thickness of the boundary layer should be taken as half of the distance between the lateral internal surface and the lateral external surface: **25** mm.

Estimation of y^+

To deal with the boundary layer, the approach chosen is to use a refinement of the meshing without the use of wall functions. This means that $y^+ < 5$, that is the adymensionalized distance of the centroid of the first layer of cells near the boundary from the boundary has to be everywhere less than five (better if $y^+ \approx 1$). The definition of this adymensionalized coordinate is the following:

$$y^+ = \frac{u_\tau \cdot y}{\nu}$$

where u_τ is the shear velocity of the cell adjacent to the wall, that has to be calculated by the simulation and which exact value is not avaliable beforehand but can be estimated with empirical correlations, y is the distance of the centroid of the cell adjacent to the wall (known by the meshing) and ν is the cynematic viscosity of the fluid (also known).

The shear or friction velocity can be estimated using the definition:

$$u_\tau = \sqrt{\frac{\tau_w}{\rho}}$$

where τ_w is the shear stress, also not available before the simulation, but that can be estimated with the formula:

$$\tau_w = C_f \cdot \frac{1}{2}\rho u_\infty^2$$

where C_f is the skin friction factor that can be estimated for example using the Schlitchting correlation as:

$$C_f = [2\log_{10} Re_\delta - 0.65]^{-2.3}$$

where the Re_δ is a Reynolds number that can be calculated as:

$$Re_\delta = \frac{\rho \cdot u_\infty \cdot \delta}{\mu}$$

where δ is the boundary layer thickness.

Assigning $\delta = 25\text{mm}$, u_∞ as the inlet velocity (for instance 0.3 $\frac{\text{m}}{\text{s}}$), $\mu = 18\text{e}{-6}\text{Pa}\,\text{s}$ and $\rho = 1.225\frac{\text{kg}}{\text{m}^3}$, the values are:

$$Re_\delta = 510, C_f = 0.02757, \tau_w = 0.001520\frac{\text{m}}{\text{s}}, u_\tau = 0.03522\frac{\text{m}}{\text{s}}, y = 0.0004\text{m}$$

where y is the centroid of the first layer of cell that is calculated inverting the definition of y^+ and setting $y^+ = 1$

$$y = \frac{y^+ \cdot \nu}{u_\tau}$$

For simulations with low velocities, that is for the mesh used with the normal heat distribution, the thickness of the first layer of the mesh is taken as **1** mm. It will be shown after running the simulations that for flows under 1000 CFM the y^+ results are everywhere approximately less than 5 satisfying the required working conditions of the turbulent SST k-ω model with the near-wall low Reynolds approach.[5]

Instead, for higher flows, the same calculations are repeated. Assigning $\delta = 25\text{mm}$, u_∞ as the inlet velocity (for instance 10 $\frac{\text{m}}{\text{s}}$), $\mu = 18\text{e}{-6}\text{Pa}\,\text{s}$ and $\rho = 1.225\frac{\text{kg}}{\text{m}^3}$, the values are:

$$Re_\delta = 17000, C_f = 0.008845, \tau_w = 0.5418\frac{\text{m}}{\text{s}}, u_\tau = 0.665\frac{\text{m}}{\text{s}}, y = 0.0002\text{m}$$

where y is the centroid of the first layer of cell that is calculated inverting the definition of y^+ and setting $y^+ = 1$

For simulations with high velocities, that is with the accident heat distribution, the thickness of the first layer of the mesh is thus taken as **0.4** mm.

Meshing on ANSYS Fluent

The software used to create the mesh is ANSYS Fluent with the Watertight Workflow settings, that is very efficient in creating prism layer meshes for complex geometries as the one of the Proton Beam Dump. Note that the number of layers in the boundary layer should be around 11 to get the previously calculated boundary layer thickness but due to convergence problems it is taken lower (this is something that could be addressed in the future). The boundary layer settings for the mesh with the normal heat distribution are:

[5] CFD Wiki y plus wall distance estimation

- Number of layers: 6
- Growth rate: 1.3
- First layer thickness: 1 mm

The total number of cells for this mesh is approximately 1400000.
The boundary layer settings for the mesh with the accident heat distribution are:

- Number of layers: 10
- Growth rate: 1.3
- First layer thickness: 0.4 mm

The total number of cells for this mesh is approximately 1600000.

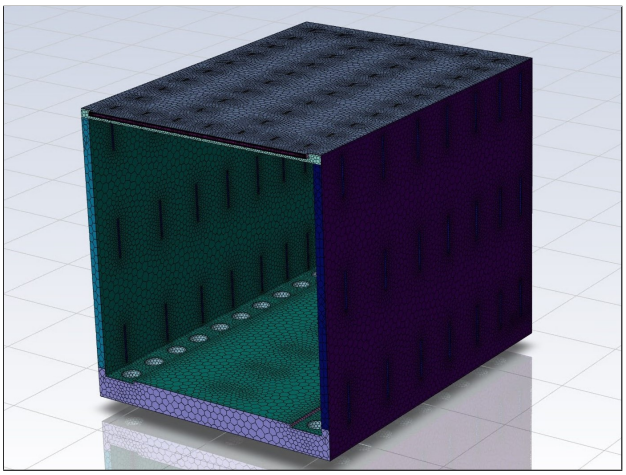

Figure 3.29: Meshing

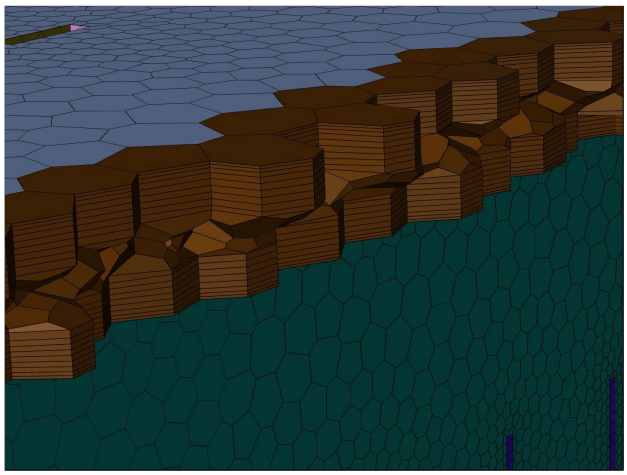

Figure 3.30: Section

3.5.2 Mesh quality

The mesh quality is pretty good for the whole body.

Figure 3.31: Fluid quality mesh

Quality Criterion	Warning Limit	Error (Failure) Limit	Worst
Max Aspect Ratio	Default (5)	Default (1000)	10.318
Min Element Quality	Default (0.05)	Default (5e-04)	0.215
Min Orthogonal Quality	Default (0.05)	Default (5e-03)	0.151
Max Skewness	Default (0.9)	Default (0.999)	0.849

3.6 Solid Boundary conditions

3.6.1 Initial temperature and external surfaces

Since the lower concrete block is in contact with the ground, the boundary condition of the lower surface is Imposed Temperature of 15 °C. Note that, in ANSYS Thermal SS, the default boundary condition for every surface where nothing is specified is imposed zero heat flux. This is the chosen as a conservative assumption for the external not-coupled surfaces of the solid.

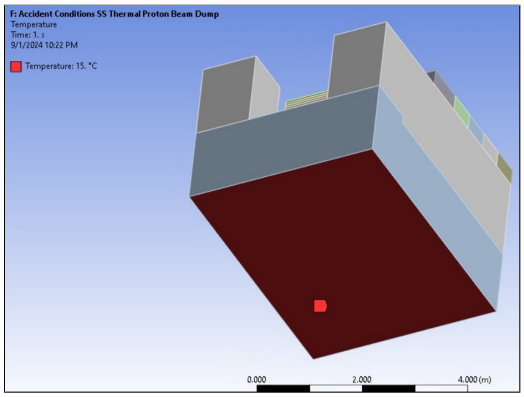

Figure 3.32: Upper external surface

3.6.2 System coupling surfaces

Below all the pictures of the coupling surfaces of the solid model and a table to remember the acronyms that the surfaces were given in the ANSYS Thermal and Fluent simulations.

Surface	Acronym
Left Internal Surface	LIS
Left External Surface	LES
Lower Internal Surface	OIS
Lower External Surface	OES
Right Internal Surface	RIS
Right External Surface	RES
Upper Internal Surface	UIS
Upper External Surface	UES
Cylinders Supports Surfaces	CSS
Right Supports Surfaces	RSS
Left Supports Surfaces	LSS
Upper Supports Surfaces	USS
Front Lower Plate	FOP
Rear Lower Plate	ROP
Rear Left Plate	RLP
Rear Right Plate	RRP
Front Left Plate	FLP
Front Right Plate	FRP
Front Upper Plate	FUP
Rear Upper Plate	RUP

Table 3.1: Surfaces and their acronyms

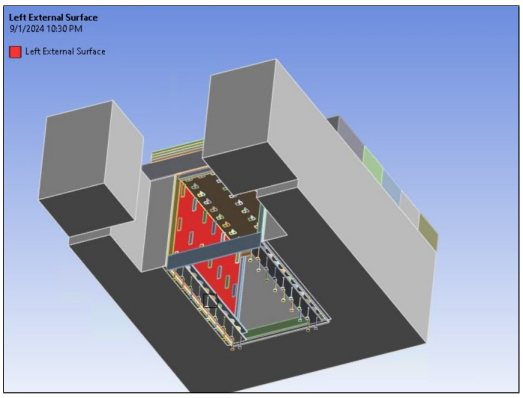

Figure 3.33: Left external surface

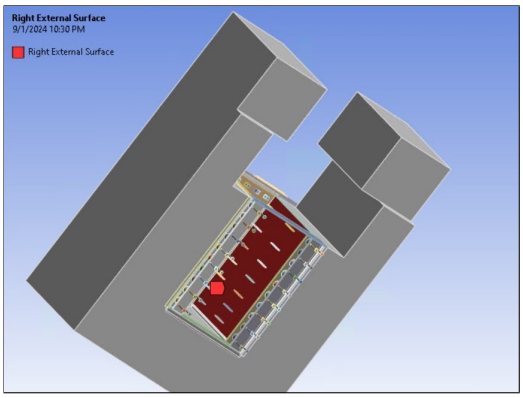

Figure 3.34: Right external surface

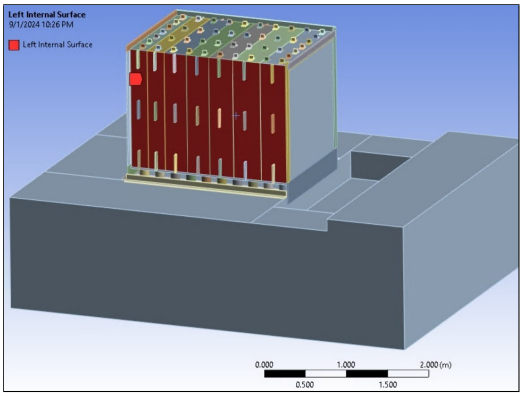

Figure 3.35: Left internal surface

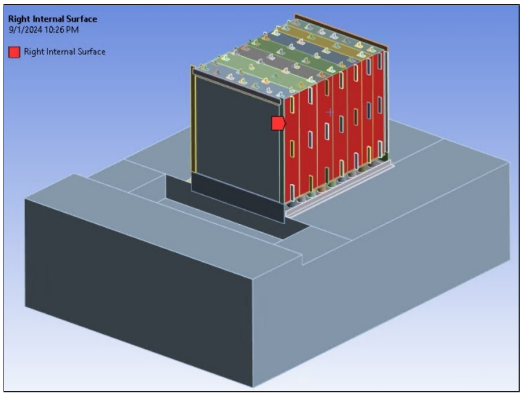

Figure 3.36: Right internal surface

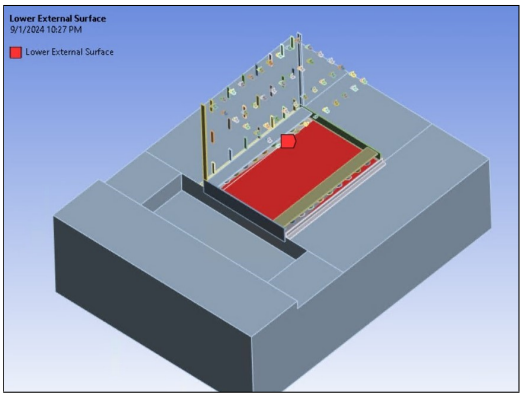

Figure 3.37: Lower external surface

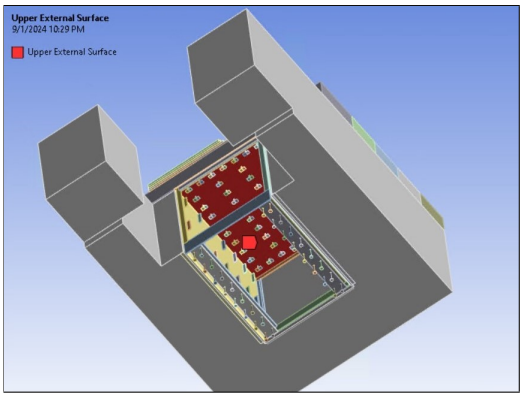

Figure 3.38: Upper external surface

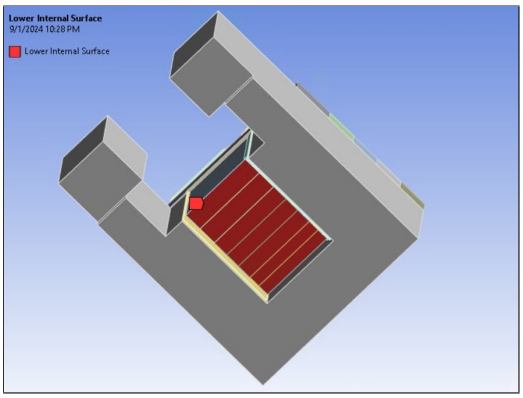

Figure 3.39: Lower internal surface

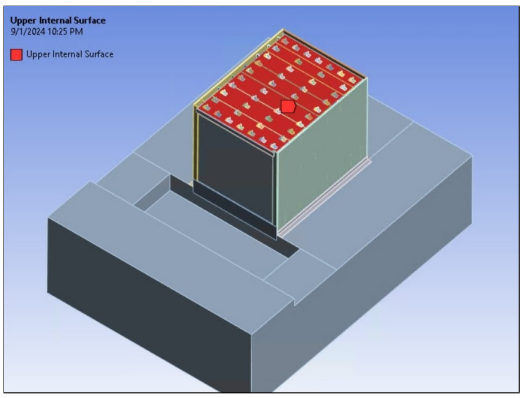

Figure 3.40: Upper internal surface

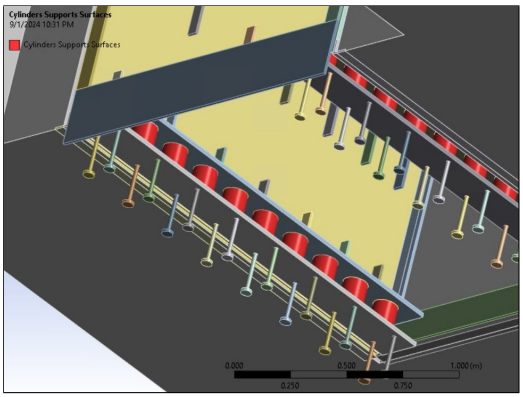

Figure 3.41: Cylindrical supports surfaces

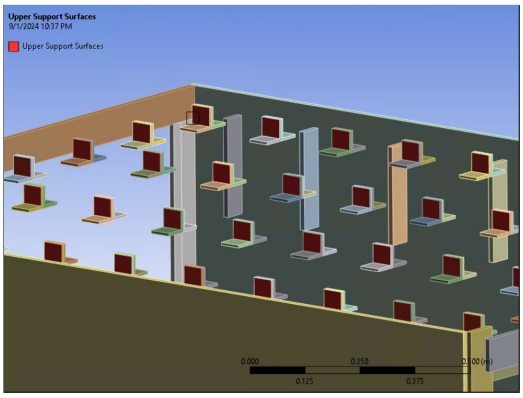

Figure 3.42: Upper supports surfaces

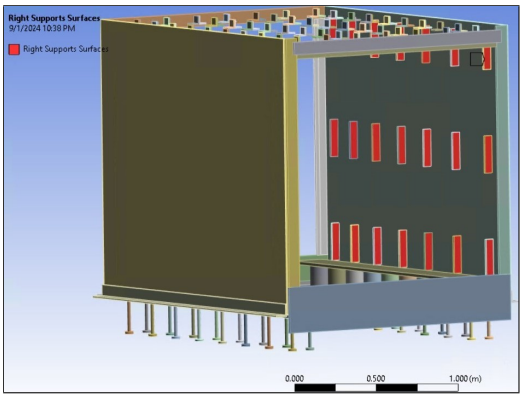

Figure 3.43: Right supports surfaces

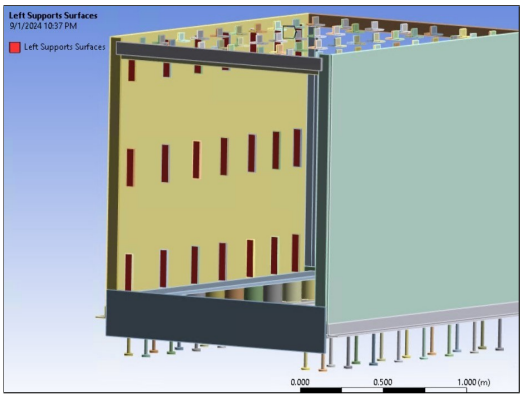

Figure 3.44: Left supports surfaces

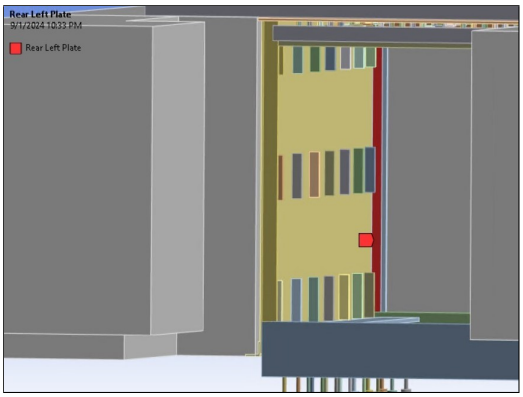

Figure 3.45: Rear left plate

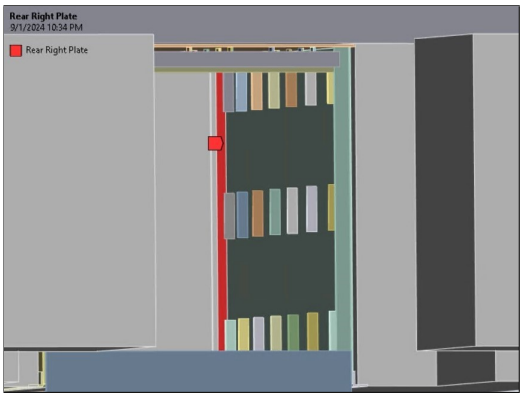

Figure 3.46: Rear right plate

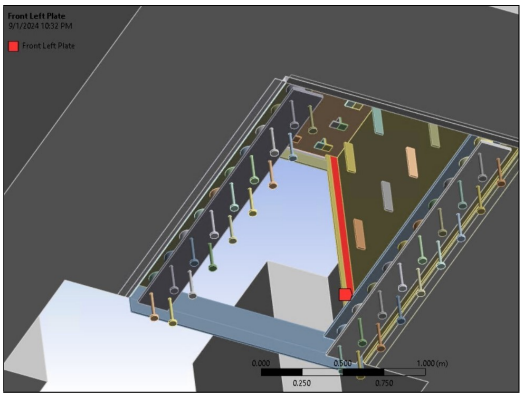

Figure 3.47: Front left plate

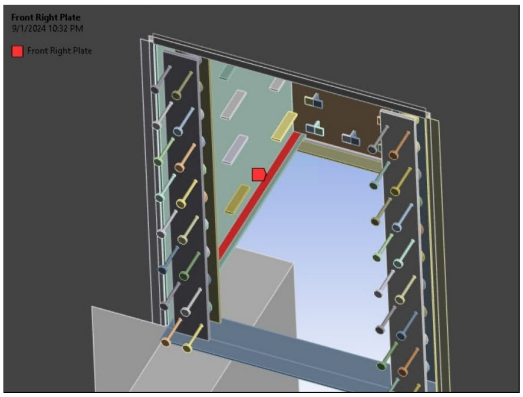

Figure 3.48: Front right plate

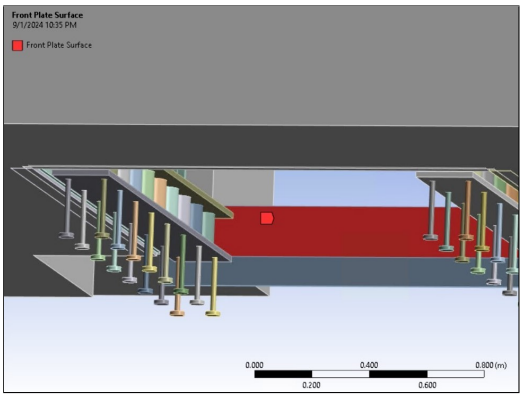

Figure 3.49: Front Lower Plate

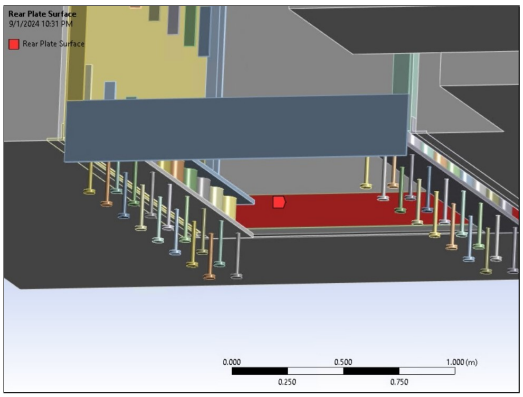

Figure 3.50: Rear Lower Plate

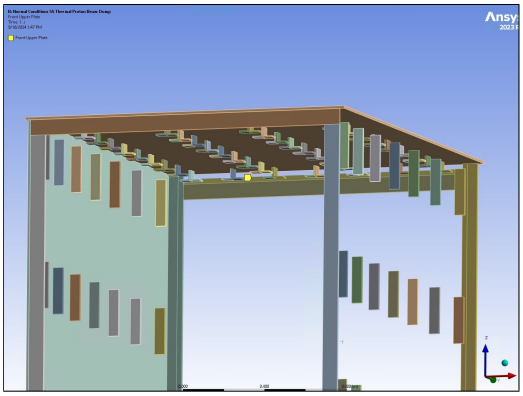

Figure 3.51: Front Upper Plate

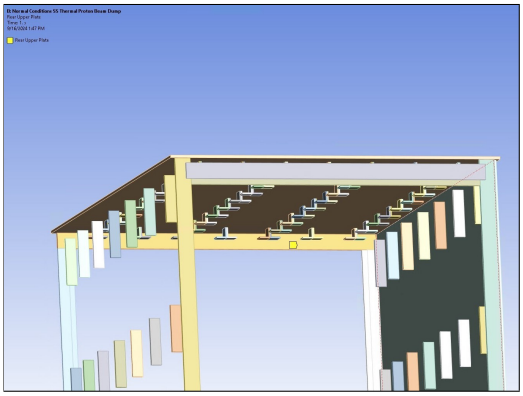

Figure 3.52: Rear Upper Plate

3.6.3 Radiation

Radiative effects are not considered due to the low temperatures reached by the simulations. An estimate of the radiative heat transfer coefficient is provided below, in the case of parallel surfaces that share the same area value.

$$HTC_{rad} = \frac{4\sigma \bar{T}^3}{\frac{1}{\epsilon_1} + \frac{1}{\epsilon_2} - 1}$$

where σ is the Stefan-Boltzmann constant, $\bar{T}$ is the arithmetic average temperature between the surfaces, ϵ_1 is the emissivity of the first material, ϵ_2 is the emissivity of the second material.

For the steel plate - steel baffle case, some guess data can be:

$$\sigma = 5.67 \cdot 10^{-8} \frac{\mathrm{W}}{\mathrm{m^2K^4}}, \bar{T} = 473\,\mathrm{K}, \epsilon_1 = \epsilon_2 = 0.08, HTC_{rad} = 1 \frac{\mathrm{mW}}{\mathrm{m^2K}}$$

For the steel baffle - concrete case, some guess data can be:

$$\sigma = 5.67 \cdot 10^{-8} \frac{\mathrm{W}}{\mathrm{m^2K^4}}, \bar{T} = 473\,^{\circ}\mathrm{C}, \epsilon_1 = 0.08, \epsilon_2 = 0.94, HTC_{rad} = 1.9 \frac{\mathrm{mW}}{\mathrm{m^2K}}$$

However, for a future simulation they should be considered activated for completeness, since their value are significative with respect to the heat transfer coefficients for static air evaluated in the paragraph below.

3.6.4 Heat conduction - static air

In some regions between the baffle and the concrete, air is not flowing and it is pretty much static. The boundary condition in this case is imposed with the Contact Tool using a thermal conductance value that is calculated as the thermal conductivity of air over the thickness of the region (being two adjacent plates). The value of the thermal conductivity of air is 25 $\frac{\text{mW}}{\text{m}\cdot\text{K}}$.[6]

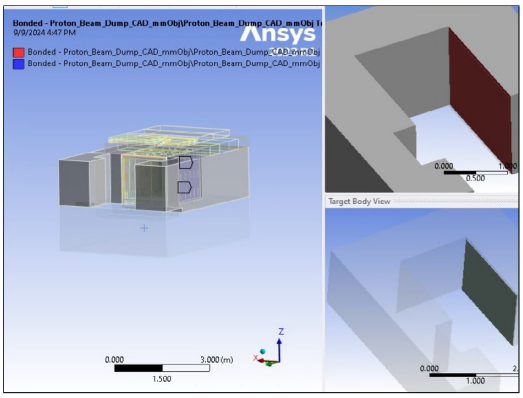

Figure 3.53: Right surface. Thickness: 25.4 mm, thermal conductance: 1 $\frac{\text{mW}}{\text{m}^2\text{K}}$

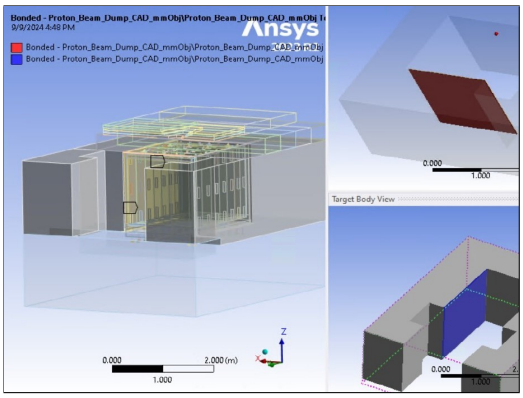

Figure 3.54: Left surface. Thickness: 25.4 mm, thermal conductance: 1 $\frac{\text{mW}}{\text{m}^2\text{K}}$

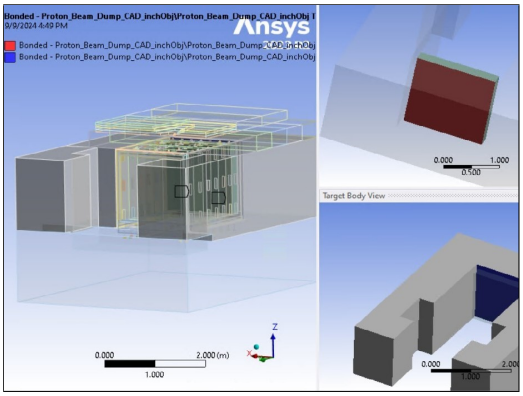

Figure 3.55: Rear surface. Thickness: 82.6 mm, thermal conductance: 0.3 $\frac{\text{mW}}{\text{m}^2\text{K}}$

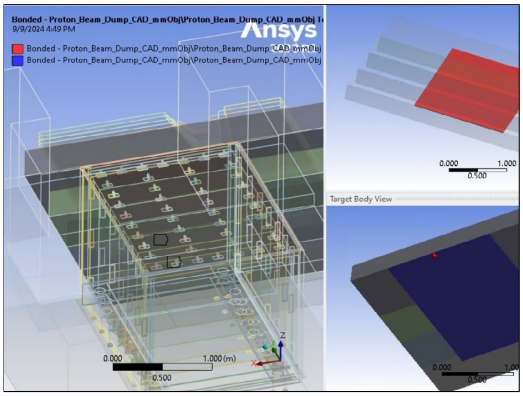

Figure 3.56: Rear surface. Thickness: 3.2 mm, thermal conductance: 7.8 $\frac{\text{mW}}{\text{m}^2\text{K}}$

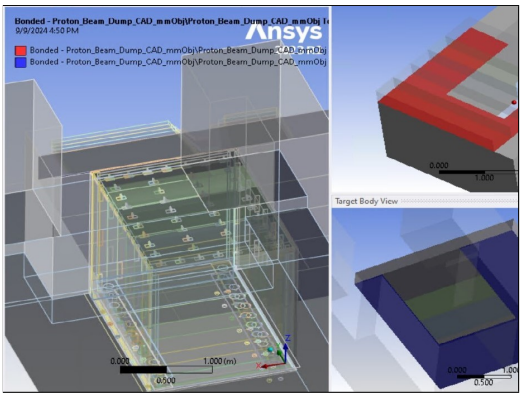

Figure 3.57: Rear surface. Thickness: 3.2 mm, thermal conductance: 7.8 $\frac{\text{mW}}{\text{m}^2\cdot\text{K}}$

[6]Realistic value assumed constant and interpolated from K. Stephan, A. Laesecke; The Thermal Conductivity of Fluid Air. J. Phys. Chem. Ref. Data 1 January 1985; 14 (1): 227–234. https://doi.org/10.1063/1.555749

Different approaches could have been used to simulate the static air. One option is to use ANSYS Fluent and create some air volumes between the baffle and the concrete with zero velocity. The problem with this approach is that the computing time would be a lot higher and the result not necessarily better because of the necessity of a fine and well-designed mesh. Using the thermal conductance, one can be sure that the computing time is reduced and the result is still accurate.

3.6.5 Heat generation

The heat generation rate is imported in ANSYS Thermal SS from a CSV file generated by a MARS Monte Carlo simulation using the block External Data. The data is available as point sources that map onto the total volume of the steel plates as seen in the picture below. The total power in case of normal operation is 1327 W, the total power in case of accident conditions is 6702 W. Note that only the normal distribution power is available at the moment, so the accident distribution is taken as the normal heat distribution scaled with a factor such that the total power is the one of the accident distribution, as you can see in the pictures below. Of course, having a more energetic proton distribution means that the power peak will be more penetrating. It was estimated that the shift is approximately 2.5 cm and since the distance between the source nodes is 7.5 cm this means that the spatial distribution can be kept as is and the scaling is sufficient.

Table of File - D:\Venturini\OneDrive\PBD Heat Removal System\PBD Heat Removal System_files\user_files\heat_distribution

	A	B	C	D	E
1	Column	Data Type	Data Unit	Data Identifier	Combined Identifier
2	A	X Coordinate	mm		Heat Distribution
3	B	Y Coordinate	mm		Heat Distribution
4	C	Z Coordinate	mm		Heat Distribution
5	D	Heat Generation	W m^-3	HeatGeneration1	Heat Distribution:HeatGeneration1

Preview of File - D:\Venturini\OneDrive\PBD Heat Removal System\PBD Heat Removal System_files\user_files\heat_distributi

	A	B	C	D
1	X Coordinate	Y Coordinate	Z Coordinate	Heat Generation
2	-712.5	-712.5	-1900	1.27E+00
3	-637.5	-712.5	-1900	1.20E+00
4	-562.5	-712.5	-1900	1.24E+00
5	-487.5	-712.5	-1900	1.85E+00
6	-412.5	-712.5	-1900	2.05E+00
7	-337.5	-712.5	-1900	2.13E+00
8	-262.5	-712.5	-1900	2.90E+00
9	-187.5	-712.5	-1900	2.94E+00
10	-112.5	-712.5	-1900	3.49E+00
11	-37.5	-712.5	-1900	4.31E+00

Figure 3.58: Preview of the normal heat distribution

Table of File - D:\Venturini\OneDrive\PBD Heat Removal System\PBD Heat Removal System_files\user_files\heat_distribution

	A	B	C	D	E
1	Column	Data Type	Data Unit	Data Identifier	Combined Identifier
2	A	X Coordinate	mm		Heat Distribution
3	B	Y Coordinate	mm		Heat Distribution
4	C	Z Coordinate	mm		Heat Distribution
5	D	Heat Generation	W m^-3	HeatGeneration1	Heat Distribution:HeatGeneration1

Preview of File - D:\Venturini\OneDrive\PBD Heat Removal System\PBD Heat Removal System_files\user_files\heat_distributi

	A	B	C	D
1	X Coordinate	Y Coordinate	Z Coordinate	Heat Generation
2	-712.5	-712.5	-1925	6.42E+00
3	-637.5	-712.5	-1925	6.08E+00
4	-562.5	-712.5	-1925	6.25E+00
5	-487.5	-712.5	-1925	9.35E+00
6	-412.5	-712.5	-1925	1.03E+01
7	-337.5	-712.5	-1925	1.07E+01
8	-262.5	-712.5	-1925	1.46E+01
9	-187.5	-712.5	-1925	1.48E+01
10	-112.5	-712.5	-1925	1.76E+01
11	-37.5	-712.5	-1925	2.18E+01

Figure 3.59: Preview of the accident heat distribution

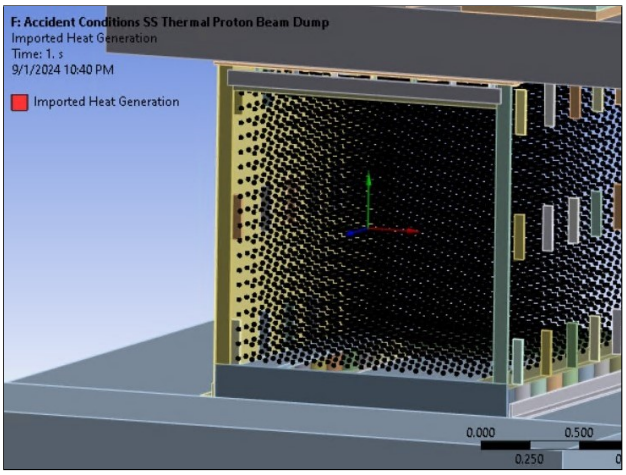

Figure 3.60: Source nodes from MARS

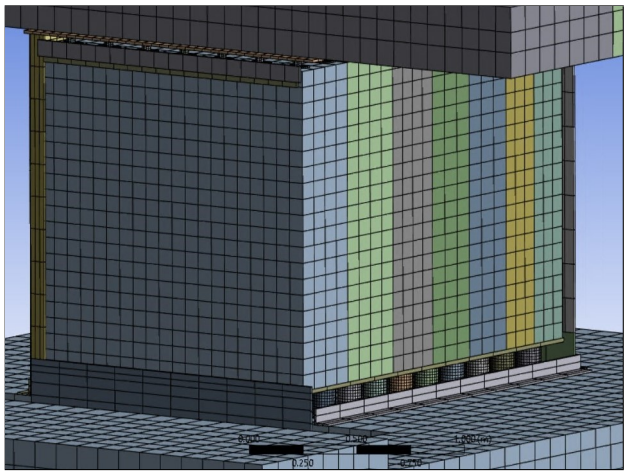

Figure 3.61: Target elements on ANSYS

3.7 Fluid Boundary conditions

3.7.1 Inlet velocity

The boundary condition for the inlet is the imposed volumetric flow. There are 12 inlets, each one with a diameter of 57 mm The velocity input is given by the following formula:

$$v[\frac{\mathrm{m}}{\mathrm{s}}] = \frac{F[CFM] \cdot 0.00047194745 \left[\frac{m^3/s}{CFM}\right]}{12 \cdot (0.057[\mathrm{m}])^2 \cdot \pi}$$

where F is the flow in CFM (cubic feet per minute), the other factor at the numerator is the conversion coefficient between CFM and $\frac{\mathrm{m}^3}{\mathrm{s}}$, and the numerator is the total input area calculated from the data above.

[CFM] value	[m/s] value
165	0.64
250	0.96
400	1.54
600	2.31
800	3.08

Table 3.2: Quick conversion table between CFM and m/s values

3.7.2 Outlet

At the outlet it is imposed the classic boundary condition of zero gauge pressure. This is not quite accurate since the pressure is zero not exactly in correspondance of the outlet but far away. In the simulations a frequent error due to this not accurate boundary condition is the presence of reverse flow and this occurs also in the simulations of this report. This is not a big problem and it can be a realistic situation: to solve this issue, it should be added a (cubic) volume connected to the previous system outlet and impose far-field boundary conditions as

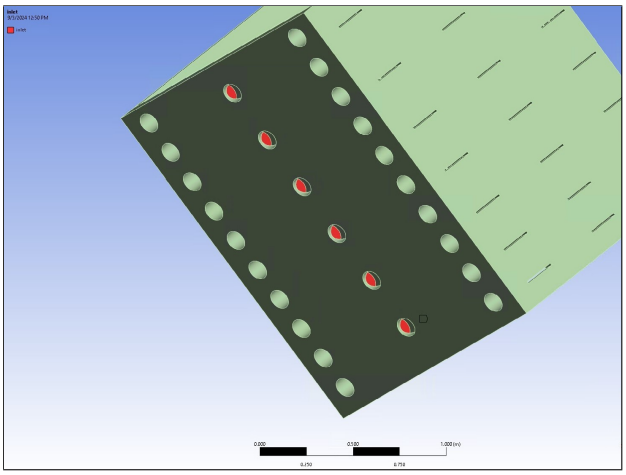

Figure 3.62: Visual of six of the twelve inlet surfaces on the bottom of the fluid volume

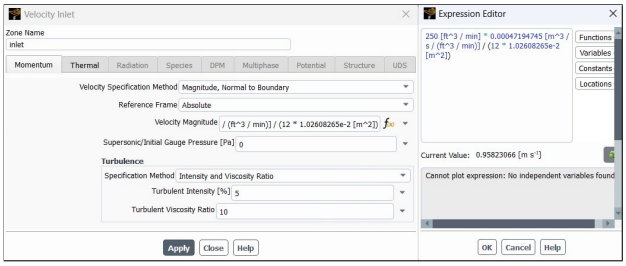

Figure 3.63: Inlet boundary conditions settings as a function

zero gauge pressure on the faces of the added volume (so quite far away from the real outlet of the system).

3.7.3 System coupling surfaces

Below the pictures of all the twenty coupled surfaces of the fluid model.

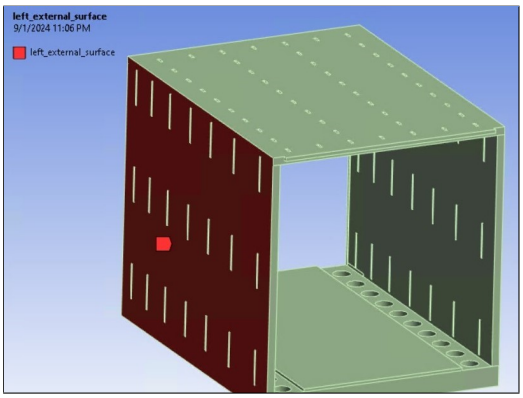

Figure 3.64: Left external surface

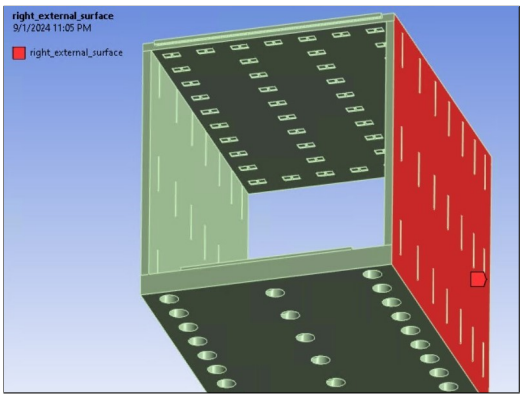

Figure 3.65: Right external surface

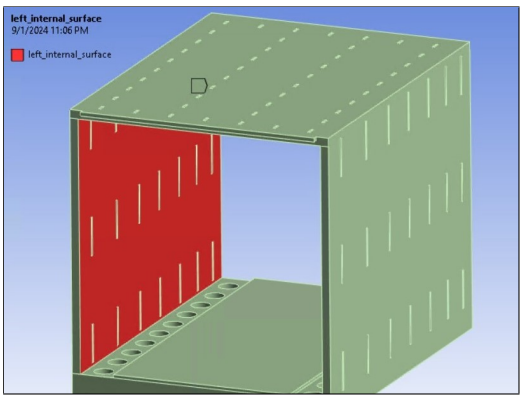

Figure 3.66: Left internal surface

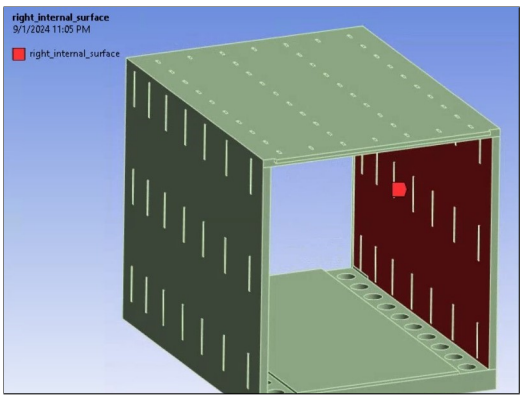

Figure 3.67: Right internal surface

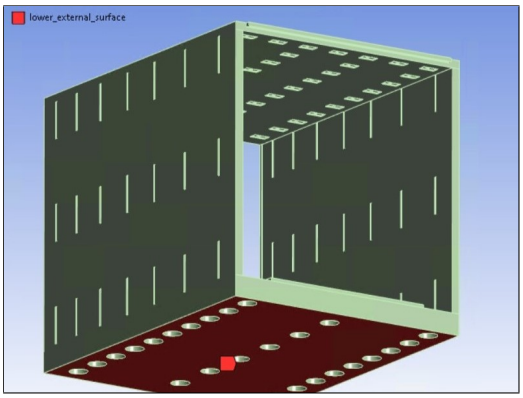

Figure 3.68: Lower external surface

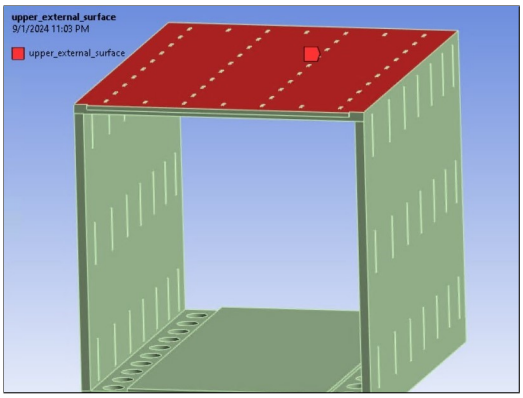

Figure 3.69: Upper external surface

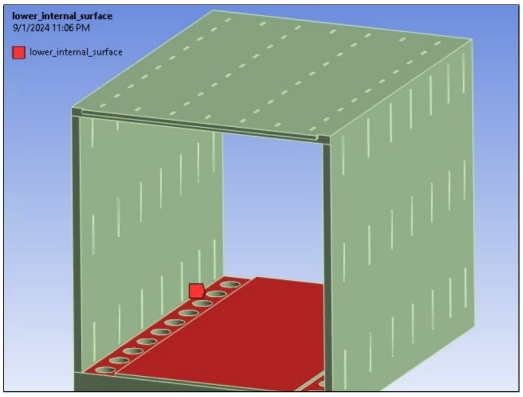

Figure 3.70: Lower internal surface

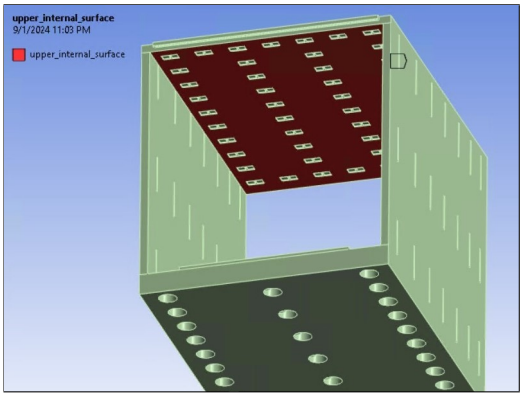

Figure 3.71: Upper internal surface

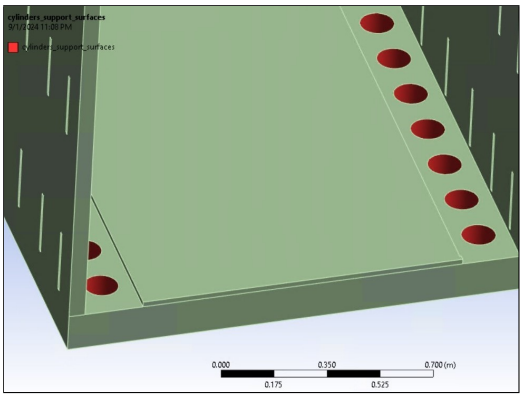

Figure 3.72: Cylinders supports surfaces

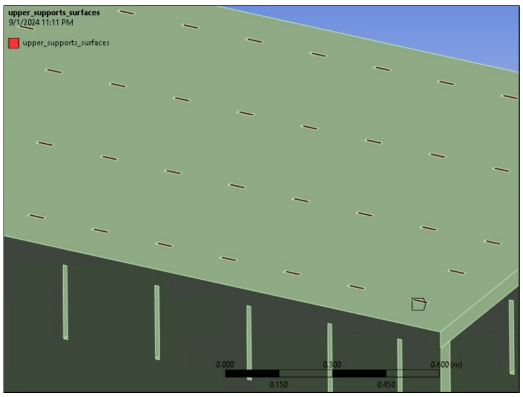

Figure 3.73: Upper supports surfaces

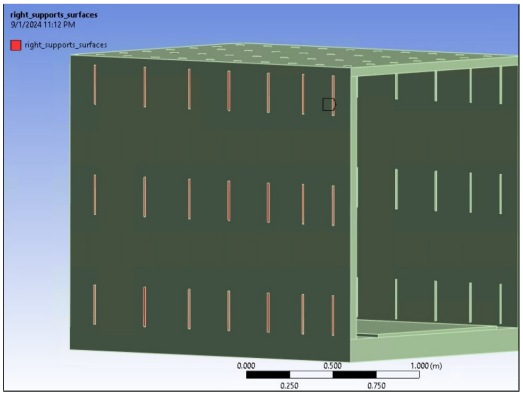

Figure 3.74: Right supports surfaces

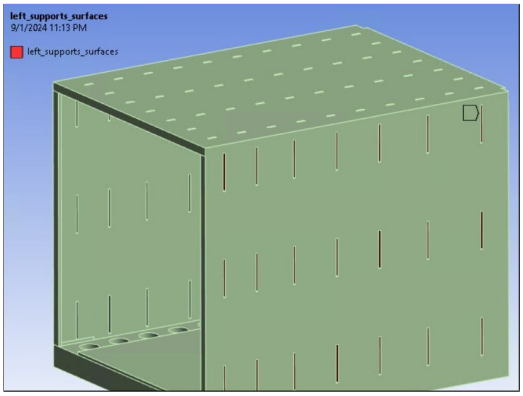

Figure 3.75: Left supports surfaces

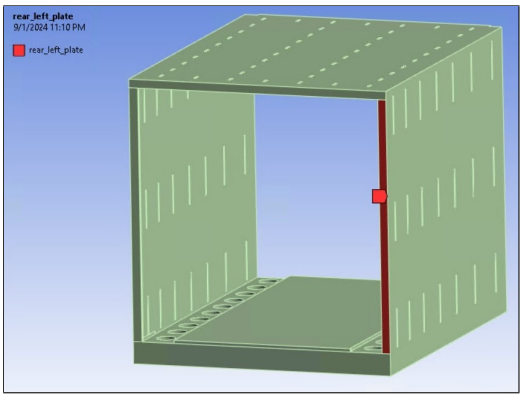

Figure 3.76: Rear left plate

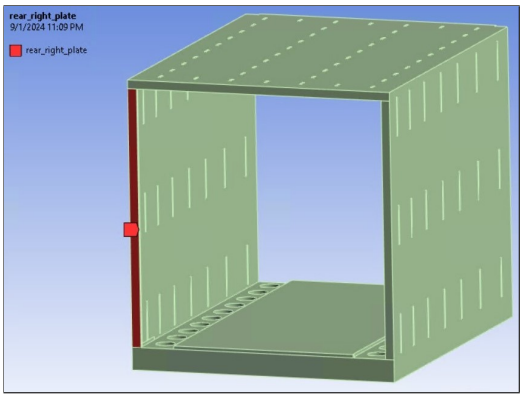

Figure 3.77: Rear right plate

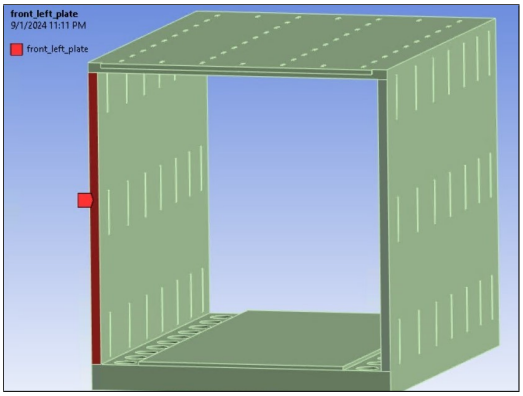

Figure 3.78: Front left plate

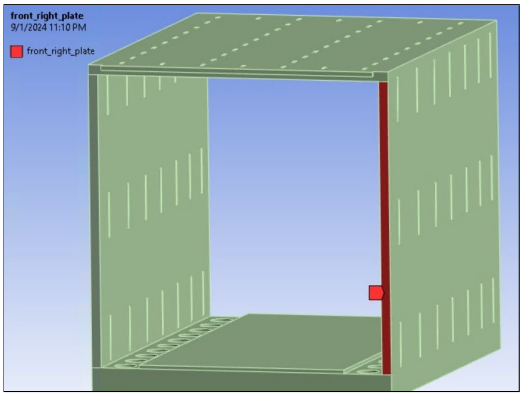

Figure 3.79: Front right plate

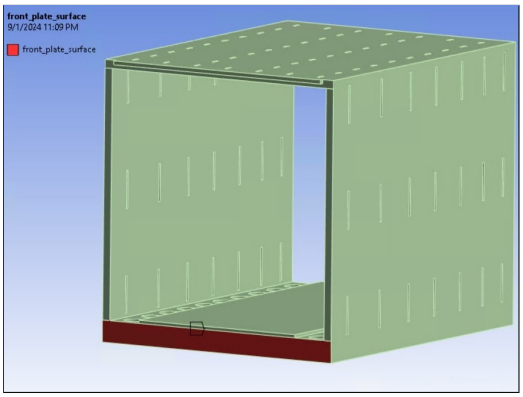

Figure 3.80: Front lower plate

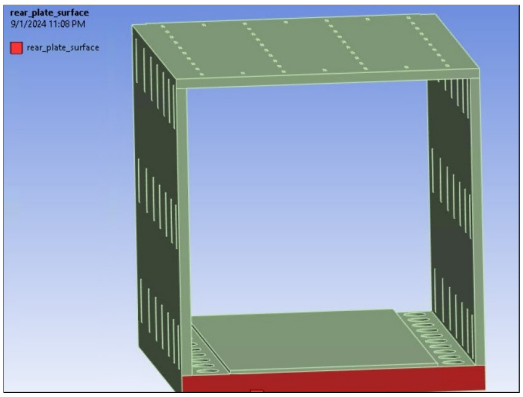

Figure 3.81: Rear lower plate

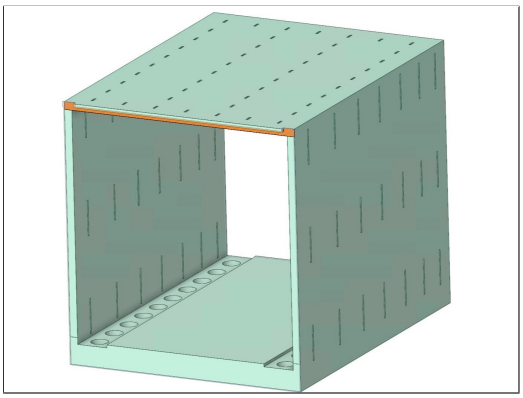
Figure 3.82: Front upper plate

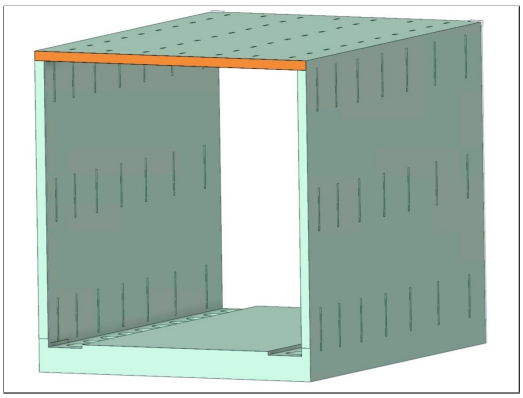
Figure 3.83: Rear lower plate

3.7.4 Compressibility

The fluid is assumed incompressible since the Mach number is always well below 0.3. The pressure-based solver is used in ANSYS Fluent, as the best solver for incompressible flows.

3.7.5 Gravity

Gravity is considered, with the standard value of 9.81 $\frac{\text{m}}{\text{s}}$

3.7.6 Radiation

Radiative effects are not considered due to the low temperatures of air and the solid.

3.8 Fluid model - laminar or turbulent?

One of the big questions of the fluid simulation was about the viscous model to use for the air. By default, ANSYS suggests that the SST k-ω can be used, but this has to be checked. The velocities of the simulations are low, and the Reynolds number not very high. Let's address the most problematic case, that is the one with volumetric flow of 165 CFM, that is the one with the lowest velocity and the airflow behaviour closest to laminar.

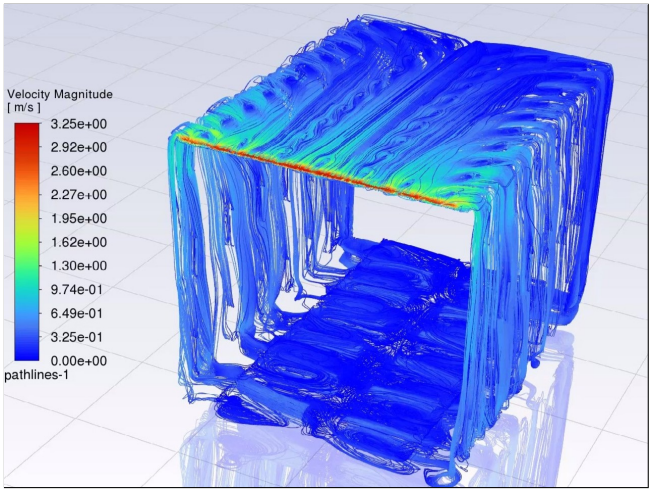

Figure 3.84: Velocities for 165 CFM airflow using the SST k-ω model

Inlet velocity	0.64 $\frac{\text{m}}{\text{s}}$
Outlet velocity	2.26 $\frac{\text{m}}{\text{s}}$
Area-Weighted average inlet cell Reynolds number	57.5
Area-Weighted average outlet cell Reynolds number	192.6
Volume-weighted average cell Reynolds number	41.9

Table 3.3: Turbulence quantities

The quantities in the table should not deceive the reader: the Reynolds number in Fluent are defined for each cell, so they are not the same Reynolds number used to check if the flow is laminar or turbulent. As a matter of fact, with a fast calculation, one can find that at the inlet:

$$v = 0.64\frac{\text{m}}{\text{s}}, \mu = 18\text{e}{-6}\text{Pa}\,\text{s}, \rho = 1.225\frac{\text{kg}}{\text{m}^3}, D = 0.28\,\text{m} \quad \text{and so} \quad Re = 11000$$

where the hydraulic diameter is taken from the calculations of the Excel file considering the lower horizontal space. So the fluid can be considered turbulent.

3.8.1 Models available

Laminar model

It is based on mass-conservation and momentum-conservation (i.e. Navier-Stokes equations without any turbulence assumption). This model should be used only when there is no turbulence and we know the flow is perfectly laminar because it is not able to simulate any turbulent effect.[7]

Standard k-ω model

The k-omega (k-ω) turbulence model is one of the most commonly used models to capture the effect of turbulent flow conditions. It belongs to the Reynolds-averaged Navier-Stokes (RANS) family of turbulence models where all the effects of turbulence are modeled. It is a low Re model, i.e., it can be used for flows with low Reynolds number where the boundary layer is relatively thick and the viscous sublayer can be resolved. It is best used for near-wall treatment.[8]

k-ϵ model

The k-ϵ turbulence model is shown instead to be reliable for free-shear flows, such as the ones with relatively small pressure gradients. It is preferred for high-Re (high Reynolds number) applications ($y^+ > 30$) where separations and reattachments of the flows are not present. It uses empirical damping functions in the viscous sub-layer region which were essentially derived for the flat plate boundary layer flows. The standard k-ω model model doesn't require these damping functions giving a better accuracy.[9]

SST k-ω

The k-epsilon model tends to show great results in the free stream region and the k-omega model has a good accuracy in the boundary layer region close to the wall. The SST k-ω combines the advantages of these two turbulence models using a blending function.

3.8.2 Model used and why

Since the geometry is quite complex, turbulence may happen even at lower Reynolds number values. Experience tells that in this case using the default SST k-ω is a good choice. Moreover, in presence of near-laminar conditions, it is known that the solution of the SST k-ω resembles the solution obtained with laminar flow. To conclude, it can be said that by trying to use the laminar model, the continuity residuals get stuck at 0.4, even simplifying the geometry, and don't decrease even increasing the number of iterations over 2000 (see the pictures below). This can be an hint that the laminar model is not the correct one to use for this case.

[7] Simscale - Laminar flow
[8] Simscale - K-Omega Turbulence Models
[9] Simscale - K-Epsilon Turbulence Models

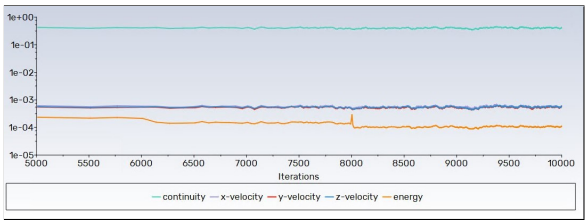

Figure 3.85: Residuals with laminar model

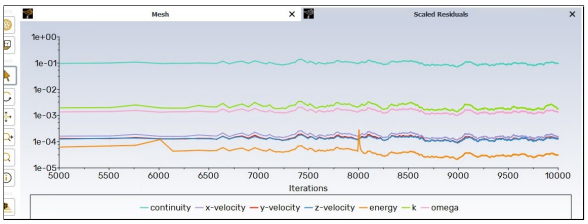

Figure 3.86: Residuals with SST k-ω model

3.8.3 Turbulence parameters

Turbulent intensity

To realistically model a given problem, it is important to define the turbulence intensity at the inlets. This parameter can be estimated as:

$$I = 0.16Re^{-1/8}$$

Here are a few examples of common estimations of the incoming turbulence intensity:

- High-turbulence (between 5% and 20%): Cases with high velocity flow inside complex geometries. Examples: heat exchangers, flow in rotating machinery like fans, engines, etc.
- Medium-turbulence (between 1% and 5%): Flow in not-so-complex geometries or low speed flows. Examples: flow in large pipes, ventilation flows, etc.
- Low-turbulence (well below 1%): Cases with fluids that stand still or highly viscous fluids, very high-quality wind tunnels. Examples: external flow across cars, submarines, aircraft, etc.

Having calculated the Reynolds value as 11000 in the previous paragraph, the value chosen for this case is the default one: **5%**.

Turbulent viscosity ratio

The turbulent viscosity ratio is directly proportional to the turbulent Reynolds number. It is large (on the order of 100 to 1000) in high-Reynolds-number boundary layers, shear layers, and fully-developed duct flows. However, at the free-stream boundaries of most external flows, is fairly small.

The value chosen for this case is the default value of **10**.

3.9 Coupled conditions

To allow a two-way convection coupling between the solid surfaces and the fluid surfaces, there is the need for three different data transfers.

- Heat transfer coefficient (Fluent) to Convection coefficient (Thermal SS)

- Near wall temperature (Fluent) to Convection reference temperature (Thermal SS)
- Temperature (Thermal SS) to Temperature (Fluent)

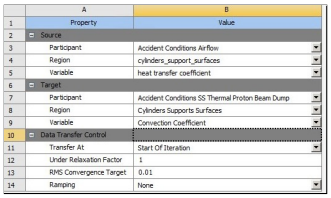

	A	B
1	Property	Value
2	Source	
3	Participant	Accident Conditions Airflow
4	Region	cylinders_support_surfaces
5	Variable	heat transfer coefficient
6	Target	
7	Participant	Accident Conditions SS Thermal Proton Beam Dump
8	Region	Cylinders Supports Surfaces
9	Variable	Convection Coefficient
10	Data Transfer Control	
11	Transfer At	Start Of Iteration
12	Under Relaxation Factor	1
13	RMS Convergence Target	0.01
14	Ramping	None

Figure 3.87: HTC transfer

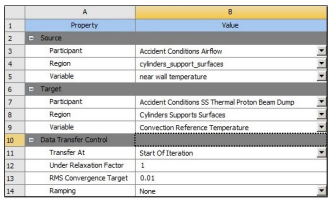

	A	B
1	Property	Value
2	Source	
3	Participant	Accident Conditions Airflow
4	Region	cylinders_support_surfaces
5	Variable	near wall temperature
6	Target	
7	Participant	Accident Conditions SS Thermal Proton Beam Dump
8	Region	Cylinders Supports Surfaces
9	Variable	Convection Reference Temperature
10	Data Transfer Control	
11	Transfer At	Start Of Iteration
12	Under Relaxation Factor	1
13	RMS Convergence Target	0.01
14	Ramping	None

Figure 3.88: Near wall temperature transfer

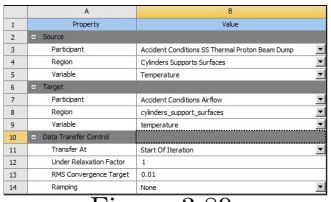

	A	B
1	Property	Value
2	Source	
3	Participant	Accident Conditions SS Thermal Proton Beam Dump
4	Region	Cylinders Supports Surfaces
5	Variable	Temperature
6	Target	
7	Participant	Accident Conditions Airflow
8	Region	cylinders_support_surfaces
9	Variable	temperature
10	Data Transfer Control	
11	Transfer At	Start Of Iteration
12	Under Relaxation Factor	1
13	RMS Convergence Target	0.01
14	Ramping	None

Figure 3.89: Temperature transfer

3.9.1 Ramping

After having tried to run the coupling tool with the default conditions, it was clear that something was not working well. The temperatures of the solid component were sent as full values from the first iterations and imposing such high temperatures to the fluid it seemed that the heat exchange was not working well. It was verified that activating the ramping option for the temperatures sent from the solid to the fluid, the results were much more realistic and compatible with global energy conservation balances that one can try by hand. The ramping option can be activated in the System Coupling block for each different data transfer. To understand how it works please consult the User Guide.

HTCs and temperatures

4.1 Heat transfer coefficients

One of the goals of the report is the double-checking of the heat transfer coefficients that were already calculated using empirical correlations in the Excel file. The main perplexities regarding these results are that the values obtained are very low: they are comparable to a case of natural circulation and not of forced circulation (as it should be, having fans that push air in).

First of all, the implementation of the correlations was checked. Some typos were corrected and all the formulas were rewritten in VBA code to be more readable. Then the HTC results were checked and found to be the correct outputs of the formulas. The fact that they are low makes sense since the airflow is very low too and the correlations do not take in consideration the geometry.

To get the final response, the results from the coupled simulations were used. ANSYS Fluent gives four different definitions of the HTC, that are described accurately below. The most sensible comparation is with the Wall adj. HTC. The results are compared below, even though the divisions of the surfaces and of the airflow paths are different between ANSYS and the Excel file, so it cannot be considered an apple-to-apple comparison.

Important note: the process to evaluate the HTC and the all temperatures on the Excel file is iterative due to the fact that air properties change slightly with temperature.

4.1.1 Derivation of the HTC from the Excel file

There are two kinds of HTC calculated from the Excel file. The first kind is the HTC derived using air properties calculated at the average bulk temperature, the second kind is the HTC derived using air properties calculated at the film temperature. To understand how these two different temperatures are calculated, please refer to section 4.2.

For every HTC, Reynolds number and Prandtl number are calculated using the same formulas:

$$Re = \frac{v \cdot D \cdot \rho}{\eta}$$
$$Pr = \frac{c_p \cdot \eta}{k}$$

where v is the velocity, D is the hydraulic diameter, ρ is the density, η is the dynamic viscosity, c_p is the specific heat and k is the thermal conductivity.

HTC calculated with properties at average bulk temperature

The HTC resulting is the minimum (i.e. conservative) value among those calculated with the following three chosen correlations.

Dittus-Boelter equation

$$HTC = \frac{Nu \cdot k}{D} \left(\frac{T_{bulk}}{T_{surf}} \right)^{0.5}$$
$$Nu = 0.023 Re^{0.8} Pr^{0.4}$$

where Nu is the Nusselt number, T_{surf} is the average surface temperature and T_{bulk} is the average bulk temperature.

Kays-Crawford equation

$$HTC = \frac{Nu \cdot k}{D} \left(\frac{T_{bulk}}{T_{surf}} \right)^{0.5}$$
$$Nu = 0.021 Re^{0.8} Pr^{0.5}$$

everything is calculated in the same way as before, but the Nusselt number has a slightly different expression.

Sieder-Tate equation

$$HTC = \frac{St \cdot c_p \cdot \dot{m}}{A} \left(\frac{T_{bulk}}{T_{surf}} \right)^{0.575}$$
$$St = 0.02 Re^{-0.2} Pr^{-0.67}$$

where $\dot{m}$ is the mass flow rate and A is the flow area.

HTC calculated with properties at film temperature

Colburn equation

$$HTC = \frac{St \cdot c_p \cdot \dot{m}}{A}$$
$$St = 0.023 Re^{-0.2} Pr^{-0.67}$$

everything is calculated as the Sieder-Tate equation except for the Stanton number where the coefficient is different. Furthermore, no temperature correction is needed since the surface temperature is equal to the film temperature.

Petukhov equation

$$HTC = \frac{Nu \cdot k}{D}$$
$$Nu = \frac{f_D \cdot Re \cdot Pr/8}{1.07 + 12.7\sqrt{f_D/8} \cdot (Pr^{0.67} - 1)}$$

In this case, the Nusselt number is calculated using the Darcy friction factor (evaluated from tables or empirical correlations). Still, no temperature correction is needed, as said before.

4.1.2 Derivation of the HTC from the ANSYS simulations

Surface HTC

The first HTC is defined as:

$$h_{eff} = \frac{q}{T_{wall} - T_{ref}}$$

where T_{ref} is the Reference Temperature of the ANSYS Fluent settings. This temperature is constant and has to be specified in the ANSYS Fluent settings by the user. This HTC should not be used if the bulk temperature changes along the flow direction, which gives it a limited usage and it is useless in a coupled simulation as the one of this report. As an example of the problems of this definition, consider this case: if the reference temperature is high, the denominator could locally become negative and one could get a negative value of the HTC: that is impossible.

Wall adjacent HTC

The second HTC is defined as:

$$h_{eff} = \frac{q}{T_w - T_{ac}}$$

where T_w is the wall face temperature and T_{ac} is the wall adjacent fluid cell temperature. This is a more accurate definition of the HTC. Note that this HTC is the one that is transferred between the simulations by the System Coupling block of ANSYS Workbench. This coefficient is not compared with the results of the Excel file because it strongly depends on the refinement of the mesh.

Wall function HTC

The third HTC, for fluid with constant density, is defined as:

$$h_{eff} = \frac{\rho \cdot c_p \cdot u^*}{T_c^*}$$

where ρ is the density, c_p is the specific heat at constant pressure, u^* is the near-wall turbulence velocity scale and T_C^* is the dimensionless law-of-the-wall temperature. This quantity

is always positive, but it is quite distant from the HTC definition one usually seeks. One advantage of this quantity is that it can be defined also without a real heat transfer.

Y+ based HTC

The fourth HTC is defined as:

$$h_{y+} = \frac{Q}{T_{wall} - T_{y+}}$$

where T_{y+} is the mean temperature at the specified $y+$. It accommodates local fluid temperature variation effects and eliminates sensitivity to near-wall mesh size. The wall adj. $y+$ value can be changed in the Reference Values settings. This heat transfer coefficient is the one compared with the results of the Excel file because it is not so dependent on the mesh, taking temperature values in the bulk of the flow. As the refernece y+ value, in the simulations the value of 25 is taken. Having seen in paragraph 4.2 that the $y+ = 1$ is equivalent to $y = 1\,\text{mm}$ this means that the temperature is calculated at $y = 25\,\text{mm}$ from the wall, approximately in the centre of the bulk region.

4.1.3 HTC decision

The HTC that will be used is the Y+ based HTC:

- It is a good and local definition
- It does not depend strongly on the refinement of the mesh
- It gives realistic values

4.2 Temperatures

Another useful comparation is between the previously available temperature results from the Excel file and the temperature results from the ANSYS coupled simulation.

4.2.1 Derivation of the temperature from the Excel file

Each flow path has a heat load assigned. For each flow path, the average air bulk temperature is calculated as:

$$T_{b,average} = T_{b,inlet} + \frac{1}{2}\frac{Q}{\dot{m} \cdot c_p}$$

where T_{inlet} is the air outlet bulk temperature of the flow path previous to the one considered, $\dot{m}$ is the air mass flow rate and Q is the thermal heat load of the considered flow path.

The outlet air bulk temperature is calculated as:

$$T_{b,outlet} = T_{b,inlet} + \frac{Q}{\dot{m} \cdot c_p}$$

The limitations of this approach are that the heat load distribution along the flow paths should be known in a very accurate way and that it assumes that all the power transferred by the proton beam is going to the air. This is not the case since the lower temperature of the concrete base is fixed and so power could possibly flow towards the ground, making it a strict conservative assumption not necessarily needed.

Average bulk temperature calculations

The surface temperature used in the first approach for the correction of the Nusselt number is calculated as:

$$T_{surface} = T_{b,average} + \frac{Q}{A \cdot HTC_b}$$

where A is the surface of the heat transfer and HTC_b is the minimum heat transfer coefficient calculated using the average bulk temperature with the respective correlations described above.

Film temperature calculations

The surface temperature used in the second approach for the calculation of the fluid properties is:

$$T_{film} = T_{b,average} + \frac{Q}{A \cdot HTC_s}$$

where A is the surface of the heat transfer and HTC_s is the minimum heat transfer coefficient calculated using the film temperature with the respective correlations described above.

4.2.2 Derivation of the temperature from the ANSYS simulation

The derivation is the result of the rules of the Finite Element Method for the solid part and of the Finite Volume Method for the fluid part, as usual.

Results

5.1 Normal conditions - 165 CFM

In this simulation, air is flowing at the fluid inlet at 165 CFM and the MARS Heat Generation distribution is that of a normal operation case (total power of 1.3 kW).

5.1.1 Solid results

Below are presented the most significant results for the solid component. Note that, for all the solid simulations, the Heat Flux has not been reported being high only locally near the fins and the upper supports (and low values everywhere else). Some annotations:

- The global maximum temperature is on the steel plates and this makes sense because of the peak of the heat generation
- The concrete maximum temperature of the concrete is near the front lower baffle plate. It is near the peak of the heat distribution and not on the top because on the bottom air has lower velocities.

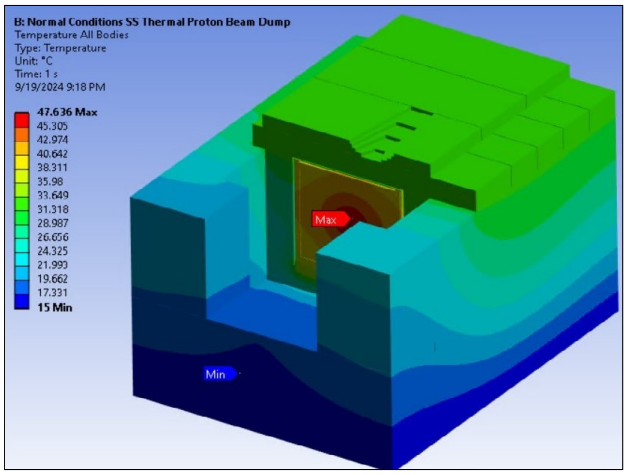

Figure 5.1: All bodies

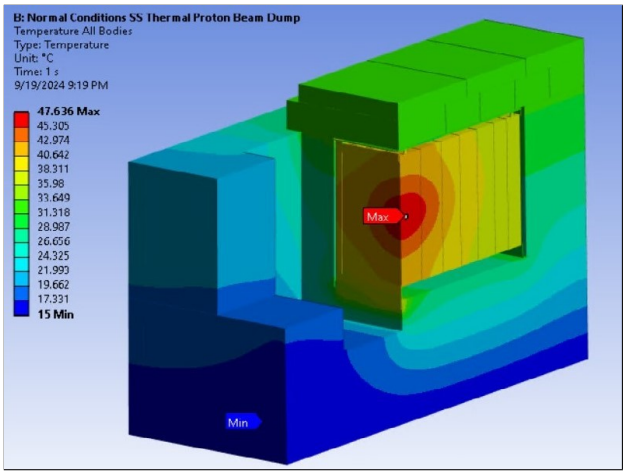

Figure 5.2: All bodies - section

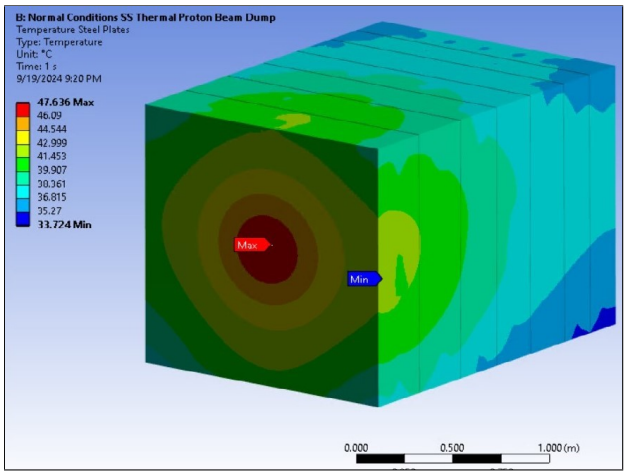

Figure 5.3: Steel plates

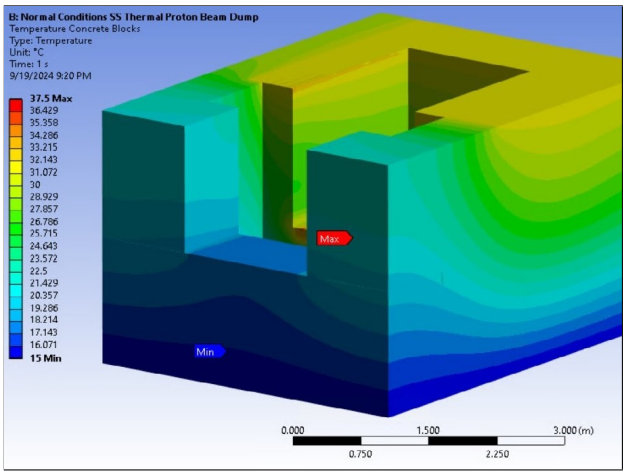

Figure 5.4: Concrete blocks

5.1.2 Fluid results

Below are presented the most significant results for the fluid component.

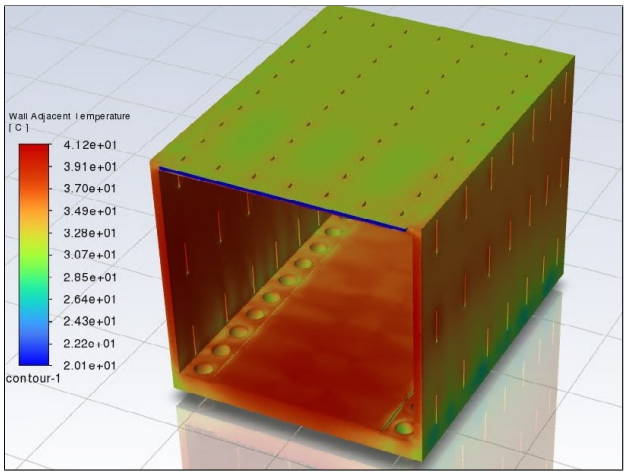

Figure 5.5: Static temperature

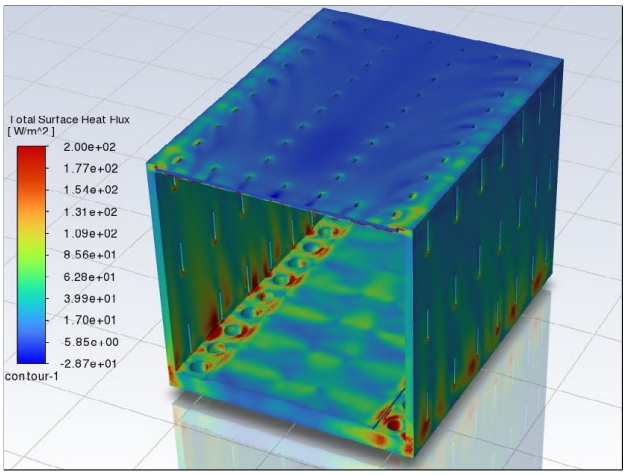

Figure 5.6: Heat flux

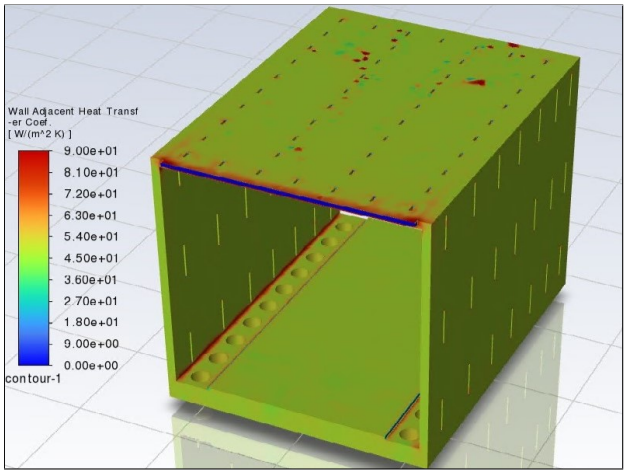

Figure 5.7: Wall adj. HTC

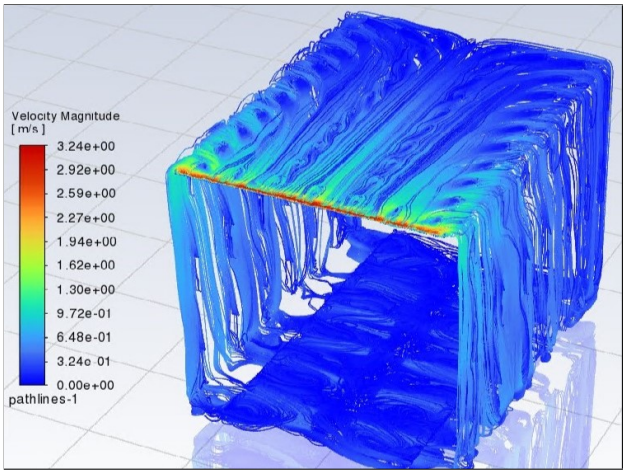

Figure 5.8: Velocity

5.1.3 HTC results

The HTCs are quite different. One reason might be that the airflow is more turbulent than supposed by the correlations used in the Excel file, so the heat removal is more efficient.

Region	Value $[W/m^2K]$
Horizontal gap under the core	1.2
Vertical gap between core and wall	2.8
Horizontal gap on top of the core - lateral flow	2.5
Horizontal gap on top of the core - vertical flow	6.8

Table 5.1: HTC values from the Excel file

Wall adj. HTC

Region	Value $[W/m^2K]$
Cylinders Supports Surfaces	3.3
Lower External Surface	2.0
Lower Internal Surface	2.0
Front Lower Plate	2.1
Left External Surface	3.1
Right External Surface	3.2
Left Internal Surface	3.0
Right Internal Surface	3.1
Rear Left Plate	1.9
Rear Right Plate	2.0
Front Left Plate	4.0
Front Right Plate	4.1
Left Supports Surfaces	3.0
Right Supports Surfaces	3.0
Upper Supports Surfaces	4.8
Upper Internal Surface	3.9
Upper External Surface	4.4
Front Upper Plate	13.0
Rear Upper Plate	1.5
Rear Lower Plate	1.5

Table 5.2: Y+ based HTC values from the ANSYS coupled simulation

5.1.4 Temperature results

Region	Value [C]
Inlet	20
Horizontal gap under the core	86.3
Vertical gap between core and wall	129.1
Horizontal gap on top of the core - lateral flow	200.4
Horizontal gap on top of the core - vertical flow	227.8

Table 5.3: Temperature values from the Excel file

Region	Value [C]
Inlet	20
Cylinders Supports Surfaces	32.5
Lower External Surface	29.2
Lower Internal Surface	37.0
Front Lower Plate	36.5
Left External Surface	34.0
Right External Surface	33.9
Left Internal Surface	37.2
Right Internal Surface	37.5
Rear Left Plate	35.0
Rear Right Plate	34.7
Front Left Plate	38.8
Front Right Plate	39.6
Left Supports Surfaces	35.5
Right Supports Surfaces	35.6
Upper Supports Surfaces	35.9
Upper Internal Surface	37.9
Upper External Surface	31.8
Front Upper Plate	37.9
Rear Upper Plate	31.7
Rear Lower Plate	30.7
Outlet	31.8

Table 5.4: Temperature values from the ANSYS coupled simulation

5.2 Normal conditions - 250 CFM

In this simulation, air is flowing at the fluid inlet at 250 CFM and the MARS Heat Generation distribution is that of a normal case (total power of 1.3 kW).

5.2.1 Solid results

Below are presented the most significant results for the solid component.

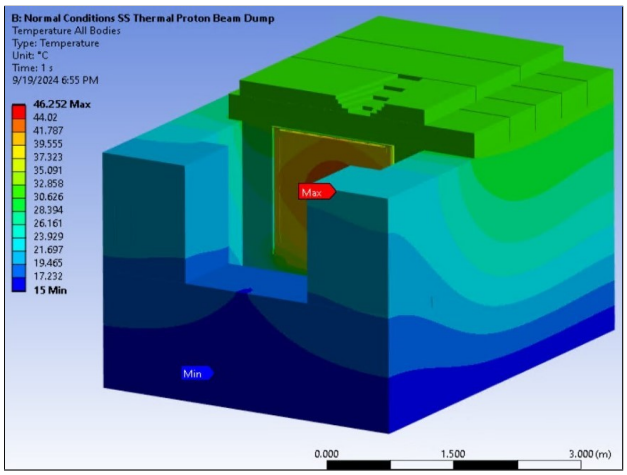

Figure 5.9: All bodies

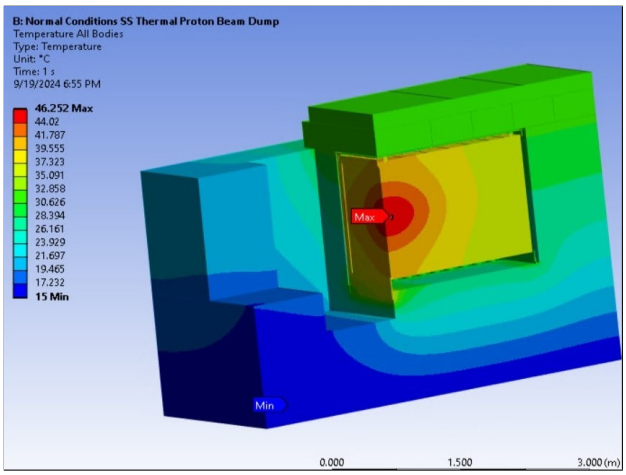

Figure 5.10: All bodies - section

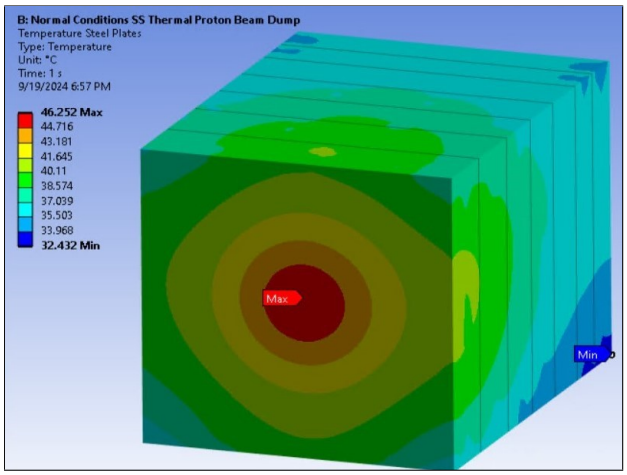

Figure 5.11: Steel plates

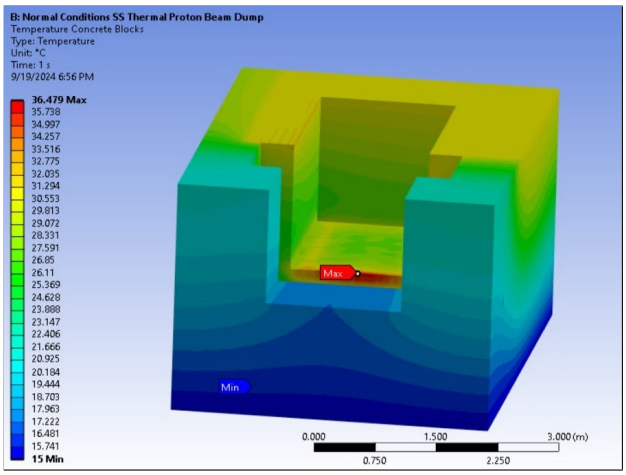

Figure 5.12: Concrete blocks

5.2.2 Fluid results

Below are presented the most significant results for the fluid component.

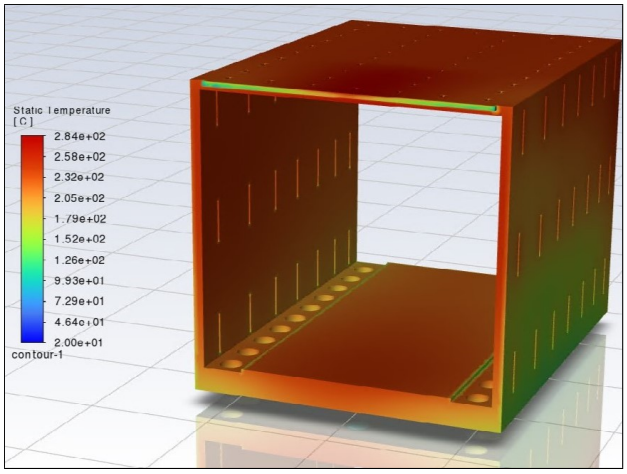

Figure 5.13: Static temperature

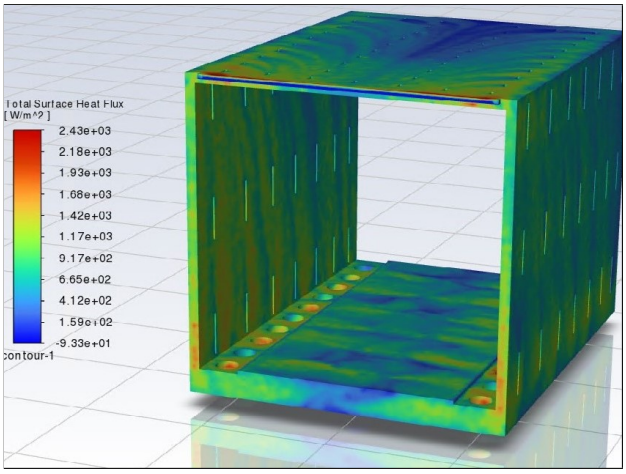

Figure 5.14: Heat flux

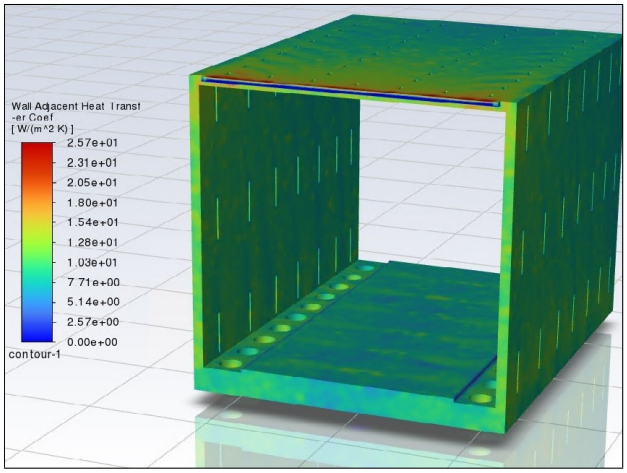

Figure 5.15: Wall adj. HTC

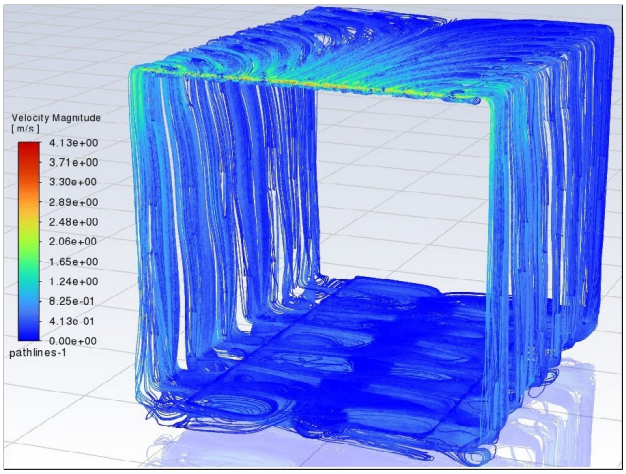

Figure 5.16: Velocity

5.2.3 HTC results

Region	Value $[W/m^2K]$
Horizontal gap under the core	1.7
Vertical gap between core and wall	3.8
Horizontal gap on top of the core - lateral flow	3.4
Horizontal gap on top of the core - vertical flow	9.2

Table 5.5: HTC values from the Excel file

Region	Value $[W/m^2K]$
Cylinders Supports Surfaces	4.5
Lower External Surface	2.8
Lower Internal Surface	2.8
Front Lower Plate	3.0
Left External Surface	4.4
Right External Surface	4.4
Left Internal Surface	4.2
Right Internal Surface	4.3
Rear Left Plate	2.8
Rear Right Plate	2.9
Front Left Plate	5.5
Front Right Plate	5.6
Left Supports Surfaces	4.1
Right Supports Surfaces	4.2
Upper Supports Surfaces	6.6
Upper Internal Surface	5.5
Upper External Surface	6.1
Front Upper Plate	17.7
Rear Upper Plate	2.1
Rear Lower Plate	2.3

Table 5.6: Y+ based HTC values from the ANSYS coupled simulation

5.2.4 Temperature results

Region	Value [C]
Inlet	20
Horizontal gap under the core	70.4
Vertical gap between core and wall	108.7
Horizontal gap on top of the core - lateral flow	175.3
Horizontal gap on top of the core - vertical flow	204.8

Table 5.7: HTC values from the Excel file

Region	Value [C]
Inlet	20
Cylinders Supports Surfaces	30.7
Lower External Surface	28.2
Lower Internal Surface	35.4
Front Lower Plate	34.8
Left External Surface	32.6
Right External Surface	32.6
Left Internal Surface	35.7
Right Internal Surface	35.9
Rear Left Plate	34.0
Rear Right Plate	33.7
Front Left Plate	37.2
Front Right Plate	37.9
Left Supports Surfaces	34.0
Right Supports Surfaces	34.0
Upper Supports Surfaces	34.6
Upper Internal Surface	36.4
Upper External Surface	31.0
Front Upper Plate	35.8
Rear Upper Plate	31.1
Rear Lower Plate	29.8
Outlet	30.3

Table 5.8: Temperature values from the ANSYS coupled simulation

5.3 Normal conditions - 400 CFM

In this simulation, air is flowing at the fluid inlet at 400 CFM and the MARS Heat Generation distribution is that of a normal case (total power of 1.3 kW).

5.3.1 Solid results

Below are presented the most significant results for the solid component.

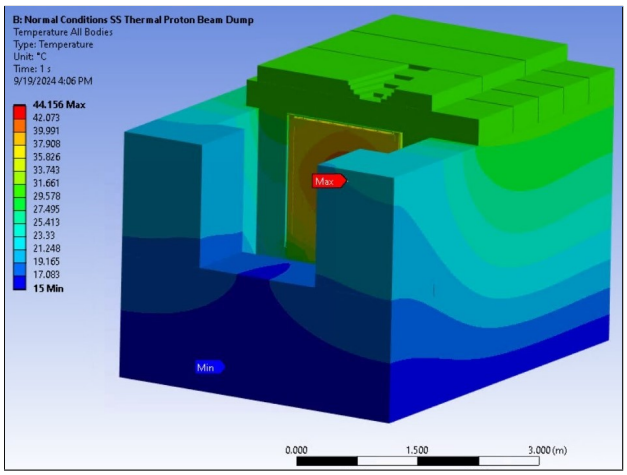

Figure 5.17: All bodies

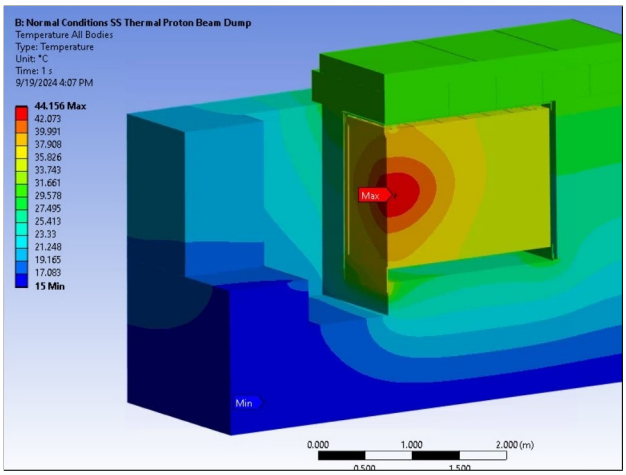

Figure 5.18: All bodies - section

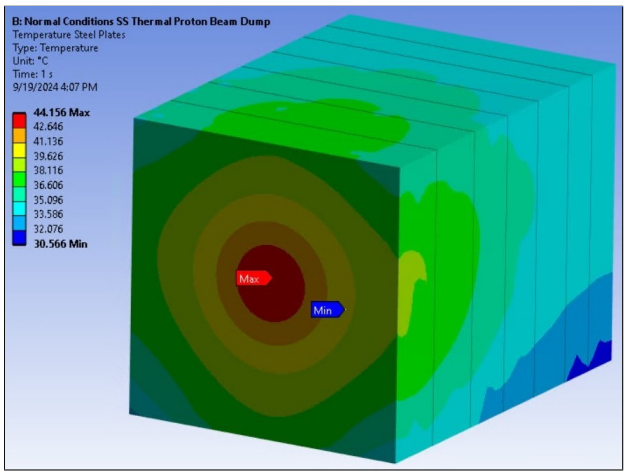

Figure 5.19: Steel plates

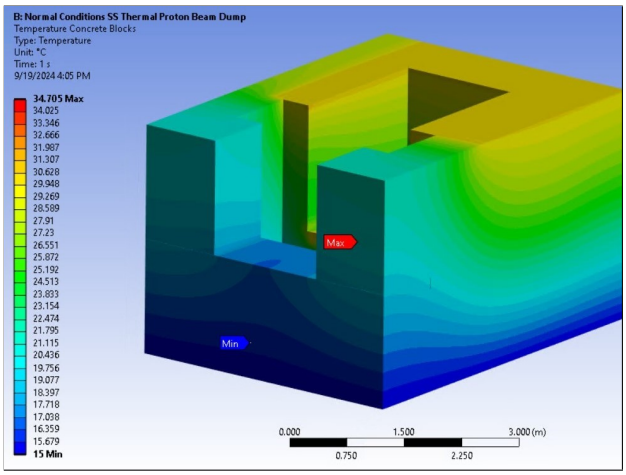

Figure 5.20: Concrete blocks

5.3.2 Fluid results

Below are presented the most significant results for the fluid component.

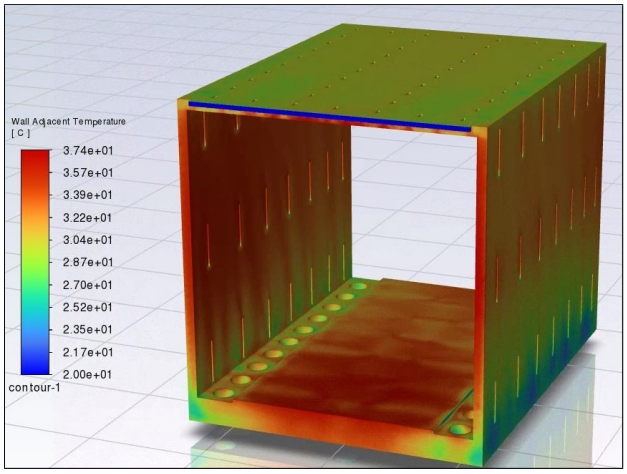

Figure 5.21: Static temperature

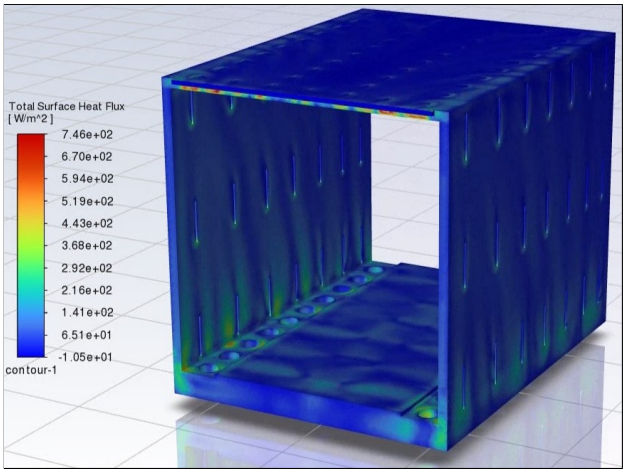

Figure 5.22: Heat flux

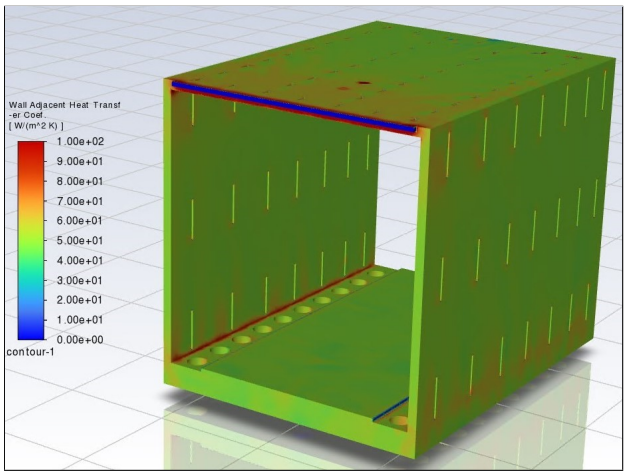

Figure 5.23: Wall adj. HTC

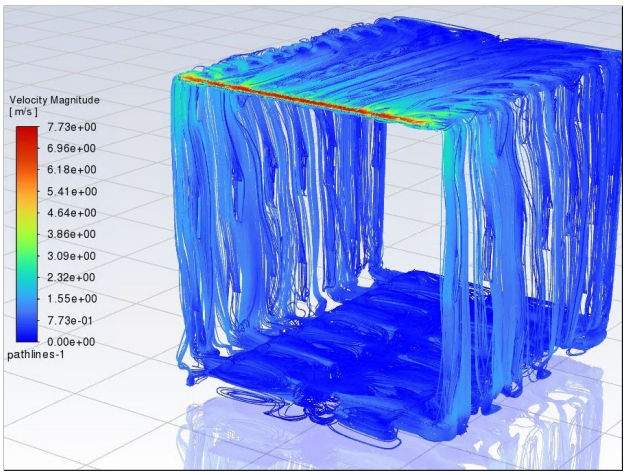

Figure 5.24: Velocity

5.3.3 HTC results

Region	Value $[W/m^2K]$
Horizontal gap under the core	1.7
Vertical gap between core and wall	3.8
Horizontal gap on top of the core - lateral flow	3.4
Horizontal gap on top of the core - vertical flow	9.2

Table 5.9: HTC values from the Excel file

Region	Value $[W/m^2K]$
Cylinders Supports Surfaces	6.7
Lower External Surface	4.0
Lower Internal Surface	4.1
Front Lower Plate	4.8
Left External Surface	6.5
Right External Surface	6.5
Left Internal Surface	6.3
Right Internal Surface	6.3
Rear Left Plate	4.3
Rear Right Plate	4.2
Front Left Plate	8.7
Front Right Plate	8.4
Left Supports Surfaces	6.1
Right Supports Surfaces	6.0
Upper Supports Surfaces	9.4
Upper Internal Surface	8.0
Upper External Surface	8.9
Front Upper Plate	25.0
Rear Upper Plate	2.9
Rear Lower Plate	3.3

Table 5.10: Y+ based HTC values from the ANSYS coupled simulation

5.3.4 Temperature results

Region	Value [C]
Inlet	20
Horizontal gap under the core	70.4
Vertical gap between core and wall	108.7
Horizontal gap on top of the core - lateral flow	175.3
Horizontal gap on top of the core - vertical flow	204.8

Table 5.11: HTC values from the Excel file

Region	Value [C]
Inlet	20
Cylinders Supports Surfaces	28.4
Lower External Surface	26.8
Lower Internal Surface	33.0
Front Lower Plate	32.4
Left External Surface	30.5
Right External Surface	30.5
Left Internal Surface	33.3
Right Internal Surface	33.5
Rear Left Plate	32.4
Rear Right Plate	32.3
Front Left Plate	34.5
Front Right Plate	35.0
Left Supports Surfaces	31.8
Right Supports Surfaces	31.9
Upper Supports Surfaces	32.4
Upper Internal Surface	34.1
Upper External Surface	29.7
Front Upper Plate	33.3
Rear Upper Plate	30.1
Rear Lower Plate	28.5
Outlet	28.6

Table 5.12: Temperature values from the ANSYS coupled simulation

5.4 Normal conditions - 600 CFM

In this simulation, air is flowing at the fluid inlet at 600 CFM and the MARS Heat Generation distribution is that of a normal case (total power of 1.3 kW).

5.4.1 Solid results

Below are presented the most significant results for the solid component.

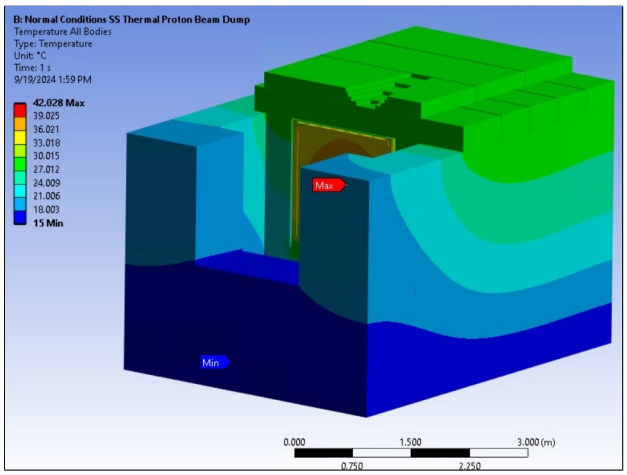

Figure 5.25: All bodies

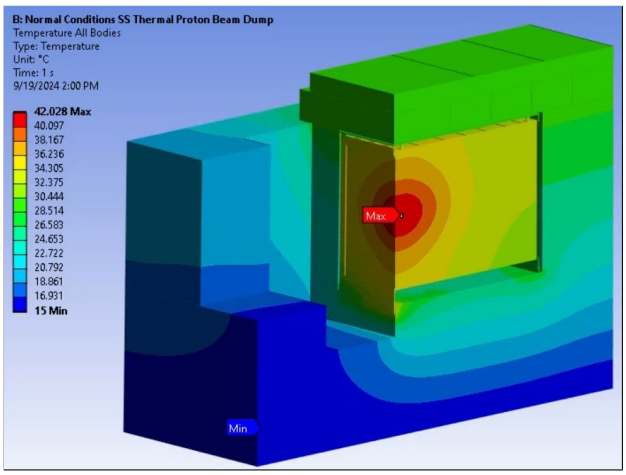

Figure 5.26: All bodies - section

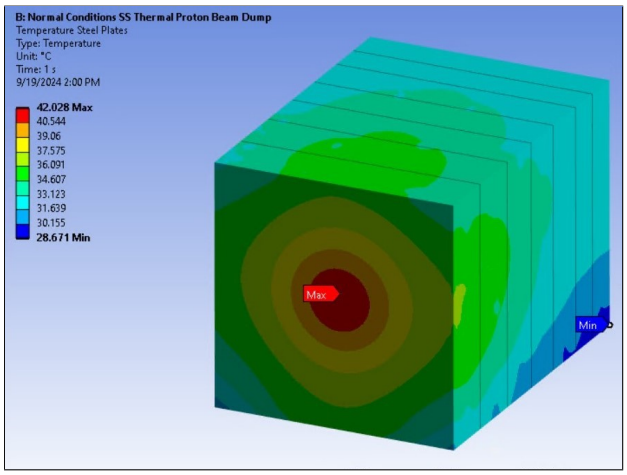

Figure 5.27: Steel plates

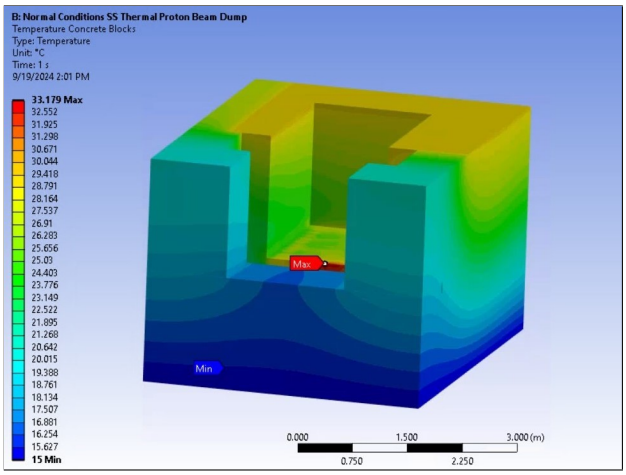

Figure 5.28: Concrete blocks

5.4.2 Fluid results

Below are presented the most significant results for the fluid component.

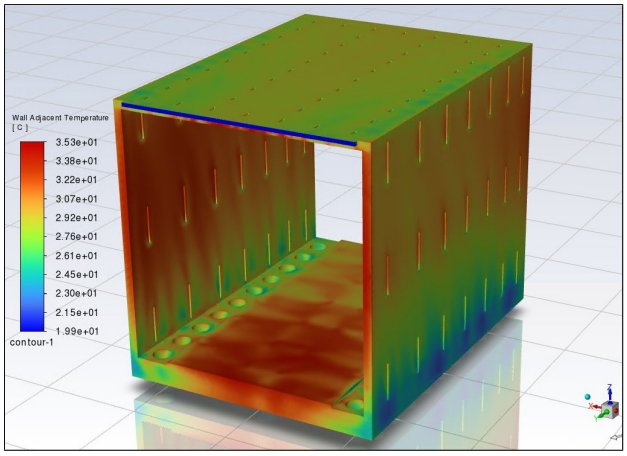

Figure 5.29: Static temperature

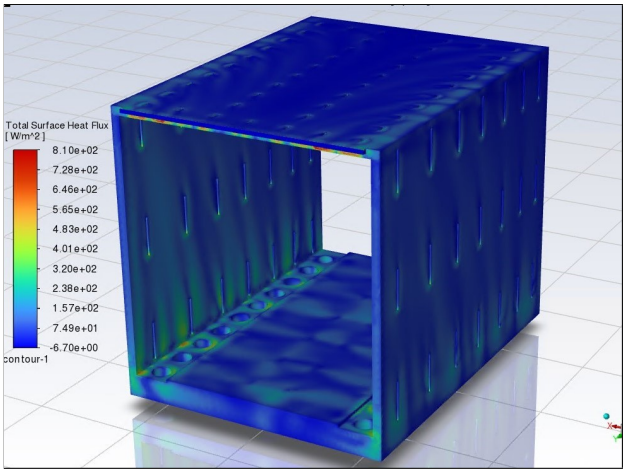

Figure 5.30: Heat flux

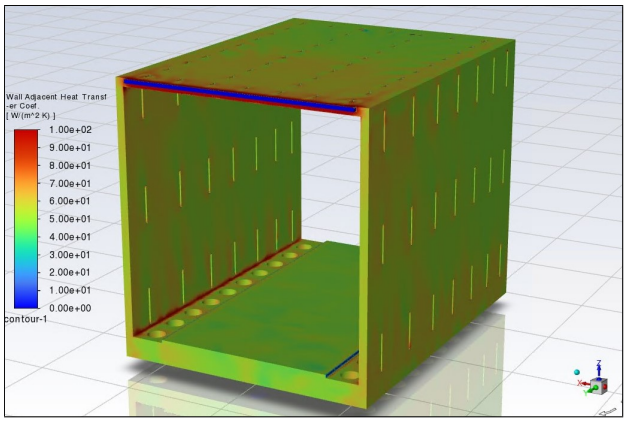

Figure 5.31: Wall adj. HTC

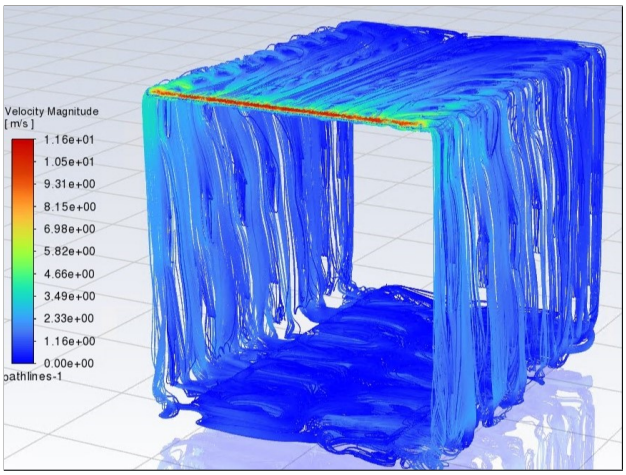

Figure 5.32: Velocity

5.4.3 HTC results

Region	Value $[W/m^2K]$
Horizontal gap under the core	1.7
Vertical gap between core and wall	3.8
Horizontal gap on top of the core - lateral flow	3.4
Horizontal gap on top of the core - vertical flow	9.2

Table 5.13: HTC values from the Excel file

Region	Value $[W/m^2K]$
Cylinders Supports Surfaces	11.8
Lower External Surface	7.1
Lower Internal Surface	7.2
Front Lower Plate	8.6
Left External Surface	11.7
Right External Surface	11.8
Left Internal Surface	11.3
Right Internal Surface	11.4
Rear Left Plate	7.9
Rear Right Plate	8.4
Front Left Plate	16.2
Front Right Plate	15.5
Left Supports Surfaces	11.0
Right Supports Surfaces	10.7
Upper Supports Surfaces	15.7
Upper Internal Surface	14.2
Upper External Surface	15.6
Front Upper Plate	39.6
Rear Upper Plate	5.0
Rear Lower Plate	6.7

Table 5.14: Y+ based HTC values from the ANSYS coupled simulation

5.4.4 Temperature results

Region	Value [C]
Inlet	20
Horizontal gap under the core	70.4
Vertical gap between core and wall	108.7
Horizontal gap on top of the core - lateral flow	175.3
Horizontal gap on top of the core - vertical flow	204.8

Table 5.15: HTC values from the Excel file

Region	Value [C]
Inlet	20
Cylinders Supports Surfaces	21.9
Lower External Surface	20.3
Lower Internal Surface	24.3
Front Lower Plate	24.2
Left External Surface	21.3
Right External Surface	21.3
Left Internal Surface	24.1
Right Internal Surface	24.4
Rear Left Plate	20.9
Rear Right Plate	20.8
Front Left Plate	25.6
Front Right Plate	26.2
Left Supports Surfaces	22.7
Right Supports Surfaces	22.8
Upper Supports Surfaces	23.4
Upper Internal Surface	24.3
Upper External Surface	21.2
Front Upper Plate	25.4
Rear Upper Plate	20.9
Rear Lower Plate	20.2
Outlet	21.9

Table 5.16: Temperature values from the ANSYS coupled simulation

5.5 Normal conditions - 800 CFM

In this simulation, air is flowing at the fluid inlet at 800 CFM and the MARS Heat Generation distribution is that of a normal case (total power of 1.3 kW).

Important note: this simulation was run with a higher number of coupling and Fluent iterations. Due to lack of time, I was able to run only this simulation and not the others. One can see that the results are much better, indicating that increasing the number of iterations could make the simulations more accurate than they are at the moment. In particular, this simulation was run with 10 total coupling iterations, a ramping to the 9th iteration and 400 Fluent iterations, whereas the other simulations of this were run with 5 total coupling iterations, a ramping to the 4th iteration and 200 Fluent iterations. As a matter of fact, one can notice that in this simulation the global energy balance check is quite satisfied, meaning that more iterations are not only suggested but probably necessary.

5.5.1 Solid results

Below are presented the most significant results for the solid component.

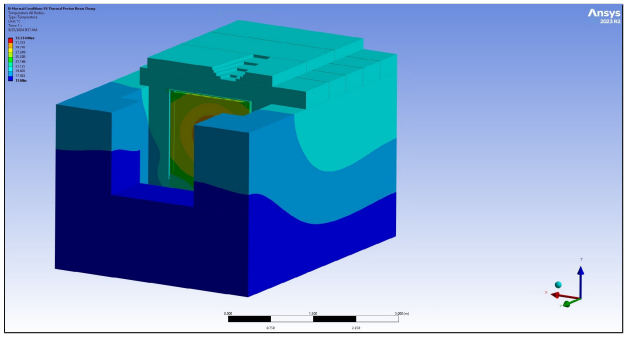

Figure 5.33: All bodies

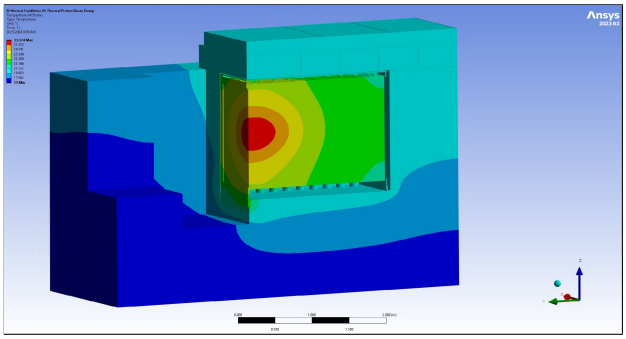

Figure 5.34: All bodies - section

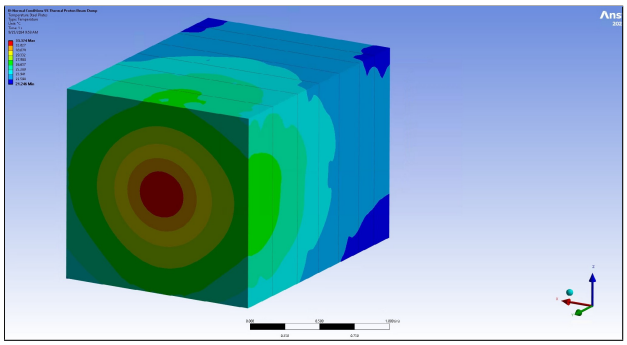

Figure 5.35: Steel plates

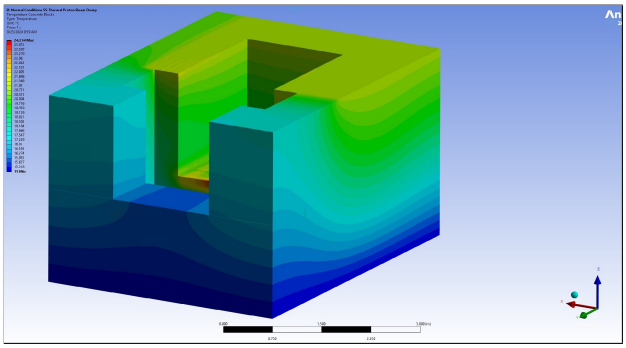

Figure 5.36: Concrete blocks

5.5.2 Fluid results

Below are presented the most significant results for the fluid component.

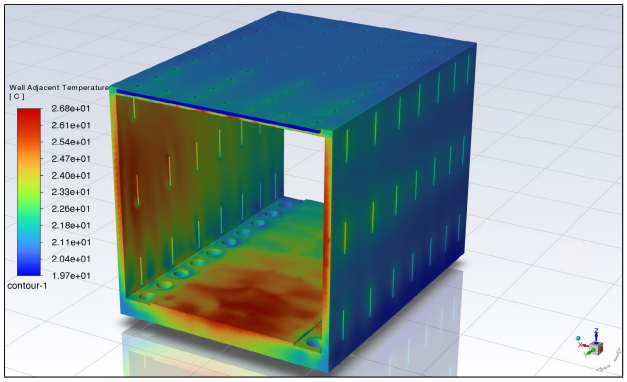

Figure 5.37: Static temperature

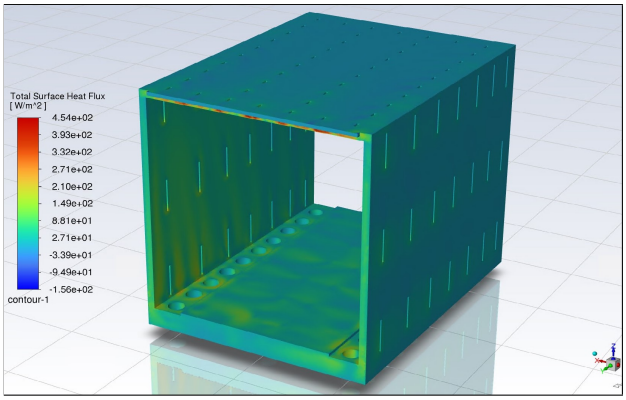

Figure 5.38: Heat flux

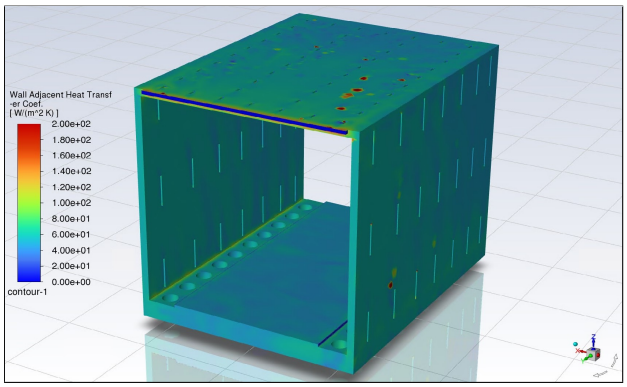

Figure 5.39: Wall adj. HTC

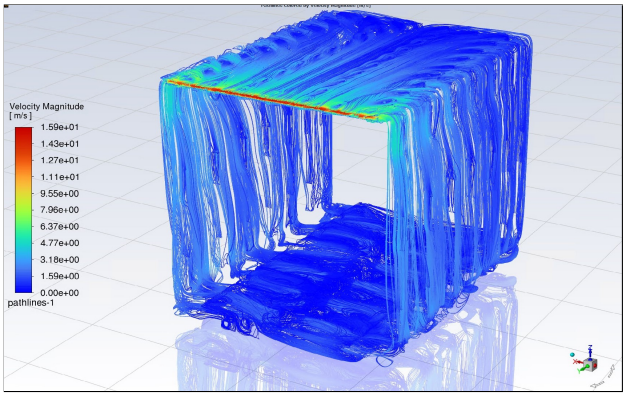

Figure 5.40: Velocity

5.5.3 HTC results

Region	Value $[W/m^2K]$
Horizontal gap under the core	1.7
Vertical gap between core and wall	3.8
Horizontal gap on top of the core - lateral flow	3.4
Horizontal gap on top of the core - vertical flow	9.2

Table 5.17: HTC values from the Excel file

Region	Value $[W/m^2K]$
Cylinders Supports Surfaces	11.7
Lower External Surface	7.0
Lower Internal Surface	7.2
Front Lower Plate	8.4
Left External Surface	11.6
Right External Surface	11.8
Left Internal Surface	11.1
Right Internal Surface	11.4
Rear Left Plate	6.7
Rear Right Plate	8.2
Front Left Plate	15.4
Front Right Plate	16.1
Left Supports Surfaces	10.5
Right Supports Surfaces	11.0
Upper Supports Surfaces	15.7
Upper Internal Surface	14.2
Upper External Surface	15.5
Front Upper Plate	39.6
Rear Upper Plate	4.5
Rear Lower Plate	6.4

Table 5.18: Y+ based HTC values from the ANSYS coupled simulation

5.5.4 Temperature results

Region	Value [C]
Inlet	20
Horizontal gap under the core	70.4
Vertical gap between core and wall	108.7
Horizontal gap on top of the core - lateral flow	175.3
Horizontal gap on top of the core - vertical flow	204.8

Table 5.19: HTC values from the Excel file

Region	Value [C]
Inlet	20
Cylinders Supports Surfaces	24.9
Lower External Surface	24.6
Lower Internal Surface	28.9
Front Lower Plate	28.8
Left External Surface	27.1
Right External Surface	27.0
Left Internal Surface	29.3
Right Internal Surface	29.4
Rear Left Plate	29.7
Rear Right Plate	29.1
Front Left Plate	30.2
Front Right Plate	30.7
Left Supports Surfaces	28.1
Right Supports Surfaces	28.0
Upper Supports Surfaces	28.9
Upper Internal Surface	30.2
Upper External Surface	27.4
Front Upper Plate	29.1
Rear Upper Plate	28.3
Rear Lower Plate	26.3
Outlet	

Table 5.20: Temperature values from the ANSYS coupled simulation

5.6 Accident conditions - 165 CFM

In this simulation, air is flowing at the fluid inlet at 165 CFM and the MARS Heat Generation distribution is that of an accident case (total power of 6.7 kW).

5.6.1 Solid results

Below are presented the most significant results for the solid component.

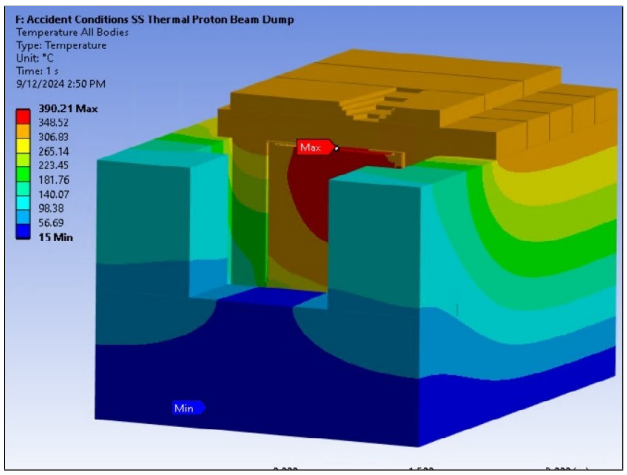

Figure 5.41: All bodies

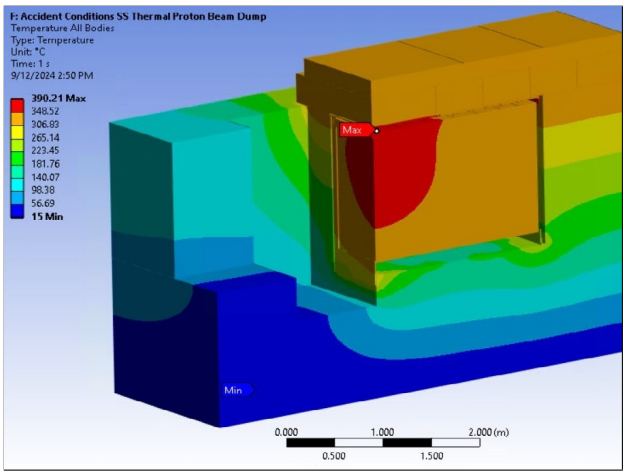

Figure 5.42: All bodies - section

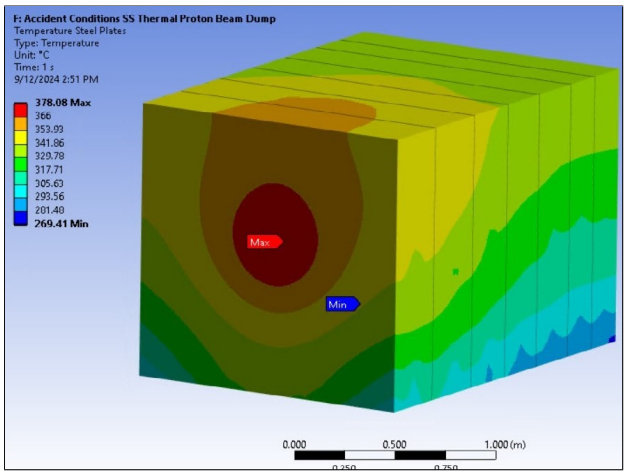

Figure 5.43: Steel plates

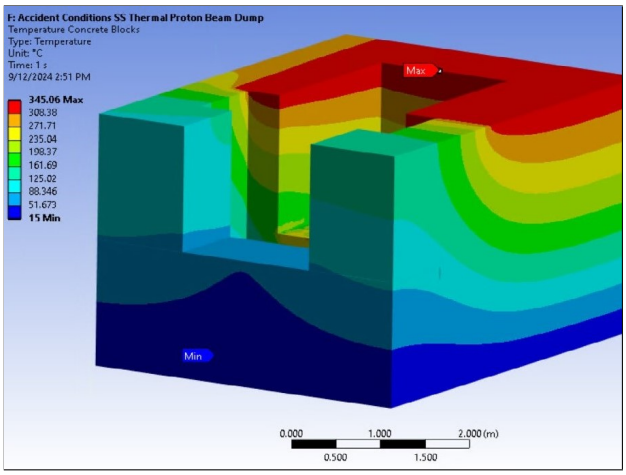

Figure 5.44: Concrete blocks

5.6.2 Fluid results

Below are presented the most significant results for the fluid component.

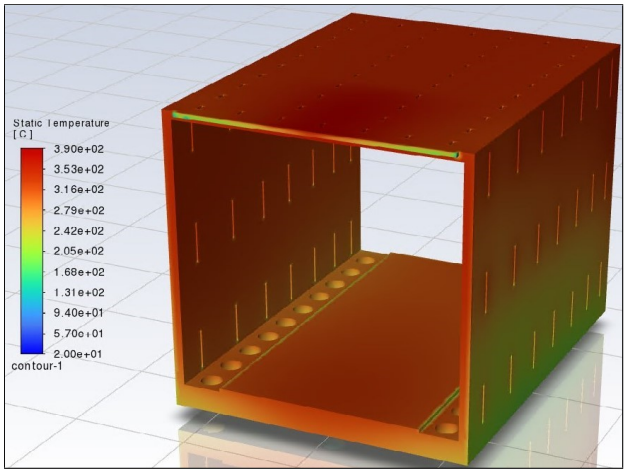

Figure 5.45: Static temperature

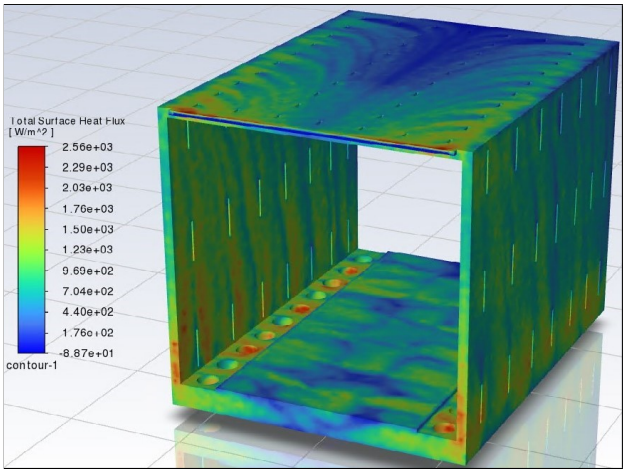

Figure 5.46: Heat flux

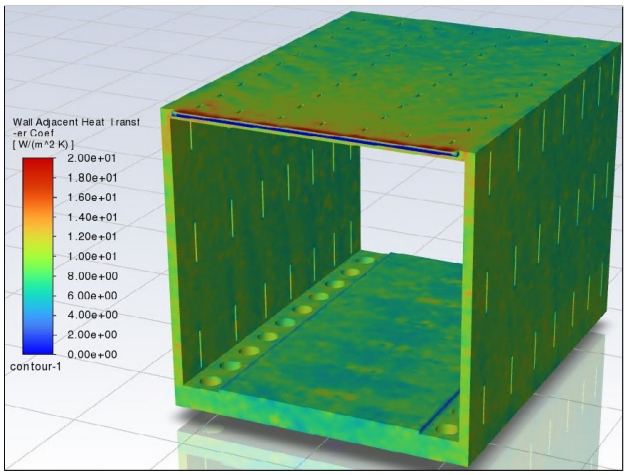

Figure 5.47: Wall adj. HTC

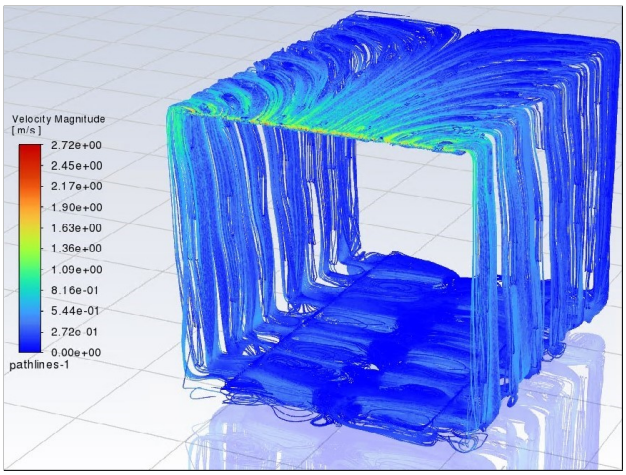

Figure 5.48: Velocity

5.6.3 HTC results

Region	Value $[W/m^2K]$
Horizontal gap under the core	1.3
Vertical gap between core and wall	Not calculable (temperature too high)
Horizontal gap on top of the core - lateral flow	Not calculable (temperature too high)
Horizontal gap on top of the core - vertical flow	Not calculable (temperature too high)

Table 5.21: HTC values from the Excel file

Region	Value $[W/m^2K]$
Cylinders Supports Surfaces	9.2
Lower External Surface	8.0
Lower Internal Surface	7.9
Front Lower Plate	7.9
Left External Surface	8.5
Right External Surface	8.6
Left Internal Surface	8.4
Right Internal Surface	8.5
Rear Left Plate	8.3
Rear Right Plate	8.0
Front Left Plate	10.5
Front Right Plate	10.3
Left Supports Surfaces	9.6
Right Supports Surfaces	9.4
Upper Supports Surfaces	9.6
Upper Internal Surface	9.4
Upper External Surface	9.0
Front Upper Plate	11.8
Rear Upper Plate	7.6
Rear Lower Plate	7.5

Table 5.22: Y+ based HTC values from the ANSYS coupled simulation

5.6.4 Temperature results

Region	Value [C]
Inlet	20
Horizontal gap under the core	307.2
Vertical gap between core and wall	>500
Horizontal gap on top of the core - lateral flow	>500
Horizontal gap on top of the core - vertical flow	>500

Table 5.23: Temperature values from the Excel file

Region	Value [C]
Inlet	20
Cylinders Supports Surfaces	257.6
Lower External Surface	199.7
Lower Internal Surface	312.0
Front Lower Plate	297.1
Left External Surface	279.6
Right External Surface	280.7
Left Internal Surface	323.4
Right Internal Surface	325.1
Rear Left Plate	317.6
Rear Right Plate	316.8
Front Left Plate	332.0
Front Right Plate	336.2
Left Supports Surfaces	307.6
Right Supports Surfaces	308.4
Upper Supports Surfaces	346.8
Upper Internal Surface	344.5
Upper External Surface	348.8
Front Upper Plate	352.1
Rear Upper Plate	348.3
Rear Lower Plate	253.7
Outlet	240.4

Table 5.24: Temperature values from the ANSYS coupled simulation

5.7 Normal conditions - No convection

In this simulation, air is not simulated. All the surfaces in contact with air are considered perfectly insulated. This could be the worst case, if for some reason the fan stop working. The MARS Heat Generation distribution is that of an normal case (total power of 1.3 kW).

5.7.1 Solid results

Below are presented the most significant results for the solid component.

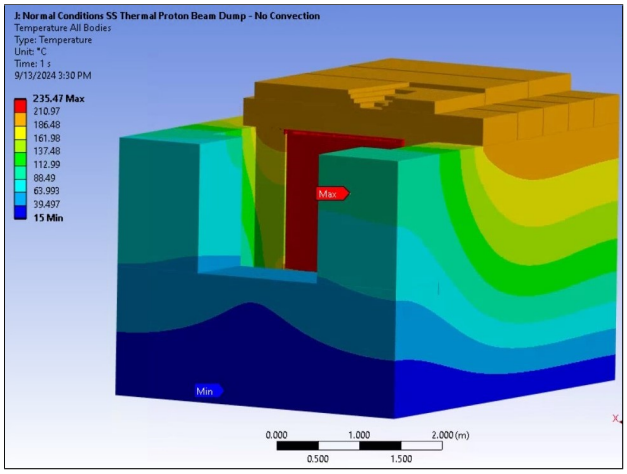

Figure 5.49: All bodies

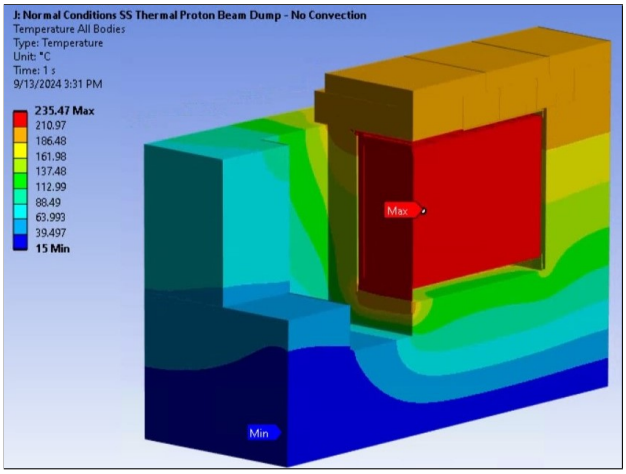

Figure 5.50: All bodies - section

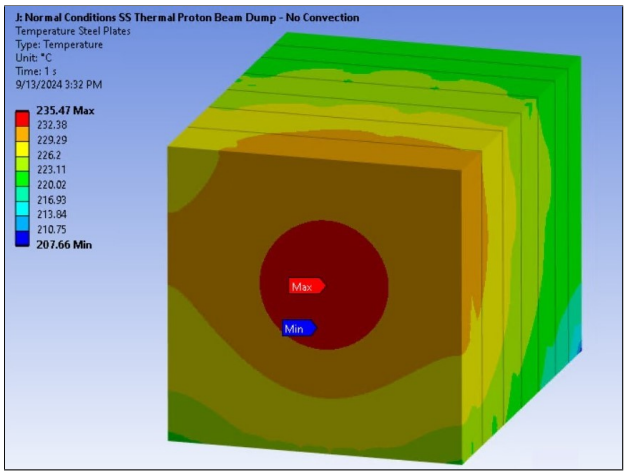

Figure 5.51: Steel plates

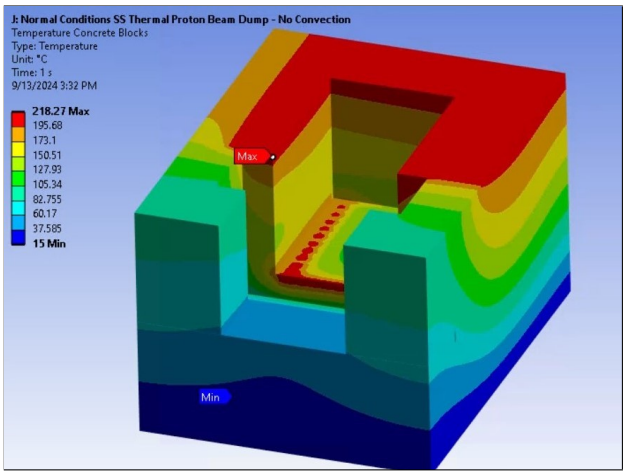

Figure 5.52: Concrete blocks

5.8 Accident conditions - No convection

In this simulation, air is not simulated. All the surfaces in contact with air are considered perfectly insulated. This could be the worst case, if for some reason the fan stop working. The MARS Heat Generation distribution is that of an accident case (total power of 6.7 kW).

5.8.1 Solid results

Below are presented the most significant results for the solid component.

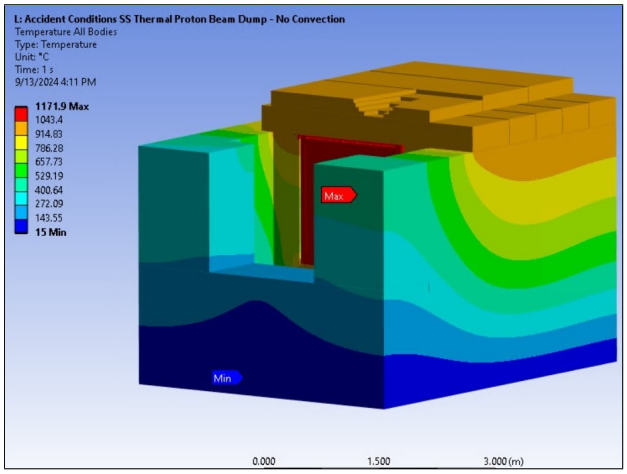

Figure 5.53: All bodies

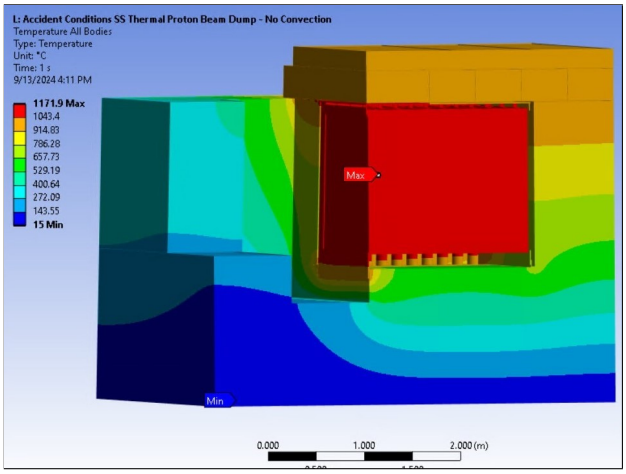

Figure 5.54: All bodies - section

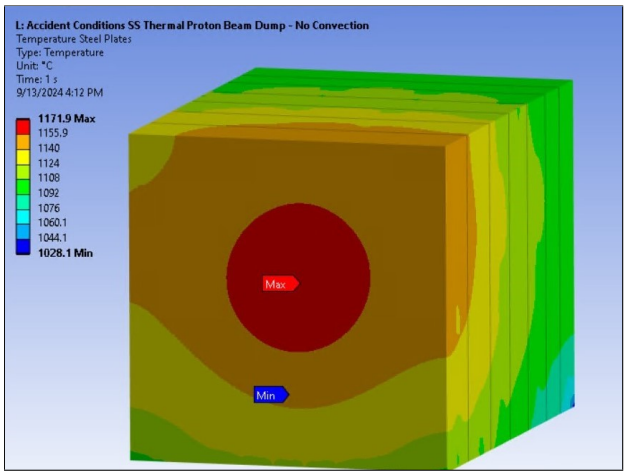

Figure 5.55: Steel plates

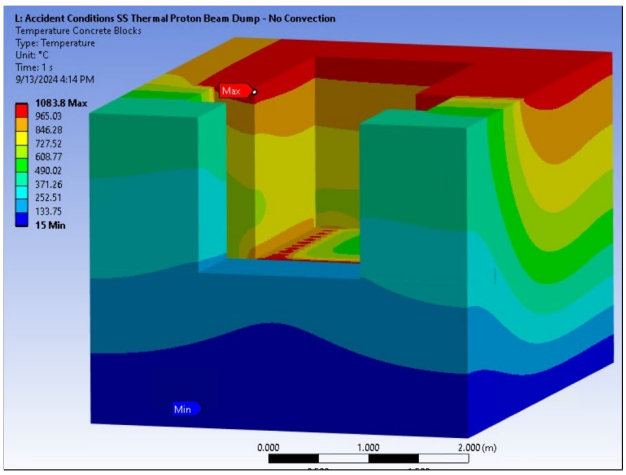

Figure 5.56: Concrete blocks

5.9 Airflow - Laminar model - 165 CFM

In this simulation, the solid is not simulated. All the surfaces in contact with the solid are considered perfectly insulated. No heat generation has been considered. This is just to check what are the differences between the laminar model and the SST k-ω model. The airflow has a volumetric flow of 165 CFM.

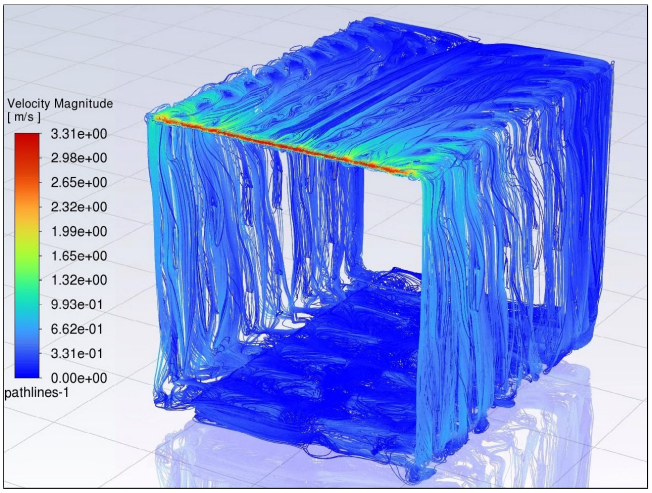

Figure 5.57: Velocities for 165 CFM airflow

Inlet velocity	0.63 $\frac{m}{s}$
Outlet velocity	2.28 $\frac{m}{s}$

Velocity quantities

5.10 Airflow - SST k-ω model - 165 CFM

In this simulation, the solid is not simulated. All the surfaces in contact with the solid are considered perfectly insulated. No heat generation has been considered. This is just to check what are the differences between the laminar model and the SST k-ω model. The airflow has a volumetric flow of 165 CFM.

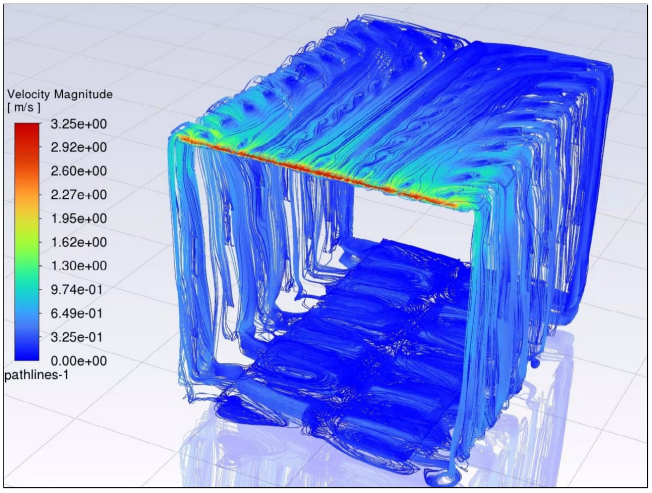

Figure 5.58: Velocities for 165 CFM airflow

Inlet velocity	0.64 $\frac{m}{s}$
Outlet velocity	2.26 $\frac{m}{s}$

Velocity quantities

Conclusions

Below, a summary table of the results of the simulations. Note that the safety factor is calculated as the ratio of the maximum concrete temperature allowable (i.e. 95 °C) over the maximum concrete temperature in the simulation, where both temperatures are expressed in Kelvin.

Heat distribution	Airflow [CFM]	Max. concrete temp. [°C]	Safety factor to 95 °C
Normal	165	37.5	1.19
Normal	250	36.5	1.19
Normal	400	34.7	1.20
Normal	600	33.1	1.20
Normal	800*	24.2	1.24
Accident	165*	77.8	1.05

Table 6.1: Summary table

*simulations run with a higher number of coupling and Fluent iterations.

6.1 Reliability of the simulations

6.1.1 Why the simulations results shuould be realistic

Solid convergence

The solid simulations all converge and do not present residual problems.

Fluent residuals

Residuals of all the Fluent simulations are low. In particular, the energy residual is below $2 \cdot 10^{-5}$, the ω and the k residuals are below $5 \cdot 10^{-3}$.

Figure 6.1: Residuals of one fluid simulation

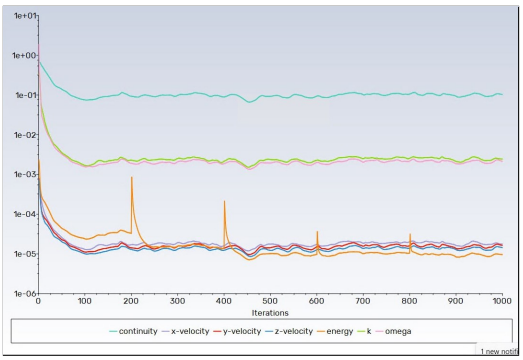

Coupled residuals

Most of the residuals of the coupling system are below 10^{-2} and below the default values of convergence.

Weighted Average	3.07E+02	3.07E+02
Interface: interface-3		
RIS T2	Converged	
RMS Change	3.57E-03	3.71E-03
Weighted Average	3.08E+02	3.08E+02
Interface: interface-4		
RES T2	Converged	
RMS Change	6.24E-03	5.83E-03
Weighted Average	3.05E+02	3.05E+02
Interface: interface-5		
UIS T2	Converged	
RMS Change	3.14E-03	3.06E-03
Weighted Average	3.09E+02	3.09E+02
Interface: interface-6		
UES T2	Converged	
RMS Change	2.64E-03	2.58E-03
Weighted Average	3.03E+02	3.03E+02
Interface: interface-7		
OIS T2	Converged	
RMS Change	3.92E-03	3.97E-03
Weighted Average	3.08E+02	3.08E+02
Interface: interface-8		
OES T2	Converged	
RMS Change	5.88E-03	6.16E-03
Weighted Average	3.01E+02	3.01E+02
Interface: interface-9		
ROP T2	Converged	
RMS Change	6.15E-03	6.26E-03
Weighted Average	3.02E+02	3.02E+02
Participant solution status		
Normal Conditions SS Thermal Proto	Converged	
Fluid Flow (Fluent with Fluent Mes	Not yet converged	

Figure 6.2: Numerical values

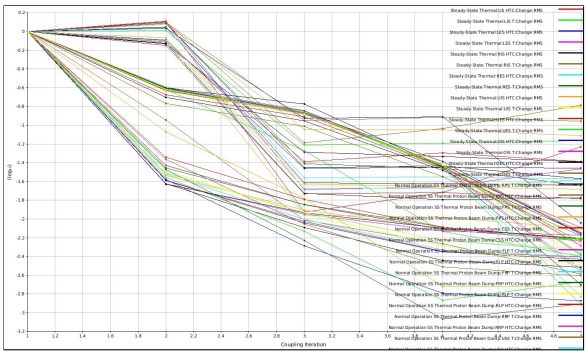

Figure 6.3: RMS over iterations

Heat distribution

The total heat generated by the heat distribution has been checked and simulations were run in which the real heat distribution was replaced by a uniform heat distribution with the same total power, getting very close results.

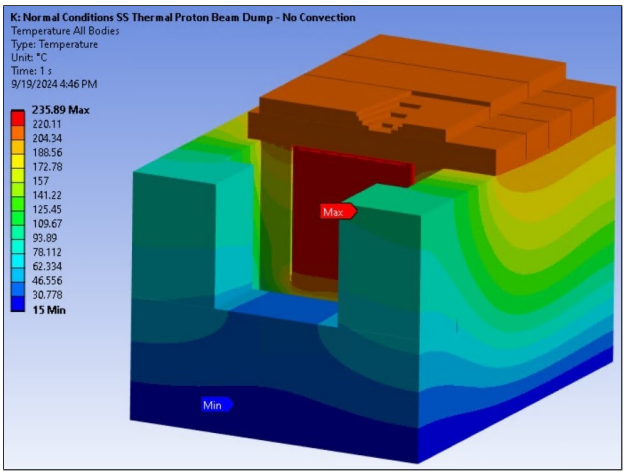

Figure 6.4: Temperature distribution with normal heat distribution without convection

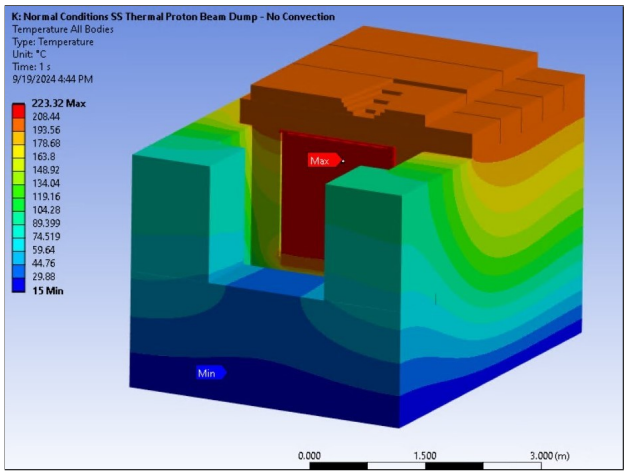

Figure 6.5: Temperature distribution with uniform heat distribution without convection

Fluent quantity convergence

Individual quantities as velocity at the outlet were observed to converge within 200 iterations and to not present oscillatory behaviour.

Figure 6.6: Convergence of velocity with iterations

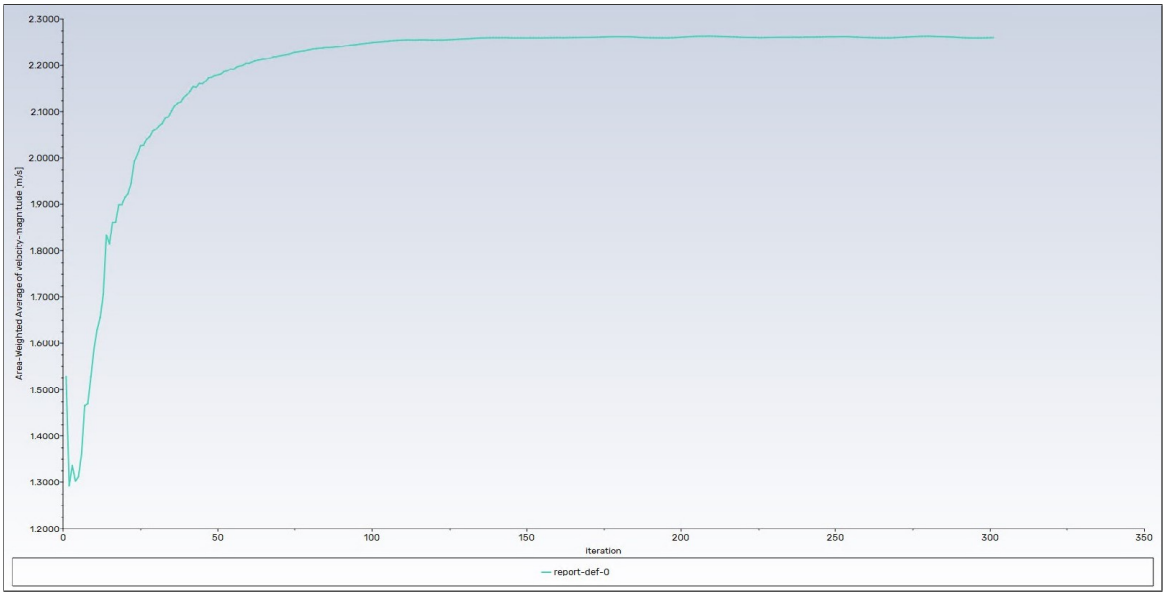

Mass flow rate balance

Mass flow rates at both the inlet and the outlet were checked for consistency. No discrepancies have been noticed between the two values.

Heat distribution	Airflow [CFM]	Inlet flow rate [kg]	Outlet flow rate [kg]
Normal	165	0.092	-0.092
Normal	250	0.14	-0.14
Normal	400	0.22	-0.22
Normal	600	0.33	-0.33
Normal	800*	0.46	-0.46
Accident	165*	0.092	-0.092

Table 6.2: Mass flow rates

*simulations run with a higher number of Fluent and coupling iterations.

Volumetric flow sensitivity analysis

Data are collected for different volumetric flows, preserving the same meshing, the same boundary conditions (for the two different cases of normal heat distribution and accident heat distribution). This is to check that varying the flow, the results vary consistently.

Turbulent quantities

Turbulent quantities as turbulence intensity and turbulent viscosity ratio have been checked and not simply assumed to be their default value. Please refer to section 3.8.3

Global heat transfer

If one thinks at the whole system, it is clear that the increase in air temperature of the simulation (that is, the difference between the mass-weighted average of the temperature at the outlet and the mass-weighted average of the temperature at the inlet evaluated by Fluent) should be similar to the increase in temperature if air takes all the power generated inside of the steel plates subtracted the power that flows through the ground on the concrete surface with the imposed temperature. So, for each case:

$$\Delta T_{\text{simulation}} \quad \text{should be equal to} \quad \Delta T_{\text{energy balance}} = \frac{Q - Q_{ext}}{c_p \dot{m}}$$

where Q is the total power generated by the proton beam, Q_{ext} is the heat that is flowing through the ground that can be found by the reaction probe in the ANSYS Thermal SS simulation, c_p is air specific heat capacity at constant pressure and $\dot{m}$ is air mass flow rate.

Heat deposited	Airflow [CFM]	$\dot{m}$ $[\frac{\text{kg}}{\text{s}}]$	Q_{ext}[W]	$\Delta T_{\text{simulation}}$[°C]	$\Delta T_{\text{energy balance}}$[°C]
1307	165	0.0954	127.7	11.8	12.9
1307	250	0.145	119.8	10.3	8.2
1307	400	0.231	108.3	8.59	5.2
1307	600	0.347	97.4	7.1	3.5
1307	800*	0.463	44.9	1.9	2.8
6225	165*	0.0920	255.3	38.5	64.5

Table 6.3: Global heat check

*simulations run with a higher number of coupling and Fluent iterations.

It is possible to see that this balance is approximately satisfied for some simulations and not satisfied for others. As already said, more coupling iterations and Fluent iterations are necessary to fully trust the results.

Number of elements of the meshes

The number of elements is pretty high. In particular:

- Elements of the solid component: 100 000
- Elements of the fluid component, normal heat distribution: 1 500 000
- Elements of the fluid component, accident heat distribution: 1 600 000

Uncoupled simulations

Uncoupled simulations were run to check the worst case (no convection) for the solid component and airflow conditions. Please refer to section 5.7

Total surface addressed

About 97% of the surface of the fluid component has been addressed with boundary conditions (coupled, inlet or outlet) for a total of 20 different individual coupled surfaces, twelve inlets and one outlet.

Turbulent flow

The viscous model used was SST k-ω and it was checked that the flow is turbulent. Please refer to section 3.8

Checking of y^+

The y^+ values were checked to be approximately under 5 for all the simulations.

Percentage of the coupled surfaces

Surfaces between solid and fluid were correctly coupled, with values up to 100

6.1.2 Why the simulations results could be more accurate

First time to do something like this

It is the first time that I do a coupled simulation, so maybe some transfers are not correctly set-up.

Properties of the fluid not temperature dependent

Air properties as specific heat at constant pressure, density and dynamic viscosity are considered constant and not dependent on the temperature.

Outlet conditions

As said in paragraph 3.7.2, the outlet conditions could be set up in a better way.

Static air on the rear face

As said in paragraph 3.6.4, air could be better simulated on the faces of the baffle.

Heat distribution not mapped perfectly

Heat distribution is not mapped perfectly due to the fact that the seven steel plates are considered separate bodies and have different thicknesses, so the meshing methods cannot reproduce exactly the spacing of the heat distribution source nodes. A solution to this problem could be considering the seven steel plates as a single body, meshing them accordingly to the spacings of the mesh. Still, it is calculated that the error on the total power is less than 8% with the current meshing and current heat generation distribution.

Fluent residuals still not too low

Fluent residuals for continuity sometimes do not drop below 10^{-1}, even after many iterations. This could be connected to the complexity of the problem and the refinement of the meshing.

Radiation

Radiation effects are not considered in both solid and fluid components.

6.2 Excel file comparisons

As it can be seen in the tables with results from the Excel file and the simulations, the HTC predicted by the correlations are very low compared to the HTC predicted by the simulations. This happens also using different Fluent HTC definitions as Wall adj. HTC, Wall function HTC. Probably this is connected to the complex geometry of the Heat Removal System and the fact that the correlations are derived for cases as pipes simpler geometries. Nevertheless, this means that air is far more useful in removing heat from the Proton Beam Dump and airflows with lower speeds can be used.

6.3 Thermal simulation comparisons

Below, a comparison between the results of the previous uncoupled simulation and the ANSYS coupled simulation.

The uncoupled simulation is obtained by imposing an imposed temperature on the bottom of the lower concrete block of 15 °C, imposing the convection boundary condition on the lateral surfaces using the HTC obtained brom the Excel file and some bulk temperatures (that it is not clear where are derived from). Radiative effects are considered (it is not clear how).

The boundary conditions for the ANSYS coupled simulation are well explained in the report.

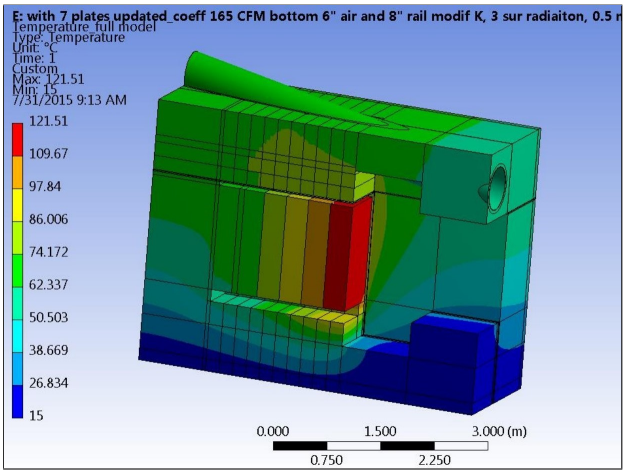

Figure 6.7: Previous temperature distribution, normal heat distribution, 165 CFM airflow

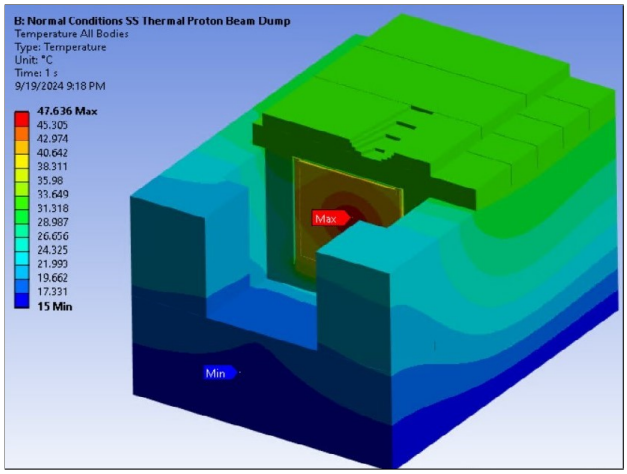

Figure 6.8: ANSYS coupled simulation, normal heat distribution, 165 CFM airflow

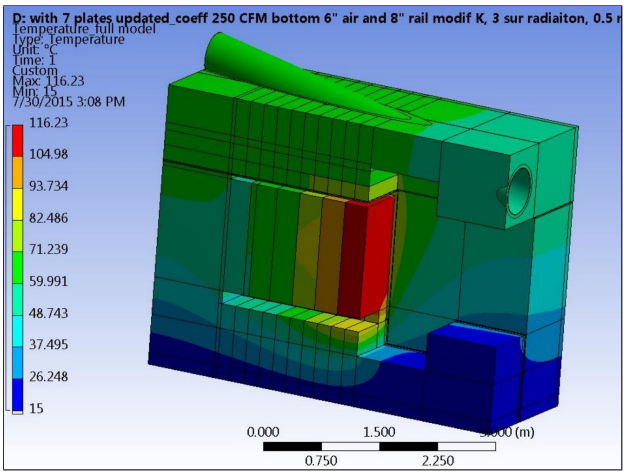

Figure 6.9: Previous temperature distribution, normal heat distribution, 250 CFM airflow

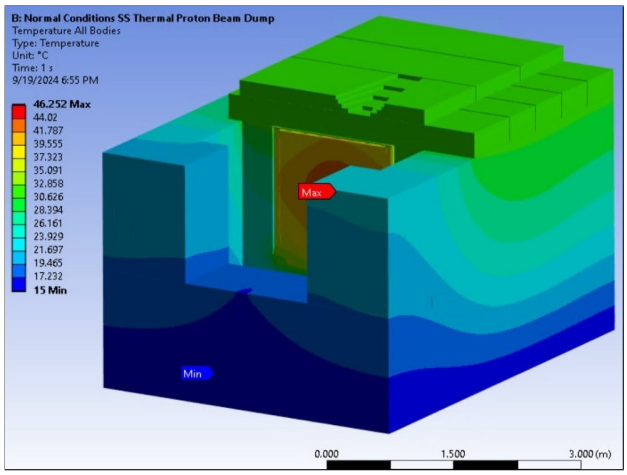

Figure 6.10: ANSYS coupled simulation, normal heat distribution, 250 CFM airflow

6.4 What to do next

There are a few things that have to be done to make sure that the simulations are giving accurate results. Here's a few, described in detail:

- **Need of a transient simulation** to know the developing of the situation in time. This has to be done by simulating the solid SS thermal alone in a transient simulation for like half a second. Then, taking the temperatures manually on the temperatures, and inputting them manually in the fluid simulation, to get the HTC and the bulk temperatures. These data have to be manually inputted as convection boundary condition in the solid simulation and the cycle repeats. Probably there is a way to write some script to do this automatically, but the System Coupling Block is useless because it would simulate the transient also of the fluid and we are not interested in the fluidodynamic transient of the fluid (it can be supposed independent from the thermodynamics transient, the change is just in the air properties).

- **Mesh sensitivity study** to check what is the role of the mesh (both solid and fluid component). The size of the geometry is big and the actual number of the elements could not be sufficient to describe what's happening. A mesh sensitivity study is carried out by taking some macroscopic quantities (velocity, temperatures, heat fluxes) and plotting them for different simulations increasing the number of elements. Take a lot of quantities and not only fluidodynamics quantities but also thermodynamics quantities because we are interested in the last ones (and I've seen that velocity converges very fast in these kind of sensitivity analysis so it's not a good indicator).

- Check the limit of **very high flow** (should tend to bring the surface temperature of the block to 20 degrees celsius) and the limit of **very low flow** (should tend to the no-convection simulation). Note: there is the possible use of laminar model in the last case, you have to check. I would expect that varying the volumetric flow, at leas a change in

the maximum temperature of a couple degrees should happen, as predicted by the global energy conservation equation paragraph.

- **Coupling iterations sensitivity study**: the total heat transmitted to the fluid is not the total heat flowing through the coupled surfaces of the solid. This means that **the heat flux and temperature** values of the coupled simulations **are not converged**. The simulations can be assumed to converge when, in Fluent, if you use the Surface Report instrument on all the surfaces, Integral Total Surface Heat Flux, the sum is the actual heat that it's being transferred from the solid (that is the total power deposited by the proton beam minus the heat that is flowing through the base, which can be obtained by the Reaction Probe on the Imposed Temperature boundary condition in the solid thermal SS simulation). Good luck.